ISSN 1980-9743

Soils and Rocks

Soils and Rocks

An International Journal of Geotechnical and Geoenvironmental Engineering

Volume 33, N. 2
May-August 2010

Soils and Rocks is an International Journal of Geotechnical and Geoenvironmental Engineering published by

ABMS - Brazilian Association for Soil Mechanics and Geotechnical Engineering
Av. Prof. Almeida Prado, 532, IPT/DEC-Prédio 54
05508-901 São Paulo, SP
Brazil

ABGE - Brazilian Association for Engineering Geology and the Environment
Av. Prof. Almeida Prado, 532, IPT/DIGEO- Prédio 59
05508-901 São Paulo, SP
Brazil

SPG – Portuguese Geotechnical Society
LNEC, Avenida do Brasil, 101
1700-066 Lisboa
Portugal

Issue Date: *August 2010*

Issue: *3,200 copies*

Manuscript Submission: *For review criteria and manuscript submission information, see Instructions for Authors at the end.*

Disclaimer: The opinions and statements published in this journal are solely the author's and not necessarily reflect the views or opinions of the publishers (ABMS, ABGE and SPG). The publishers do not accept any liability arising in any way from the opinions, statements and use of the information presented.

SOILS and ROCKS

An International Journal of Geotechnical and Geoenvironmental Engineering

Soils and Rocks publishes papers in English in the broad fields of Geotechnical Engineering, Engineering Geology and Geo-environmental Engineering. The Journal is published in April, August and December. Subscription price is US$ 90.00 per year. The journal, with the name "Solos e Rochas", was first published in 1978 by the Graduate School of Engineering-Federal University of Rio de Janeiro (COPPE-UFRJ). In 1980 it became the official magazine of the Brazilian Association for Soil Mechanics and Geotechnical Engineering (ABMS), acquiring the national character that had been the intention of its founders. In 1986 it also became the official Journal of the Brazilian Association for Engineering Geology and the Environment (ABGE) and in 1999 became the Latin American Geotechnical Journal, following the support of Latin-American representatives gathered for the Pan-American Conference of Guadalajara (1996). In 2007 the journal acquired the status of an international journal under the name of Soils and Rocks, published by the Brazilian Association for Soil Mechanics and Geotechnical Engineering (ABMS), Brazilian Association for Engineering Geology and the Environment (ABGE) and Portuguese Geotechnical Society (SPG).

Soils and Rocks

1978,	1 (1, 2)
1979,	1 (3), 2 (1,2)
1980-1983,	3-6 (1, 2, 3)
1984,	7 (single number)
1985-1987,	8-10 (1, 2, 3)
1988-1990,	11-13 (single number)
1991-1992,	14-15 (1, 2)
1993,	16 (1, 2, 3, 4)
1994-2009,	17-32 (1, 2, 3)
2010,	**33 (1, 2,**

ISSN 1980-9743 CDU 624.131.1

ISSN 1980-9743

SOILS and ROCKS

An International Journal of Geotechnical and Geoenvironmental Engineering

Publication of

ABMS - Brazilian Association for Soil Mechanics and Geotechnical Engineering

ABGE - Brazilian Association for Engineering Geology and the Environment

SPG - Portuguese Geotechnical Society

Volume 33, N. 2, May-August 2010

Table of Contents

Articles

Assessment of Long-Term Settlement Prediction Models for Municipal Solid Wastes Disposed in an Experimental Landfill

Gustavo Ferreira Simões, Cícero Antonio Antunes Catapreta

Abstract. Settlement evaluation in sanitary landfills is a complex process, due to the waste heterogeneity, time-varying properties and influencing factors and mechanisms, such as mechanical compression due to the load application and creep, and physical-chemical and biological processes caused by the wastes decomposition. Many empirical models of analysis and long-term settlement prediction are reported in the literature, which require the application to real case studies in order to be validated. In this paper, four models of long-term settlement prediction (Rheological, Hyperbolic, Composite and Meruelo models) reported in the literature were applied to assess the mechanical behavior of an experimental landfill, composed of 6 different cells of municipal solid waste. Concerning the long-term settlement prediction, the results enabled a critical evaluation of the models, pointing out some advantages and limitations. During the monitoring period of 3 years, significant vertical strains were observed (of up to 22%) in relation to the initial height of the experimental landfill, which can be considered high and is due to fresh wastes with high organic content disposed. The results also suggest that the operational procedures influenced the settlements in the experimental landfill. The long-term settlement prediction indicated a final strain range from 22% to 42%, with respect to initial waste height and the composite model presented better comparisons between field measurements and predictions.
Keywords: sanitary landfill, solid wastes, monitoring, settlement, experimental landfill, settlement prediction models.

1. Introduction

As pointed out by many authors (*e.g.* El-Fadel *et al.*, 1999), landfills remains an essential part of waste management system and in many countries the only economic form of municipal solid waste (MSW) disposal. The need to reuse landfills sites after closure associated with the large long-term vertical strains observed in these structures are enhancing waste settlements studies, mainly concerning the validation of long-term settlement prediction models.

MSW deposited in landfills suffer large long-term settlements, associated with volume reduction caused by the decomposition of organic solids, and also by physical creep of MSW skeleton (Sowers, 1973; Park *et al.*, 2002), leading to an increase in storage capacity.

Mechanisms governing the settlement occurrence in MSW landfills are many and complex and less known than in soils, due to waste particles deformability, heterogeneity of the material, particles of varied sizes, and to the loss of solids due to biodegradation (Sowers, 1973; Gabr *et al.*, 2000). Liu *et al.* (2006) mention that landfill settlement can be attributed to both mechanical compression and biological decomposition of solids. According to Hossain *et al.* (2003), with the enhancement of the waste decomposition, compressibility properties and, subsequently, the rate and magnitude of waste settlement change.

According to Edil *et al.* (1990) and Simões & Campos (2002), the identification of the mechanisms of settlement development in MSW landfills is important for the interpretation of geomechanical behavior, proposition of long-term settlement models and carrying out long-term simulations. The main factors affecting the MWS settlements include:

- Waste composition and biodegradable material content;
- Initial unit weight and void ratio;
- Landfill dimensions;
- Compaction methods;
- Stress history, involving all the filling stages;
- Wastes pre-treatment (incineration, composting and others);
- Leachate level and fluctuations;
- Existence of gases collection and extraction systems;
- Environmental factors, such as moisture content, temperature and gases present or generated by the biologic decomposition of waste.

As cited by Singh (2005), the total amount of settlement is dependent on the amount of mechanical compaction applied when placing the waste, the percentage of organics in the waste stream and the waste-to-soil ratio within the landfill. Mechanical compaction will reduce voids in the waste pile and allow placement of a larger vol-

Gustavo Ferreira Simões, DSc, Associate Professor, Departamento de Engenharia de Transportes e Geotecnia, Escola de Engenharia, Universidade Federal de Minas Gerais, Belo Horizonte, MG, Brazil. e-mail: gustavo@etg.ufmg.br.
Cícero Antonio Antunes Catapreta, DSc, Civil Engineer, Urban Cleansing Authority of Belo Horizonte, Belo Horizonte, MG, Brazil.
Submitted on December 22, 2008; Final Acceptance on June 6, 2009; Discussion open until December 31, 2010.

ume of waste within a geometry profile defined in the design, but there are other processes that affect settlement after placement. These processes, including particle migration, biodegradation and collapse of matter, may increase the long-term settlement rate.

According to Park & Lee (2002) the most important cause of long-term settlements is generally the volume reduction caused by organic solids decomposition, which may continue for a very long period and is dependent of biodegradable organic solids content. Liu *et al.* (2006) mention that the decomposition of organic material in landfills causes a considerable amount of settlement as the organic material is converted into decomposition products, such as liquids and gases, mainly methane and carbon dioxide. Wall & Zeiss (1995) describes that the biodegradation components of long-term compression, or bioconsolidation, is due to a four stage process (hydrolysis, acidogenesis, acetogenesis, methanogenesis) by which solid organic particles present in the waste are solubilized and converted to methane and carbon dioxide. Long-term settlements due to waste decomposition can theoretically reach 40% of the original thickness and can last for several years after closure in a continuous decreasing rate, depending on stabilization processes within the landfill (El-Fadel *et al.*, 1999).

Estimation of total settlement of sanitary landfills range from 25% to 50% of the landfill initial height (Edgers *et al.*, 1992; Wall & Zeiss, 1995; Ling *et al.*, 1998). This volume reduction caused by settlements can increase the landfill capacity and its life time. Besides, waste compression makes the landfill slopes less steep, contributing to the landfill stability and allowing future vertical expansions.

However, the settlement occurrence is undesirable in landfill maintenance, since it may lead to surface ponding and accumulation of water in the top of the landfill, development of cracks and failures of the cover system, deterioration of the leachate and gases drainage systems and safety issues (Bjarngard & Edgers, 1990; Edgers *et al.*, 1992; Ling *et al.*, 1998; Singh, 2005). Settlement occurrence can also be indicative of slope failures or, in more common situations, it changes the landfill surface configuration, causing irregular alterations in the surface drainage systems.

Several approaches and models for estimating landfill settlement have been proposed. These models, summarized in Liu *et al.* (2006), can be divided into the following categories: (i) consolidation models, based on Terzaghi's consolidation theory; (ii) rheological models; (iii) biodegradation models, which account for organic matter decomposition processes; (iv) regression models, which use common functions, such as logarithmic, hyperbolic and bi-linear, to simulate the landfill settlement.

As pointed out by Marques *et al.* (2003), each of these approaches addresses at least one of the three important mechanisms of MSW compression: (i) immediate response to applied loading; (ii) time-dependent mechanical creep, and (iii) biological decomposition of the waste. The models proposed by Simões & Campos (2002) and Marques *et al.* (2003) incorporate three separate expressions to explicitly account for all three mechanisms of MSW compression.

In this work, four long-term settlement prediction models presented in the literature, and described below, were investigated to evaluate the Belo Horizonte Experimental Sanitary Landfill behavior and the long-term settlement prediction. In this analysis a critical evaluation of the models performance was made, verifying their advantages and limitations. The models were selected in order to represent three of the categories cited previously, empirical (hyperbolic), rheological (composite and rheological) and biodegradation (Meruelo).

This study aims to contribute to the understanding of sanitary landfills mechanical behavior, concerning the long-term settlements. Usually, as a result of operational procedures in sanitary landfills, the initial settlements monitoring time occurs after the landfill closure or after some deformation has been observed. Landfills operating in real scale with the monitoring beginning immediately after closure are not common. In this study, the settlement monitoring started immediately after the experimental landfill filling.

Some considerations regarding the applicability of four long-term settlement prediction models mentioned in the literature are discussed in this study, trying to assess their advantages and limitations, as well as analyzing the parameters obtained by fitting field data to the models and trying to compare them to the results given in the literature.

The study is completed with the simulation using the four long-term settlement models, whose results are compared with the experimental landfill monitoring field data, allowing the identification of which model is more suitable to represent the observed data.

2. Long-Term Settlement Prediction Models Evaluated

2.1. Rheological model

The Rheological Model (Edil *et al.*, 1990) is composed of two elements: a Hookean element (of constant *a*) in series to a Kelvin element (a Hookean element, of constant *b*, associated in parallel to a Newtonian element, of viscosity $\lambda/\mathbf{b}$), as presented in Fig. 1.

After a stress increment, that can be originated by the weight of the waste or by applied loads in the surface, the Hookean element of constant *a* is compressed immediately, similar to the primary compression in soils. The compression of the Kelvin element is delayed by the dashpot, in a similar way to the secondary compression under constant effective stress in soils. The load is, then, progressively transferred for the second Hookean element. After a certain time, the whole effective stress will be supported by the two

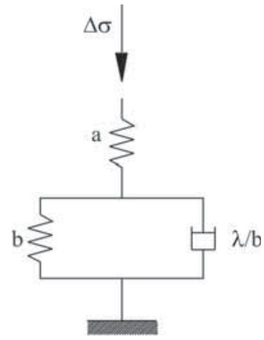

Figure 1 - Rheological model.

Hookean elements. This physical model can be represented by the mathematical expression (Eq. (1)):

$$\Delta H(t) = H \times \Delta\sigma \left[a + b\left(1 - e^{-\frac{\lambda}{b}t}\right)\right] \tag{1}$$

where: ΔH = settlement (m); a = primary compressibility parameter (kPa^{-1}); b = secondary compressibility parameter (kPa^{-1}); λ/b = rate of secondary compression (day^{-1}); $\Delta\sigma$ = compressive stress (kPa); H = initial height of MSW landfill (m); and t = time (day).

2.2. Hyperbolic function

The Hyperbolic Model was proposed by Ling *et al.* (1998), and is represented by the following expression (Eq. (2)).

$$S = \frac{t}{\frac{1}{\rho_0} + \frac{t}{S_{ult}}} \tag{2}$$

where t = difference between the time of interest and initial time ($t = t_i - t_o$) (day); S = difference between settlement at time ti and initial settlement ($S = S$i - So) (m); ρ_o = initial rate of settlement; S_{ult} = final settlement (m). The parameters ρ_o and S_{ult} may be determined through t/S *vs.* t relationship by conducting a linear regression analysis (Eq. (3)).

$$\frac{t}{S} = \frac{1}{\rho_0} + \frac{t}{S_{ult}} \tag{3}$$

2.3. Composite compressibility model

The composite biological model (Marques *et al.*, 2003) incorporates three mechanisms for one-dimensional compression of MSW: instantaneous response to loading from overlying layers, mechanical creep associated with the stresses from self-weight and the weight of overlying layers and biological decomposition.

The mechanisms of this model can be represented by three rheological components, as presented in Fig. 2. A Hookean element (primary mechanical compression), associated with a Kelvin element (secondary mechanical compression), represented by the association of a Hookean element and a Newton element (dashpot), and a third body (secondary biological compression) represented by the association in parallel of a finite compression element and dashpot.

Analytically, the model can be expressed as (Eq. (4)):

$$\varepsilon = \frac{\Delta H}{H} = C'_c \log\left(\frac{\sigma_0 + \Delta\sigma}{\sigma_0}\right) + \Delta\sigma \times b(1 - e^{-ct'}) + E_{DG}(1 - e^{-dt''}) \tag{4}$$

where ε = deformation (%); H = height (m); ΔH = settlement (m); C'_C = compression ratio (primary mechanical compression); σ_0 = initial vertical stress (kPa); $\Delta\sigma$ = change in vertical stress (kPa); b = coefficient of mechanical creep (secondary compression) (kPa^{-1}); c = rate constant for mechanical creep (secondary compression) (day^{-1}); E_{DG} = total amount of strain that can occur due to biological decomposition; d = rate constant for biological decomposition (day^{-1}); t'' = time since placement of the waste in the landfill; t' = time since application of the stress increment.

2.4. Meruelo model

Described in Diaz *et al.* (1995) and Espinace *et al.* (1999), this model is based on the loss of mass of the degraded materials that occurs during the anaerobic phase, which is conditioned by the organic matter hydrolysis rate. The loss of mass and consequent volume reduction is associated to the expected settlement (ΔH). The model is valid only for the long-term settlement prediction under the action of the decomposition processes (secondary compression due to waste biodegradation) (Eq. (5)).

$$\Delta H = \alpha \times H \times \mathrm{COD}\left[1 - \left(\frac{1}{K_h \times t_c}\right) \times (e^{-K_h(t - t_c)} - e^{-K_h t})\right] \tag{5}$$

where α = coefficient of mass loss; H = height of MSW landfill (m); COD = biodegradable organic matter present

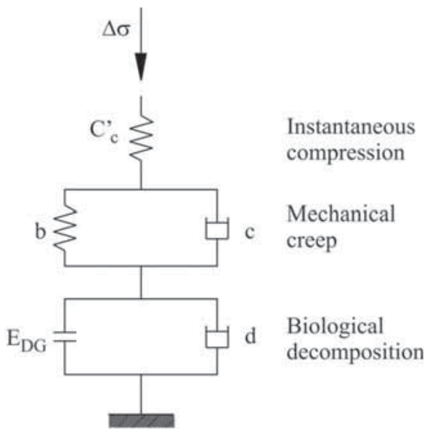

Figure 2 - Composite compressibility model.

in the wastes; t_c = time of landfill construction (day); K_h = hydrolysis coefficient (day^{-1}); t = time (day).

3. Material and Methods

3.1. Experimental landfill

The construction of the experimental landfill aimed to investigate the influence of operational aspects, mainly those concerning waste compaction, in the behavior of sanitary landfills. The study was carried out with the construction and monitoring of an experimental landfill for municipal solid wastes disposal, operating in real scale. The study also aimed at evaluating the mechanical behavior of the landfill and the evolution of the physical and chemical parameters of the leachate and gases generated, as well as evaluating the water balance and the performance of the landfill final cover (Catapreta, 2008). The focus of this paper is on long-term settlement analysis and modeling.

The experimental landfill is located at BR 040 Solid Waste Treatment Facility, in Belo Horizonte City, Minas Gerais State, Brazil, and it covers an area of about 5.26 x 10^3 m^2, with a total initial height of 3.8 m (3.2 m of waste and 0.60 m of final cover). About 8.6 x 10^3 mg of MSW, corresponding to 11.55 x 10^3 m^3, were disposed in the experimental landfill.

The construction of the experimental landfill was carried out between June of 2004 and May of 2005. The initial earthworks involved the removal of the existent vegetation layer and regularization of the area, to enable the liner and leachate collection system installation. The liner was composed of a support layer, constituted of 0.40 m compacted silty-clay soil, a synthetic flexible asphaltic membrane, 4.0 mm thick, and a protection layer, constituted of 0.30 m compacted silty-clay soil. Over the liner, the leachate collection system, composed of gravel-filled trenches, was constructed. All these construction stages were subjected to quality control, involving topographical measurements and field and laboratory tests carried out in earthen materials used.

The MSW disposal in the experimental landfill took one month, from May to June of 2005, and involved a series of controlled operational procedures. The filling procedures consisted of spreading the wastes in thin layers on the working face of the landfill and compaction with Track-Type Tractors, with weight of 17 mg. The daily waste densities were obtained using topographical measurements carried out at the end of each day and the weight of wastes disposed, obtained in Belo Horizonte Sanitary Landfill weighting facility.

The experimental landfill was divided in 6 cells (strips), which were filled with the same type of waste, but subjected to different compaction conditions. The field compaction energy (number of compactor equipment passes) and slope of working face were varied in order to obtain different initial densities for each cell, and consequently, to enable the evaluation of the influence of these aspects in the settlements.

The final cover of the cells was installed just after the filling phase. In 50% of the landfill, an evaporative final cover, constituted of 0.60 m thick compacted clay (permeability of 10^{-8} m.s^{-1}), was constructed. On the other half of the landfill, a capillary barrier, constituted of 0.30 m thick recycled demolition and construction waste layer under 0.30 m thick compacted clay (permeability of 10^{-8} m.s^{-1}), was constructed.

Immediately after the final cover construction, 18 settlement plates were installed, 3 on each cell. Figure 3 shows the experimental landfill, indicating the 6 cells and the installed settlement plates (SP 01 to SP 18).

The design and construction of this experimental landfill were carried out aiming the uniformity of waste composition. The average gravimetric composition of MSW disposed in all experimental landfill cells was: organic matter: 62%; paper and cardboard: 10%; plastics: 11%; metals: 2%; glasses: 3%; construction and demolition wastes: 3%; rubber, foam and ceramics: 1%; wood, textiles and leather: 4%; others: 5%. Based on Tchobanoglous *et al.* (1993), the methodology to obtain gravimetric composition consisted in quartering, sampling, segregation in categories

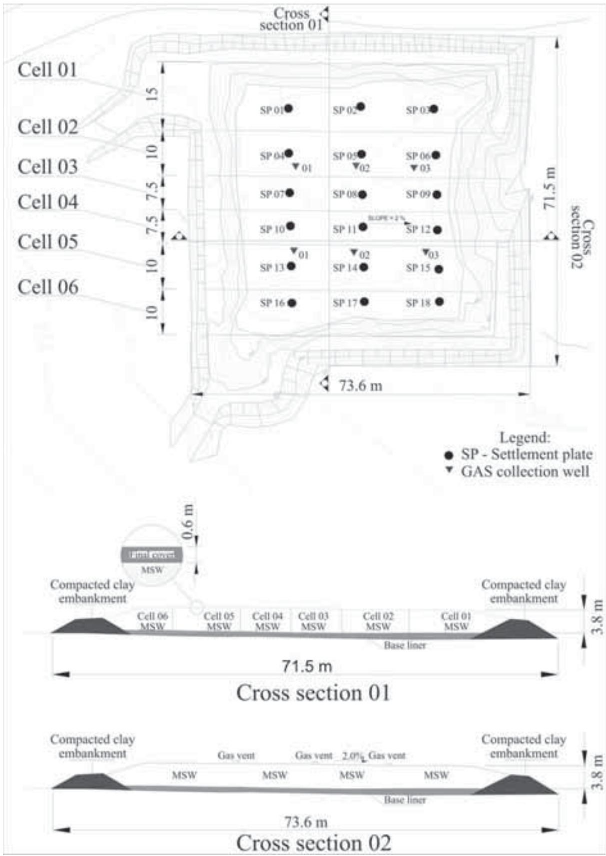

Figure 3 - Experimental landfill.

and weighting. The initial average moisture content was 60% in wet basis.

3.2. Settlement measurements

The settlement monitoring was carried out using the installed settlement plates, as showed in Fig. 3. These settlement plates were constituted of a concrete block with a steel rod, to allow the measurements, and were installed between the wastes surface and the final cover. The distribution of the settlement plates aimed at establishing the relationship between observed settlements, operation methods and initial waste densities in each cell. The settlements were measured using conventional topographical equipments.

The settlement analysis was performed using the average settlements observed for each group of plates, for each cell. To obtain and validate this average, the non-parametric Tukey Test (Larsen & Marx, 1986) was carried out. This test allows establishing the minimum significant difference, or in other words, the smallest average difference of samples that should be taken as statistically significant.

The settlement monitoring started immediately after the end of the experimental landfill construction and spanned over a period of approximately 3 years, from June 2005 to September 2008. Considering the geotechnical properties and the homogeneity of the soil underneath the experimental landfill associated with the low stresses induced by the experimental landfill, the long-term foundation settlements were not considered.

3.3. Settlement models calibration and simulation

The settlements analysis was accomplished considering the field data observed during the period of 3 years and were divided in two stages. In first stage, denominated Phase I, the first year monitoring data were used to calibrate the models. With the parameters obtained, a simulation of the second year was carried out to verify if the models adjusts to the field data observed.

In the second stage, described as Phase II, the 3 years monitoring data were used to calibrate the models and to simulate the long-term settlement for a period of 30 years.

The calibration of the models and long term simulation were obtained using a spreadsheet. For each cell settlement data, the best parameters of each model were achieved using an interactive approximation procedure, where the deviations (D), defined as the average of the square differences between the fitted and field data (Eq. (6)), were minimized.

$$D = \frac{\sum \left(Y - \overline{Y} \right)^2}{n} \qquad (6)$$

where: Y = fitted values; $\overline{Y}$ = field values; n = number of data.

4. Results and Discussion

The Tukey test indicated that the settlements observed in the set of three plates installed on each cell, could be represented by the average value. Therefore the influence of the small differences observed between the end of filling of each cell and the beginning of settlement monitoring were eliminated.

Table 1 shows the average settlement observed for the first and third years, as well as the cells initial densities. Figure 4 presents the curves of average measured settlement for each cell *vs.* time. As it can be observed the settlement plates presented a similar movement, however with different strain rates for each cell.

Considering that the MSW moisture content in all cells was similar, about 60% as described previously, the wet waste density was considered in the analysis.

The results suggest that the total vertical strains observed during the monitoring period are influenced by the initial wastes densities, with the larger settlements associated with the larger initial wastes densities. This observation is clear when Cells 2 and 4 are compared, where the settlement presented the smallest and highest values, respectively.

This result seems, in fact, contrary to the expected since wastes with same composition and smaller initial

Table 1 - Settlements observed in the experimental landfill.

Cell	Settlement plates	Settlement (m)		Average Settlement (m)		Waste density (kN.m^{-3})
		Year 1	Year 3	Year 1	Year 3	
1	1	0.372	0.615	0.341	0.593	7.3
	2	0.319	0.583			
	3	0.331	0.581			
2	4	0.358	0.625	0.352	0.623	5.8
	5	0.313	0.626			
	6	0.386	0.617			
3	7	0.396	0.655	0.387	0.646	8.1
	8	0.351	0.584			
	9	0.414	0.698			
4	10	0.461	0.712	0.425	0.717	8.2
	11	0.385	0.655			
	12	0.430	0.782			
5	13	0.402	0.644	0.402	0.684	8.1
	14	0.356	0.612			
	15	0.449	0.796			
6	16	0.345	0.594	0.376	0.642	8.0
	17	0.334	0.560			
	18	0.449	0.771			

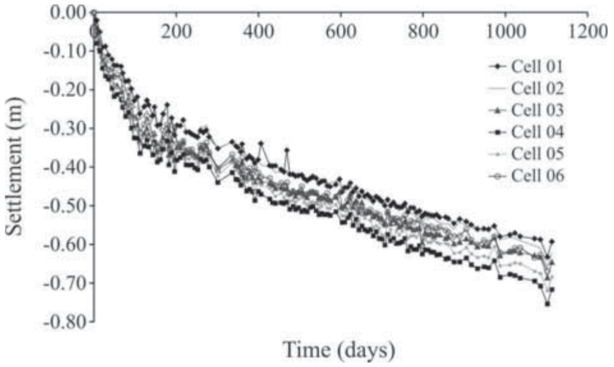

Figure 4 - Settlements observed in the experimental landfill.

densities tend to present higher settlements, mainly when subjected to stress increments. However this influence may not have affected the results, since the only stress increment was imposed by the final cover, which was similar for all cells. Considering the long-term behavior, although more compressible, the wastes with smaller densities are subject to smaller stresses due to self weight and the wastes with larger initial densities and, despite the lower compressibility, would be subject to larger stresses due to self weight. That could be contributing to the occurrence of larger settlements in the cells with larger initial densities.

4.1. Phase I calibration

The initial calibration, called Phase I, used the first year field data. The parameters and deviations obtained are shown in Table 2. The four models presented small and similar deviations, showing a good agreement between the fitted and observed data. As can be observed in Fig. 5, all the models presented a similar pattern, which can be attributed to the small number of records used in the calibration.

The parameters obtained in Phase I calibration were used to predict the settlements of the complete monitoring period (3 years). The comparison of the models results and the field data is shown in Table 3 and Fig. 6. As it can be seen in Fig. 6 and despite the small deviations observed in the calibration (Table 2), the models were not able to predict correctly the 3-year field data. All the models underestimate the settlements. Relations between predicted and measured settlements of up to 84% were observed. This confirms the need of larger set of data to predict more accurately landfill settlements.

4.2. Phase II calibration

The second calibration, called Phase II, used the three-year field data. The parameters and deviations obtained are shown in Table 4. The deviations observed are higher than those obtained for Phase I calibration. As can be observed in Fig. 7, all the models presented a similar pattern, excepting the Composite model, which presented better results, with lower deviations.

Table 2 - Obtained parameters for the Phase I calibration.

Cell	Rheological model			Hyperbolic model			Composite model					Meruelo model		
	D (x 10^4)	λ/b (x 10^3)	b (x 10^3)	D (x 10^4)	ρ_o (x 10^3)	S_{ult}	D (x 10^4)	b (x 10^3)	c (x 10^3)	Edg (x 10^3)	d	D (x 10^4)	α	K_h (x 10^3)
	m	day^{-1}	kPa^{-1}	m		m	m	kPa^{-1}	day^{-1}	-	day^{-1}	m	-	day^{-1}
1	2.4	9.17	9.44	2.3	3.90	0.466	2.2	8.24	8.02	6.96	0.102	2.6	0.19	7.06
2	3.3	11.54	11.34	2.9	4.95	0.426	2.9	9.30	9.50	10.79	0.151	3.0	0.18	8.85
3	3.4	13.41	9.22	3.1	6.81	0.470	2.8	7.75	11.28	12.24	0.303	3.0	0.20	10.27
4	4.2	14.12	9.83	3.4	7.91	0.502	3.1	8.16	11.18	17.37	0.357	3.1	0.22	10.77
5	3.9	12.94	9.57	3.5	6.78	0.490	3.2	8.14	10.72	13.28	0.408	3.3	0.21	9.94
6	4.1	11.41	9.31	3.9	5.54	0.483	3.6	8.07	9.63	10.83	0.222	3.8	0.20	8.80

D: deviation.

Table 3 - Settlement prediction for 3 years using parameters of Phase I.

Cell	Field data	Rheological model		Hyperbolic model		Composite model		Meruelo model	
	(m)	(m)	R (%)	(m)	R (%)	(m)	R (%)	(m)	R (%)
1	0.593	0.353	68.01	0.421	40.94	0.375	58.31	0.363	63.36
2	0.622	0.337	84.62	0.395	57.35	0.352	76.33	0.348	78.82
3	0.646	0.382	68.80	0.443	45.76	0.397	62.64	0.391	64.98
4	0.717	0.413	73.60	0.475	50.81	0.428	67.52	0.425	68.47
5	0.684	0.397	72.34	0.460	48.52	0.412	65.84	0.407	67.86
6	0.669	0.381	75.37	0.448	49.49	0.399	67.72	0.392	70.58

R: ratio between modeled and field data.

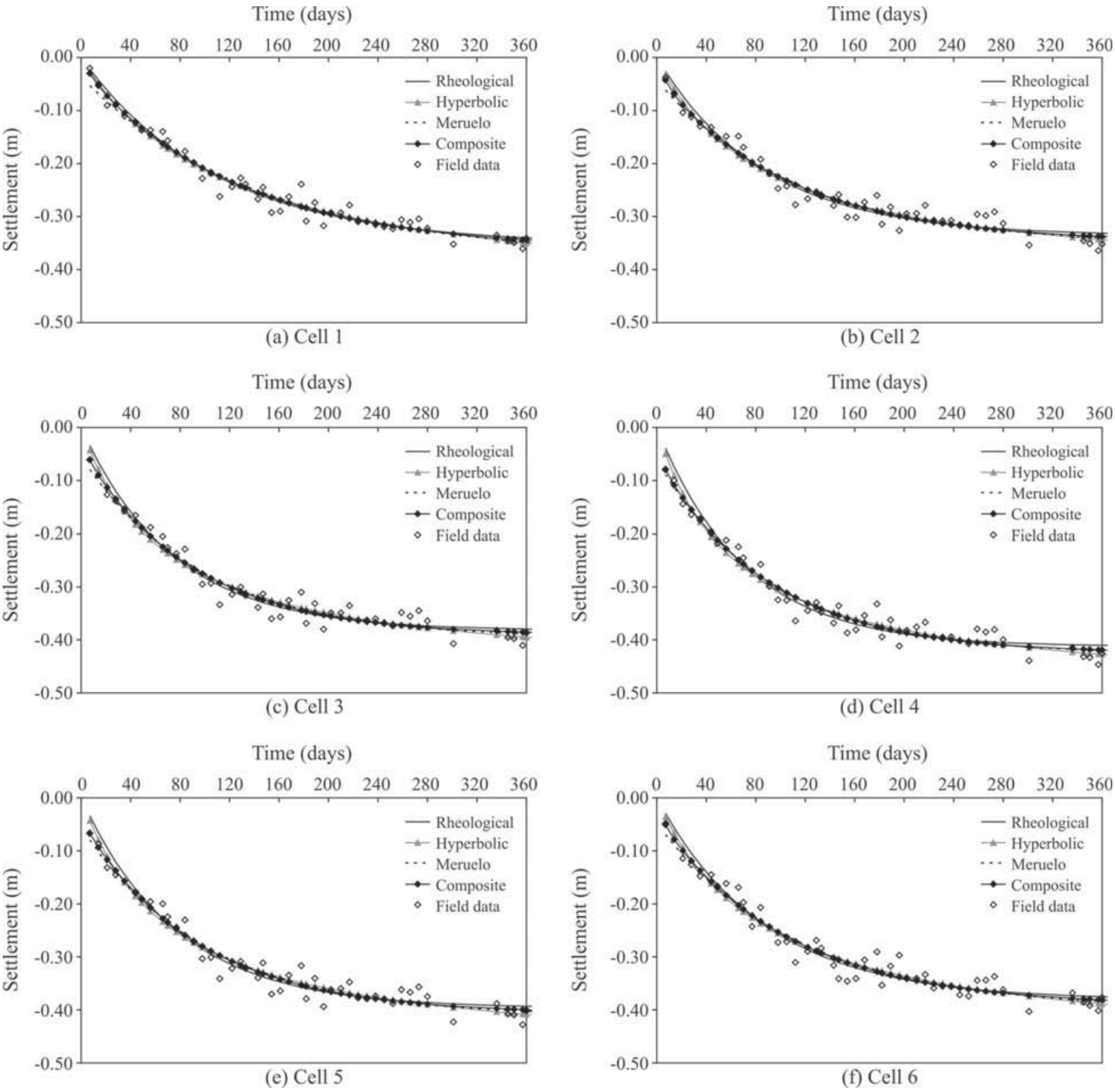

Figure 5 - Calibration of settlement models with the observed field data for Phase I (1 year).

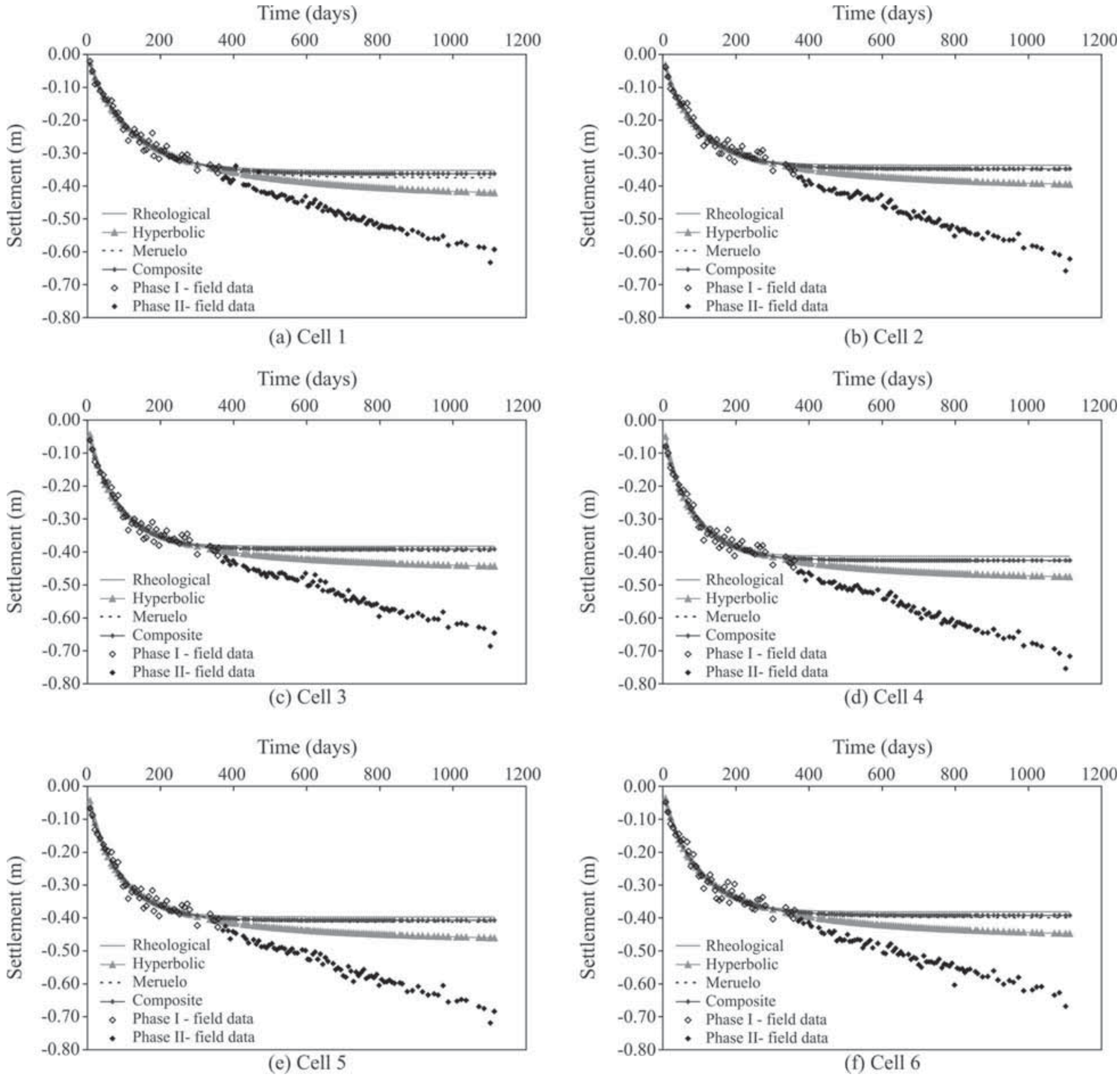

Figure 6 - Comparison of models results and field data using Phase I parameters.

Correlations between calculated and measured strains (settlement to initial height ratio) using Phase II calibrated parameters are shown in Fig. 8. The composite model was the only model to predict adequately the long term settlements.

Based on the results from the calibrations of Phase II, some remarks about the parameters obtained can be done.

Initial settlement rates observed for the Hyperbolic Model varied between 2.35 x 10^{-3} and 3.88 x 10^{-3} m.day^{-1} (Cells 1 and 4), similar to the rates observed by Ling *et al.* (1998): 1 x 10^{-3} and 3.0 x 10^{-3} m.day^{-1}. As Cell 1 presented a smaller density than Cell 4, the results suggest that the smaller the density, the smaller the settlement rates.

Despite the good fitting obtained for Phase I Calibration, for the total period of monitoring (Phase II) the Rheological Model presented a poor fitting. The compressibility parameters of the model were similar to the ones mentioned in the literature. The smallest secondary compression rate (λ/b) was observed for Cell 2, presenting values close to 3.31 x 10^{-3} day^{-1}, while the largest value was 4.46 x 10^{-3} day^{-1}, for Cell 4. Similar values were observed by Park *et al.* (2002).

The Meruelo Model has the advantage of representing the degradation process, which is important for the long-term settlement prediction. For this model, the observed values of mass loss coefficient (α), around 0.29 to

Table 4 - Obtained parameters for the Phase II calibration.

Cell	Rheological model			Hyperbolic model			Composite model					Meruelo model		
	D (x 10^4)	λ/b	b	D (x 10^4)	ρ_o	S_{ult}	D (x 10^4)	b	c	Edg	d	D (x 10^4)	α	K_h
		(x 10^3)	(x 10^3)		(x 10^3)			(x 10^3)	(x 10^3)	(x 10^3)				(x 10^3)
	m	day^{-1}	kPa^{-1}	m		m	m	kPa^{-1}	day^{-1}	-	day^{-1}	m	-	day^{-1}
1	10.2	3.32	14.80	5.7	2.35	0.70	1.3	18.89	0.64	64.20	0.0160	7.8	0.29	3.01
2	15.3	3.31	18.91	9.6	2.48	0.71	2.0	29.62	0.48	64.63	0.0209	12.0	0.29	3.00
3	21.0	4.46	13.63	11.6	3.55	0.68	2.1	26.84	0.34	85.45	0.0207	16.6	0.29	4.00
4	26.7	4.44	14.70	15.0	3.88	0.74	2.1	35.04	0.28	92.70	0.0223	21.1	0.32	3.98
5	22.1	4.24	14.37	12.5	3.51	0.72	2.3	27.35	0.36	86.63	0.0205	17.4	0.31	3.81
6	16.8	4.07	13.88	9.4	3.15	0.70	2.4	20.70	0.49	79.97	0.0182	13.2	0.29	3.67

D: deviation.

0.32, are similar to those described by Palma (1995), who observed variations between 0.15 and 0.50. The hydrolysis coefficient (K_h) presented values varying between 3.0 x 10^{-3} and 4.0 x 10^{-3} day^{-1}, smaller than the results obtained by Palma (1995). However, the values presented in the literature for such parameters are not common, and usually relations between them and landfill height are not obtained.

For the Composite Model were obtained values varying between 18.89 x 10^{-3} and 35.04 x 10^{-3} kPa^{-1} (Cells 1 and 4) for the secondary mechanical compression coefficient (b); 0.28 x 10^{-3} to 0.64 x 10^{-3} day^{-1} (Cells 4 and 1) for the secondary mechanical compression rate (c); 64.20 x 10^{-3} to 92.70 x 10^{-3} (Cells 1 and 4) for the secondary biological compression coefficient (E_{DG}); and 0.0160 to 0.0223 day^{-1} (Cells 1 and 4) for the secondary biological compression rate (d). Marques *et al.* (2003) observed average values of 5.27 x 10^{-4} kPa^{-1} for the secondary mechanical compression coefficient (b); 1.79 x 10^{-3} day^{-1} for the secondary mechanical compression rate (c); 0.159 for the coefficient of secondary biological compression (E_{DG}); and 1.14x10^{-3} day^{-1} for the secondary biological compression rate (d).

The composite model presented the lowest deviations (D) for Phase I and Phase II calibrations, showing a good fit of the model results to the field data. It should also be considered that this model has one more fitting parameter than the other used models, what probably makes it more accurate than the others. Besides, this model couples mechanical creep and biodegradation effects individually.

4.3. Settlement prediction

The parameters obtained in the calibration of Phase II were used to predict the long-term settlement, considering a period of 30 years. Table 5 and Fig. 9 show the results. As some of the models consider the occurrence of long-term settlement due to the biodegradation, it was chosen a longer period for settlement evaluation, in order to estimate the period of waste stabilization. Certainly, if a more extensive monitoring period were used in the calibration, it would be possible to accomplish a more accurate settlement prediction.

The composite and hyperbolic models results presented a tendency to stabilization at larger times, when compared to the rheological and Meruelo models, however with different settlement rates and final settlements. Considering the presence of slowly degradable organic wastes (such as fractions containing lignine), it is expected that complete stabilization of the landfill takes place only in the long-term.

It must be pointed out the difference between the final settlements predicted by composite and hyperbolic models. The final vertical strain predicted by the composite model has an average of 42% and the hyperbolic model 22%, with respect to the initial height of the cells. These results are similar to values suggested in the literature.

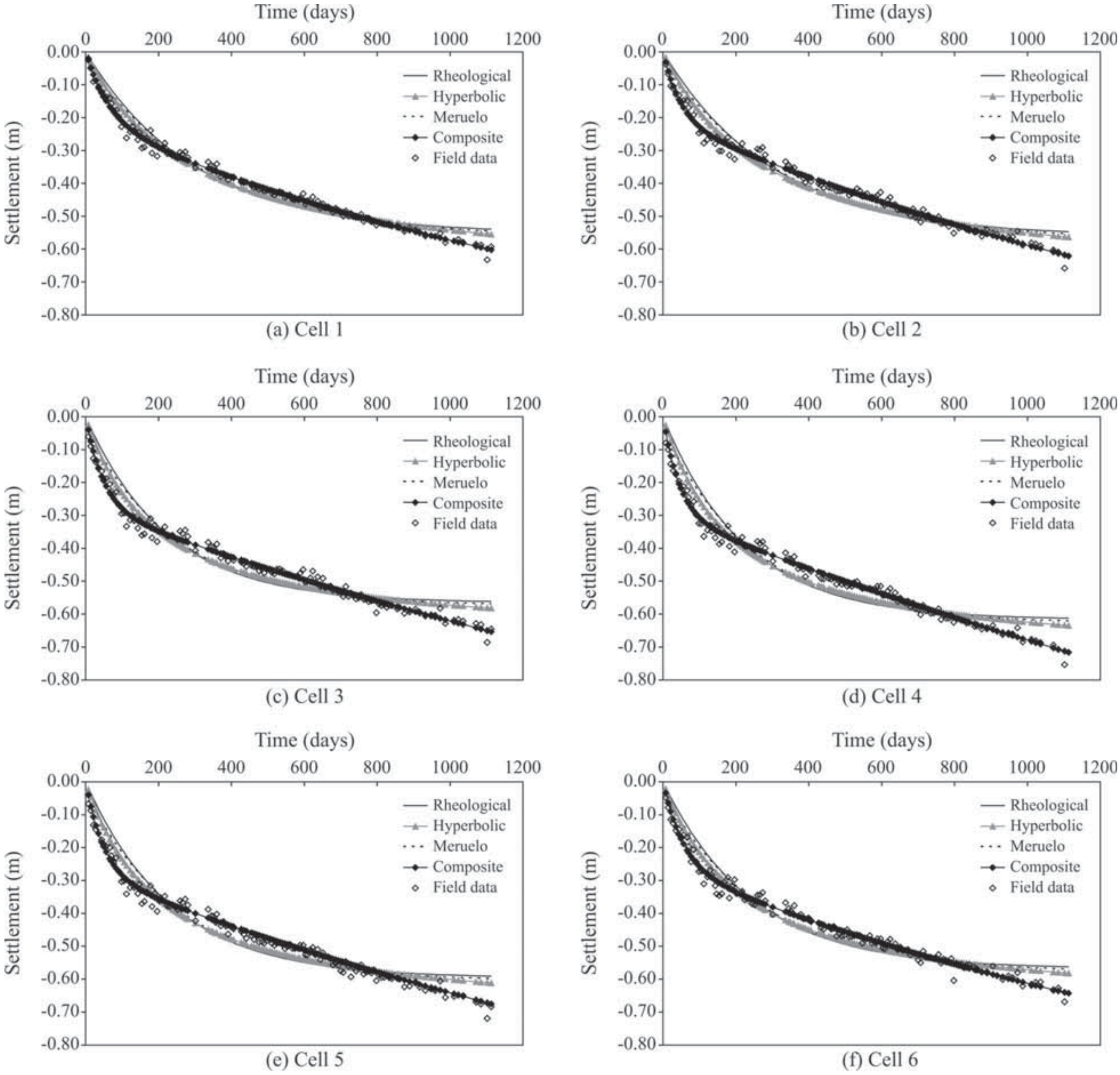

Figure 7 - Calibration of settlement models with the observed field data for Phase II (3 years).

The rheological and Meruelo models did not present satisfactory results, since the values observed in the long-term settlement prediction are indicating that the landfill would have reached the final phase of stabilization in approximately 3 years after wastes disposal, which, according to settlement field data that are still been collected is not happening (Catapreta, 2008).

5.Conclusions

The analysis of the vertical strains observed in the experimental landfill contributed to a better understanding of the waste settlement, allowing a critical assessment of the considered models, through the calibration of the field data and long-term settlement prediction.

The results demonstrate that settlement prediction in sanitary landfills is complex, what can be attributed to the wastes heterogeneity and the mechanisms involved in the process.

Limitations of some of the models considered in this study were verified, showing that long-term settlement prediction in MSW Landfill may not be restricted to the use of a single model. The use and comparison of different models should be considered and used to define final settlements ranges.

For a monitoring period of 3 years, the observed results indicated significant vertical strains, of up to 22% in relation to the initial height of the experimental landfill, what can be considered high and may be due to the fresh-

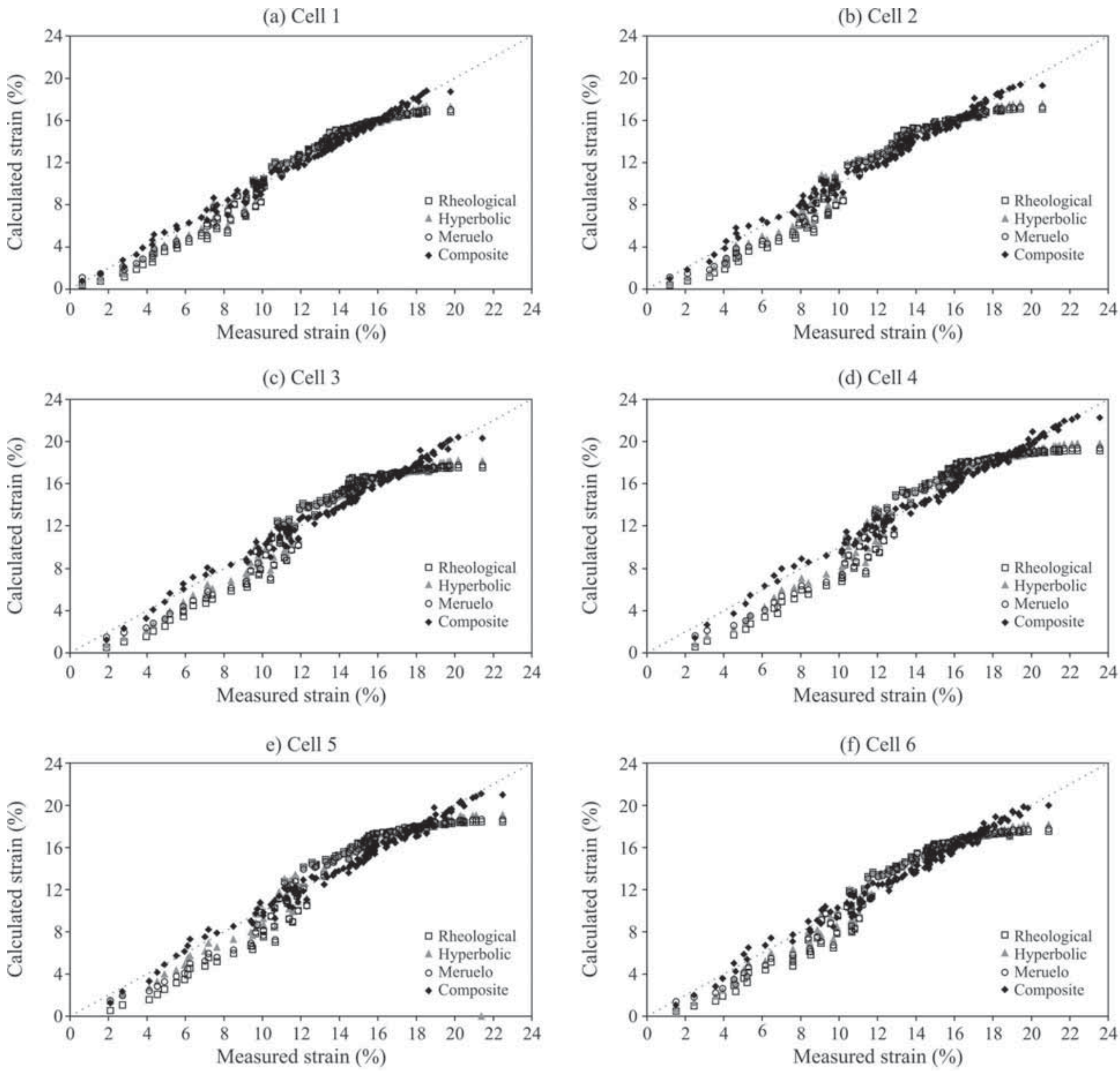

Figure 8 - Comparison of modeled and field strains using Phase II calibrated parameters.

Table 5 - 30-years Settlement prediction (m).

Cell	Rheological model	Hyperbolic model	Composite model	Meruelo model
1	0.553	0.686	0.986	0.564
2	0.561	0.690	1.199	0.576
3	0.565	0.671	1.462	0.575
4	0.617	0.731	1.808	0.627
5	0.596	0.711	1.480	0.606
6	0.568	0.685	1.169	0.578

ness and high organic content of the wastes being disposed.

The results obtained for the long-term settlement prediction with the rheological and Meruelo models indicate that the landfill would be reaching the final phase of stabilization in approximately 3 years after wastes landfilling. However, the settlement, leachate and gases monitoring that were carried out suggested that this stabilization has not occurred (Catapreta, 2008).

Others factors, related to mass loss, such as gas production and pressure, and position of gas vents, may also influence landfill settlements. However the monitoring program included only gas quality monitoring. Some tests

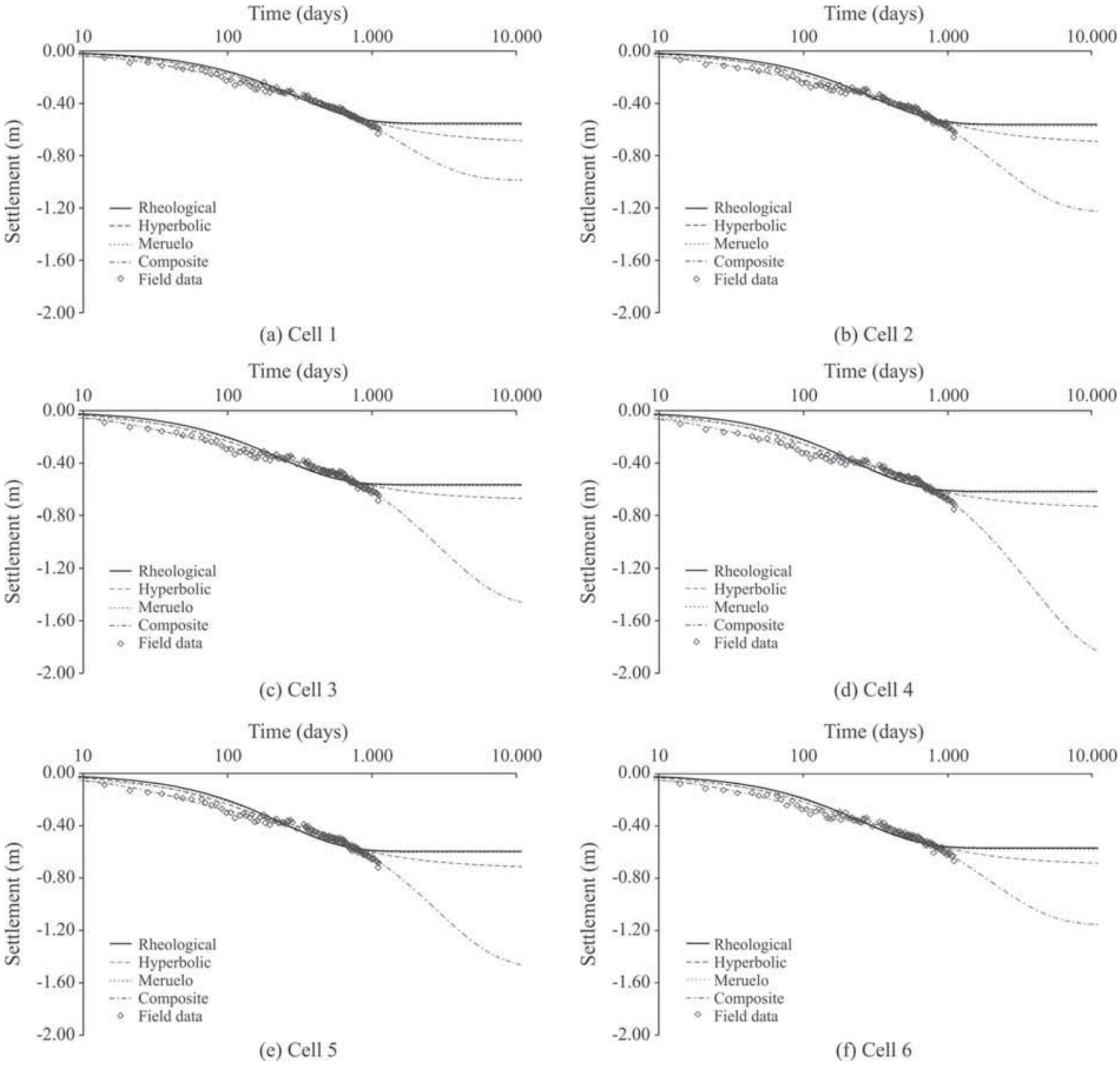

Figure 9 - Long-term settlement prediction.

were carried out to measure flow rates at gas vents, but the results indicated very small values, suggesting that the location of the vents did not influence the settlements in the experimental landfill.

The composite and hyperbolic models suggest settlements stabilization at larger times when compared to the rheological and Meruelo models, however with different settlement rates and final settlements. Considering these two models, a range of 22% to 42% of final strains could be suggested for long-term settlement prediction.

It should also be considered that the main reason for some models fit better than others may be due to the fact that they have more fitting parameters, enabling curve shapes that more closely resembles the field data.

Considering the mechanical component of the long-term settlement, the results also suggest that the operational procedures interfered directly in long-term settlements in sanitary landfills, indicating that the higher the initial densities, the higher are the stresses within the waste mass and, consequently, the larger are the long-term settlements.

Acknowledgments

The authors would like to acknowledge the Urban Cleansing Authority of Belo Horizonte for their assistance and co-operation with this study.

References

Bjarngard, A. & Edgers, L. (1990) Settlements of municipal solid waste landfills. Proceedings 13th Annual Madison Waste Conference, Madison, Wisconsin, v. 1, pp. 192-205.

Catapreta, C.A.A. (2008) Behavior of an Experimental Landfill: Assessment of Design, Construction and Operation Influence. PhD Thesis, Escola de Engenharia, Universidade Federal de Minas Gerais, 337 pp.

Diaz, J.G.L.; Narea, M.S.; Sanchez-Alciturri, J.M.; Ibarra, A.A., Monzon, I.T.; Gonzalez, J.P. & Lamia, M.F. (1995) Estimating material losses in sanitary landfills through biological degradation. Proceedings, 5th International Landfill Symposium – Sardinia 95, Cagliari, Italy, pp. 203-208.

Edgers, L.; Noble, J.J. & Williams, E. (1992) A biologic model for long term settlement in landfills. Proceedings of Mediterranean Conference on Environmental Geotechnology, Environmental Geotechnology, Cesme, Turkey, pp. 177-184.

Edil, T.B.; Ranguete, V.J. & Wuellner, W.W. (1990) Settlement of municipal refuse. Landva, A. & Knowles, G. D. (eds) Geotechnics of Waste Fills – Theory and Practice. American Society for Testing and Materials, Philadelphia, pp. 225-239.

El-Fadel, M.; Shazbak, S.; Saliby, E. & Lechie, J. (1999) Comparative assessment of settlement models for municipal solid waste landfill applications. Waste Management & Research, v. 17:5, p. 347-368.

Espinace, R.; Palma, G. & Sanchez-Alciturri, J.M. (1999) Experiencias de aplicacion de modelos para la determinacion de los assentamientos de rellenos sanitarios. Proceedings XI Panamerican Conference on Soil Mechanics and Foundation Engineering, Foz do Iguaçu, Brazil.

Gabr, M.A.; Hossain, M.S. & Barlaz, M.A. (2000) Solid waste settlement with leachate recirculation. Geotech. News, v. 18:2, p. 50-55.

Hossain, M.S.; Gabr, M.A. & Barlaz, M.A. (2003) Relationship of compressibility parameters to municipal solid waste decomposition. Journal of Geotechnical and Geoenvironmental Engineering, v. 129:12, p. 1251-1158.

Larsen, R.J. & M.L. Marx. (1986) An Introduction to Mathematical Statistics and its Applications, 2nd ed. Prentice-Hall International, Englewood Cliffs, 630 pp.

Ling, H.I.; Leshchinsky, D.; Mohri, Y. & Kawabata, T. (1998) Estimation of municipal solid waste landfill settlement. Journal of Geotechnical and Geoenvironmental Engineering, v. 124:1, p. 21-28.

Liu, C.N.; Chen, R.H. & Chen, K.S. (2006) Unsaturated consolidation theory for the prediction of long-term municipal solid waste landfill settlement. Waste Management & Research, v. 24:1, p. 80-91.

Marques, A.C.M.; Filz, G.M. & Vilar, O.M. (2003) Composite compressibility model for municipal solid waste. Journal of Geotechnical And Geoenvironmental Engineering, v. 129:4, p. 372-378.

Palma, J.H. (1995) Comportamiento Geotécnico de Vertederos Controlados de Residuos Sólidos Urbanos. Tesis Doctoral, Universidad de Cantabria, Santander, 294 pp.

Park, H.I. & Lee, S.R. (2002) Long-term settlement behavior of MSW landfills with various fill ages. Waste Management & Research, v. 20:3, p. 259-268.

Park II, H.; Lee, S.R. & Do, N.Y. (2002) Evaluation of decomposition effect on long-term settlement prediction for fresh municipal solid waste. Journal of Geotechnical and Geoenvironmental Engineering, v. 128:2, p. 107-118.

Simões, G.F. & Campos, T.M.P. (2002) A coupled mechanical and biological model to estimate settlements in solid waste landfills. Proceedings 4th International Symposium on Environmental Geotechnics, Rio de Janeiro, v. 1, pp. 283-288.

Singh, P. (2005) Landfill settlement effects. Proceedings 70th Annual Conference, Workshop And Expo, Rotorua, New Zeland.

Sowers, G.F. (1973) Settlement of waste disposal fills. Proceedings 8th International Conference on Soil Mechanics Foundation Engineering, Moscow, v. 2, pp. 207-210.

Tchobanoglous, G.; Theisen, H. & Vigil, S. (1993) Integrated Solid Waste Management: Engineering Principles and Management Issues, 1st ed. McGraw-Hill Book Company, New York, 978 pp.

Wall, D.K. & Zeiss, C. (1995) Municipal landfill biodegradation and settlement. Journal of Environmental Engineering, v. 121:3, p. 214-224.

Hydraulic Conductivity and Shear Strength Behavior of Compacted Lateritic Soil-Bentonite Mixtures Used for Sanitary Landfill Liners

Juliana Azoia Lukiantchuki, Edmundo Rogério Esquivel

Abstract. The use of soil-bentonite mixtures for sanitary landfill liners with the purpose of retaining pollutants is becoming very common. This work shows the results of hydraulic conductivity and shear strength tests performed with soil-bentonite mixtures with bentonite contents of 3%, 5% and 7%. Additionally, shear strength test results carried out with a mixture with bentonite content of 9%, are shown. The selected natural soil for this research is a lateritic residual clayey sand originated from Adamantina Formation sandstones of the Bauru Group. Samples of this soil were collected in the Pindorama County, which is located in the northeast of the State of Sao Paulo, Brazil. The hydraulic conductivity tests were performed with rigid and flexible wall permeameters. Test results show that mixtures with bentonite content higher than 6% are suitable, in terms of hydraulic conductivity, for the construction of sanitary landfill liners. The shear strength parameters of natural soil and mixtures were assessed by performing undrained triaxial compression tests and unconfined compression tests. It was found that there is a tendency showing that the cohesion increases when the bentonite content is increased. The addition of bentonite to natural soil causes the friction angle to decrease. However, it cannot be concluded from test results, that the higher the bentonite content, the lower the friction angle. In terms of shear strength, the unconfined compression test results have shown that mixtures with bentonite content of 5% are suitable for the construction of sanitary landfill liners when relative compaction is equal or higher than 95%.

Keywords: sanitary landfill, liners, bentonite, hydraulic conductivity, shear strength.

1. Introduction

In the last decades, the population growth and industrial expansion have caused serious problems, such as contaminant waste production and unsafe waste disposal. Waste decomposition produces gases and liquids, which may cause soil and groundwater contamination. At present, more importance has been given to this subject due to the concerns with the environmental protection. For this reason, many researchers (Rowe, 2001; Daniel, 1984, 1989 and 1993; Daniel & Koerner, 1995; Gleason *et al.*, 1997, Daniel & Wu., 1993; Rowe *et al.*, 2004; McBean *et al.*, 1995; Tripathi & Viswanadham, 2005; Sivapullaiah *et al.*, 2000; Anderson & Hee, 1995; Farnezi & Leite, 2007; Kumar & Yong, 2002, Magistris *et al.*, 1998) have discussed the issue concerning the adequate final waste disposal.

Among other factors, the efficiency of solid waste landfills depends on the liner performance. Liners are low hydraulic conductivity layers used in solid waste landfills to minimize infiltration of leachate into the groundwater (Dixon *et al.*, 1999). Such layers should show some basic characteristics such as low hydraulic conductivity, suitable shear strength, and durability. Materials used as liners may be either synthetic (geomembranes or geosynthetic clay liners) or natural (compacted clays or soil-bentonite mixtures).

Since soil liners serve as primary barrier to liquid movement, they should be composed of soils with a high percentage of clay-sized particles. In the case of places where the local soils show high hydraulic conductivity, suitable liners are constructed either with imported soils from other places or with local soils, improved by adding very fine materials, such as bentonite (McBean *et al.*, 1995).

Bentonites are clay minerals of the smectite group. Water is easily absorbed between the layers of smectite, causing swelling of the clay and consequently lowering its hydraulic conductivity. Because of its intense swelling and CEC (cation exchange capacity) properties, bentonite is widely used in the construction of liners. The sodium bentonite is frequently used for the construction of liners because its expansion is higher than that of the calcium bentonite. Consequently, the hydraulic conductivity of the sodium bentonite is lower than that of the calcium bentonite (Gleason *et al.*, 1997; Khera, 1995; Daniel & Koerner, 1995; Hoeks *et al.*, 1987, Mollins *et al.*, 1996).

According to Rowe (2001), the successful construction of soil-bentonite liners with low hydraulic conductivity depends on: (a) obtaining and maintaining a

Juliana Azoia Lukiantchuki, M.Sc, Doctoral Student, Departamento de Geotecnia, Escola de Engenharia de São Carlos, Universidade de São Paulo, São Carlos, SP, Brazil. e-mail: jazoia@yahoo.com.br.
Edmundo Rogério Esquivel, D.Sc, Professor, Departamento de Geotecnia, Escola de Engenharia de São Carlos, Universidade de São Paulo, São Carlos, SP, Brazil. e-mail: esquivel@sc.usp.br.
Submitted on December 16, 2008; Final Acceptance on June 22, 2009; Discussion open until December 31, 2010.

homogeneous mixture of the base soil with bentonite, avoiding segregation prior to and during placement; (b) compaction and water content control during placement; (c) reduced lift thickness to ensure uniform mixing of soil and bentonite.

The process of mixing soil and bentonite in the field may be done using motor grader blades and/or grids. According to Gouveia Filho (2006), the efficiency of the homogenization, when using this process, is very reasonable. Before mixing, the existing soil must be broken up and cleaned, with gravel and roots being removed. After mixing, the soil-bentonite mixture should be compacted according to the project recommendations, in terms of dry unit weight and optimum water content (Gouveia Filho, 2006).

When designing a soil-bentonite liner, it is important to find the optimum proportion of bentonite and water content on a site-specific basis. This can be achieved by preparing different soil mixtures with different bentonite contents and different water contents. Then laboratory hydraulic conductivity tests are performed on compacted specimens. Rowe (2001) reported that in barriers built with soil-bentonite mixtures, the bentonite content typically ranges between 4% and 10%, which leads to hydraulic conductivities ranging between 10^{-9} m.s^{-1} and 10^{-11} m.s^{-1}. Previous studies (Daniel, 1993) reported that in mixtures even with low bentonite content, the hydraulic conductivity could be reduced up to four orders of magnitude, as shown in Fig. 1.

When selecting materials for liner construction, if only the hydraulic conductivity characteristics are considered without taking into account the material shear strength, the liner performance can be negatively affected. Liner integrity, among other factors, is fundamental for waste landfill success (Boscov, 2008). Generally, liners undergo different states of stress, which may lead to failure. Thus, it is important to evaluate the shear strength of the materials used in the liner construction, in order to perform the required stability analyses.

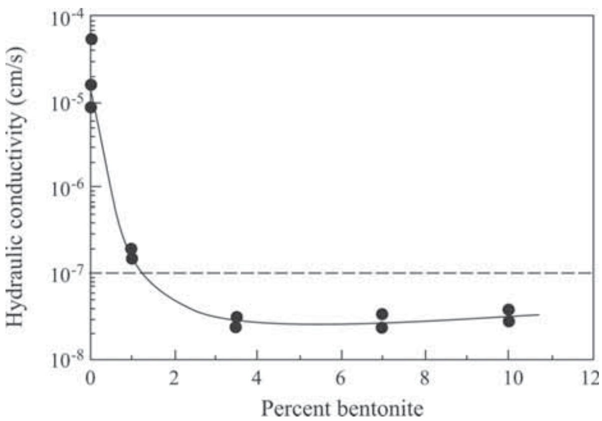

Figure 1 - Hydraulic conductivity *vs.* bentonite content (Daniel, 1993).

The addition of bentonite to a natural soil may modify its shear strength parameters. Chalermyanont & Arrykul (2005) reported that in barriers compacted with soil-bentonite, the cohesion and the friction angle increased and decreased, respectively, with the increase of the bentonite content.

The present paper describes the results of hydraulic conductivity and shear strength tests performed with natural soil and soil-bentonite mixtures. The natural soil used is a typical lateritic clayey sand found in the Southeast of Brazil. Hydraulic conductivity tests were performed with natural soil and three different soil-bentonite mixtures, with bentonite contents of 3%, 5% and 7%. The natural soil was tested in a rigid-wall permeameter and the soil-bentonite mixtures in flexible-wall permeameters. The shear strength parameters of the compacted soil and compacted mixtures were obtained through consolidated undrained triaxial compression tests (CU) and unconfined compression tests. In this case, shear strength tests were also carried out with a mixture with bentonite content of 9%.

2. Materials and Methods

2.1. Materials

Disturbed samples were collected in an industrial landfill located in Pindorama, São Paulo State, Brazil. The typical soil of this area is a lateritic residual clayey sand originated from Adamantina Formation sandstones of the Bauru Group. The natural soil was classified as lateritic soil according to the methylene blue adsorption test results (Lukiantchuki, 2007). Table 1 shows cation exchange capacity (CEC), specific surface (SS), clay activity (CA) and mineralogical composition of natural soil.

Figure 2 shows the grain size distribution of the natural soil and the bentonite used for mixtures (ABNT, 1984). Clay, silt and sand contents were about 22%, 14% and 64%, respectively. The uniformity coefficient (C_U) and the coefficient of gradation (C_C) are equal to 85 and 5, respectively.

The clay content of the bentonite was about 74%. According to the Unified Soil Classification the natural soil was classified as clayey sand (*SC*).

In the present work, besides the natural soil, three different soil-bentonite mixtures were studied, with bentonite contents of 3%, 5% and 7%. The natural soil and the mixtures were respectively designated by *S00*, *S03*, *S05* and *S07*, according to the bentonite contents. Further information about mixture preparation can be obtained in Lu-

Table 1 - Natural soil properties.

CEC (cmol kg^{-1})	4.39
SS (m^{2}g^{-1})	34.25
CA	6.45 (normal)
Mineralogical composition	kaolinite (dominant)

Table 2 - Natural soil and mixtures properties.

		S00	*S03*	*S05*	*S07*	Bentonite
Gs		2.61	2.67	2.67	2.68	2.83
Atterberg limits (ABNT,1984)	w_L (%)	26	36	39	42	455
	w_P (%)	17	16	17	17	54
	I_P (%)	9	20	22	25	401
Unified soil classification		*SC*	*SC*	*SC*	*SC*	-

G_s = specific gravity. w_L = liquid limit. w_P = plastic limit. I_P = plasticity index.

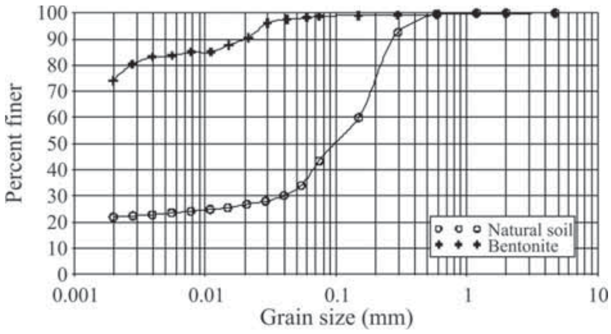

Figure 2 - Grain size distribution of natural soil and bentonite (ABNT, 1984).

kiantchuki (2007). Figure 3 shows the grain size distribution of the mixtures. Since the mixture bentonite content is relatively low, the grain size distribution curves are very alike. Some properties of natural soil, bentonite and soil-bentonite mixtures are shown in Table 2. According to X-ray diffraction test results, the bentonite used in this research is mineralogically composed of sodium smectite and low quartz. The bentonite chemical composition is show in Table 3.

2.2. Compaction test

Compaction tests were carried out to assess optimum water contents and maximum dry unit weights for natural soil and sand-bentonite mixtures. Proctor compaction tests were performed using standard effort (ABNT, 1986).

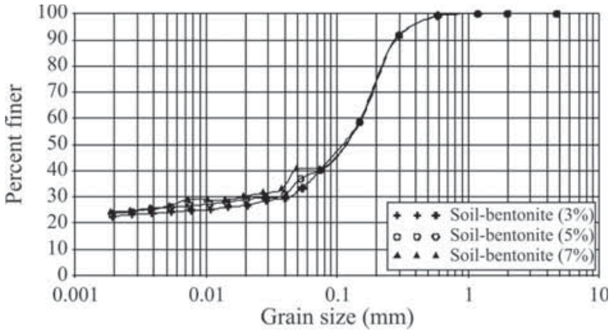

Figure 3 - Grain size distribution of soil-bentonite mixtures (ABNT, 1984).

For sample preparation, first, water was added to the dry soil-bentonite mixtures. Next, the specimens were sealed in plastic bags and left to hydrated for at least 24 h prior to compaction.

2.3. Hydraulic conductivity tests

The hydraulic conductivity tests were performed with natural soil and soil-bentonite mixtures with bentonite contents of 3%, 5% and 7%. These tests were carried out with three different specimens at each bentonite content. Specimens were molded at optimum water content and 95% of maximum dry unit weight. For the natural soil, the tests were performed with four different specimens in a rigid-wall permeameter (ABNT, 2000). The sample diameter and height were 50 mm and 100 mm, respectively.

The tests with soil-bentonite mixtures were performed using the flexible-wall permeameter (FWP) technique. In this case, the sample diameter and height were 100 mm and 100 mm, respectively. The FWP tests were conducted with a constant volume hydraulic system (closed system). The permeameter was connected to three different pressure sources, providing sample confinement, backpressure saturation and hydraulic gradient. Figure 4 shows the closed hydraulic system developed by Dourado (2003).

In this test, the specimen was placed between filter paper sheets and porous discs, and sealed with a rubber membrane, as shown in Fig. 5. The porous discs were previously saturated with water.

Table 3 - Bentonite chemical composition.

Chemical component	Percent
Silicon dioxide (SiO_2)	60.2
Aluminum oxide (Al_2O_3)	18.5
Ferric oxide (Fe_2O_3)	7.2
Magnesium oxide (MgO)	2.0
Calcium oxide (CaO)	2.4
Sodium oxide (Na_2O)	2.5
Titanium dioxide (TiO_2)	0.9
Potassium oxide (K_2O)	0.53

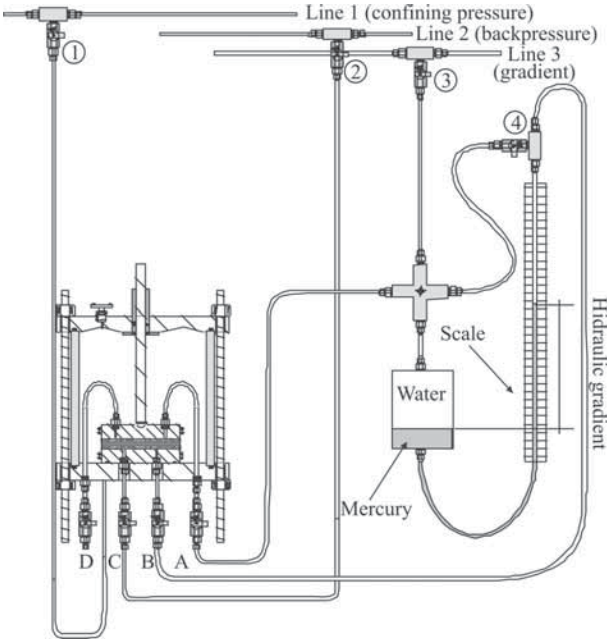

Figure 4 - Closed hydraulic control system (Dourado, 2003).

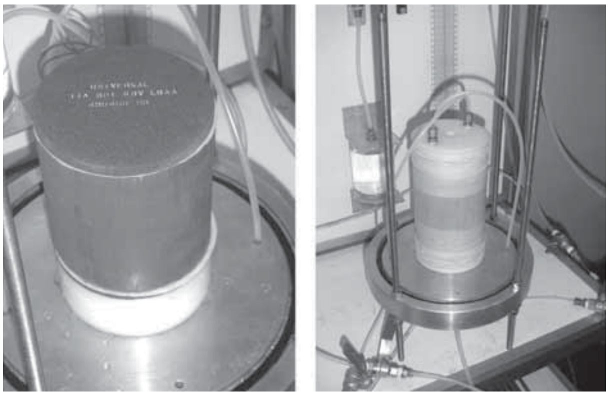

Figure 5 - Details of specimen assembly in the flexible-wall permeameter.

The FWP test comprised two stages: saturation and percolation. The specimen was initially saturated by applying the backpressure and the confining pressure, simultaneously. According to Head (1986), the saturation degree can be evaluated through the pore-pressure parameter B, which is defined as:

$$B = \frac{\Delta u}{\Delta \sigma_3} \tag{1}$$

where Δu is the pore pressure variation and $\Delta\sigma_3$ is the confining pressure variation. The tests were conducted by increasing the pressure in steps of 50 kPa, maintaining a difference of 10 kPa between the confining pressure and the backpressure. The specimens were considered fully saturated when $B \geq 0.90$, which was confirmed through index properties tests, performed after the FWP tests.

After full saturation, a flow through the sample was imposed by increasing pressure in line 3, creating a hydraulic gradient between the specimen top and bottom (Fig. 4). The initial hydraulic gradient adopted was 10, as recommended by ASTM (2001). The pressure increase caused the mercury in the capillary tube to heave, indicating the hydraulic gradient level. The hydraulic conductivity k (m.s^{-1}) was calculated by Eq. (2), measuring the variation with time of the mercury column height:

$$k = \frac{a \times A}{(a + A)\left(\frac{\gamma_{Hg}}{\gamma_w} - 1\right)} \times \frac{L}{S \times \Delta t} \times \ln\left(\frac{Y_i}{Y_{i+1}}\right) \tag{2}$$

where a = the capillary tube cross section area (m^2); A = mercury container cross section area (m^2); γ_{Hg} = mercury unit weight (kN.m^{-2}); γ_w = water unit weight (kN.m^{-2}); L = specimen height (m); S = specimen cross section area (m^2); Y_i and Y_{i+1} = mercury column height at instants t_i and t_{i+1}, respectively (m); Δt = elapsed time between the readings of Y_i and Y_{i+1} (s).

2.4. Shear strength tests

Shear strength parameters (cohesion and friction angle) of the natural soil and sand-bentonite mixtures were assessed by carrying out a series of consolidated undrained (CU) triaxial tests (ASTM, 1995). Specimens were molded at optimum water content and 85% of maximum dry unit weight. Shear strength tests were performed with natural soil and soil-bentonite mixtures with bentonite contents of 3%, 5%, 7% and 9% at three different confining pressures (50 kPa, 100 kPa and 200 kPa). The extra soil-bentonite mixture with bentonite content of 9% was designated *S09*. Specimen shearing rate of 0.2 mm/min was adopted based on the full consolidation time (Head, 1986).

The undrained shear strength of the natural soil and sand-bentonite mixtures were assessed by means of unconfined compression tests. For each relative compaction value (85%, 90% and 95%), one specimen was molded, which was tested under unconfined compression.

3. Results and Discussion

3.1. Compaction test results

Natural soil and soil-bentonite mixtures compaction test results are shown in Table 4 and Fig. 6. It can be noticed that the higher the bentonite content, the lower the maximum dry unit weight. Also, there is a tendency showing that the higher the bentonite content, the higher the optimum water content, although for mixtures *S03* and *S05* the optimum water contents are alike. These soil-bentonite behaviors are very similar to those found by Chalermyanont & Arrykul (2005).

Table 4 - Compaction characteristics.

	S00	S03	S05	S07
$\gamma_{dmáx}$ (kN.m^{-3})	18.90	18.50	18.30	17.8
w_{op} (%)	13.0	14.5	14.5	15.5

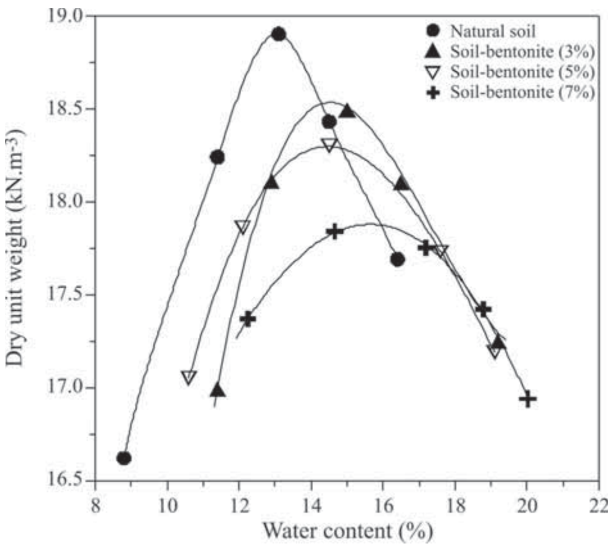

Figure 6 - Compaction curves for natural soil and soil-bentonite mixtures.

Figure 7 shows the influence of the bentonite content on some mixture properties. It can be noticed that the variation of the liquid limit (W_L) with bentonite content is approximately linear, whereas the plastic limit (W_P) remains almost constant. Consequently, the addition of bentonite significantly increased the plasticity (I_P) of the natural soil. These Atterberg limit behaviors were also observed by Magistris *et al.* (1998).

Many researchers reported noticeable changes in the compaction parameters as a result of bentonite addition to natural soil (Magistris *et al.*, 1998; Chalermyanont & Arrykul, 2005; Kumar & Yong, 2002; Farnezi & Leite, 2007). However, the observed behaviors of the compaction parameters show different trends. According to Magistris *et al.* (1998) the interpretation of these apparently erratic behaviors can be justified by comparing the particle size distribution parameters of the granular soils adopted as basic material (matrix). These authors also reported that the higher the bentonite content, the higher the optimum water content. However, the rate of increase appears to be less evident for the mixtures with well graded matrices and higher hygroscopic water contents, likely due to the hydration of bentonite particles.

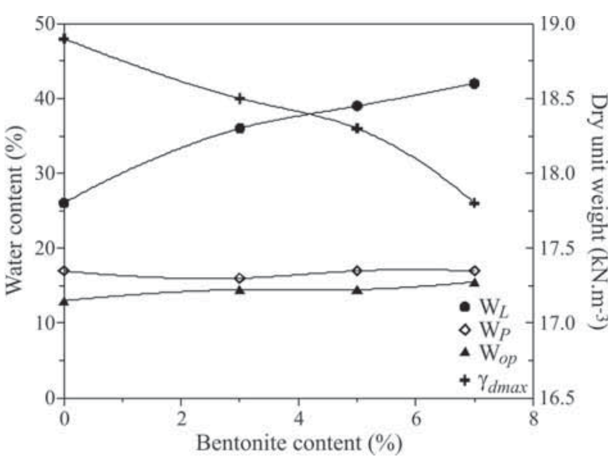

Figure 7 - Variation of some properties with the bentonite content.

3.2. Hydraulic conductivity test results

Figures 8 and 9 show the hydraulic conductivity test results for natural soil and soil-bentonite mixtures, respectively. Table 5 shows the average values of hydraulic conductivity.

It was observed that the higher the bentonite content, the lower the hydraulic conductivity. For mixtures with bentonite content of 7%, the hydraulic conductivity was reduced about four orders of magnitude when compared to the natural soil. This behavior has been also observed by other researchers (Daniel, 1993; Tripathi & Viswanadham, 2005; Chalermyanont & Arrykul, 2005).

Figure 10 shows the variation of hydraulic conductivity average with bentonite content. The reduction in hydraulic conductivity occurs due to high mineralogical activity of bentonite. Absorbing water, the bentonite particles swell, fill the pores of the coarse matrix and obstruct the free water flow (Magistris *et al.*, 1998).

The usual municipal waste standards for compacted soil liners state that the hydraulic conductivity should be less than 10^{-9} m/s. Therefore, according to laboratory tests,

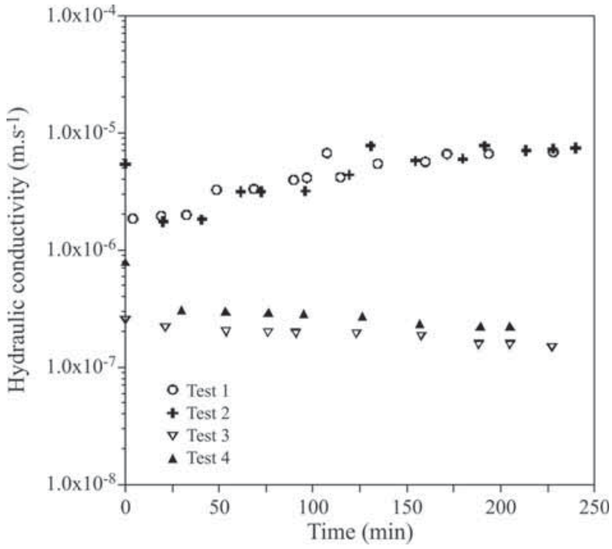

Figure 8 - Hydraulic conductivity test results for natural soil.

the compacted soil-bentonite mixtures with bentonite content higher than 6% fulfill the requirements for liners. However, it must be taken into account that hydraulic conductivity in the field will be generally higher than that measured in laboratory tests (Daniel, 1984). In a research conducted by Ferrari (2005), the hydraulic conductivity obtained in the field was very similar to that one obtained in laboratory. According to the same author, this can be accomplished when some precautions are taken, including proper bentonite hydration, homogeneous mixtures of base soil with bentonite and reduced lift thickness to ensure uniform mixing of soil and bentonite.

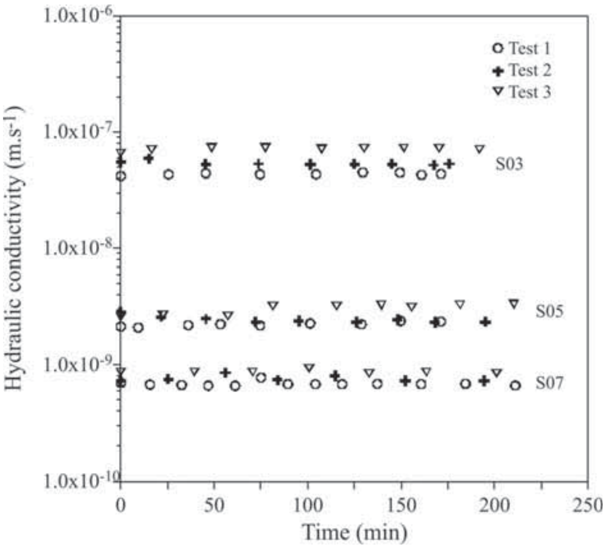

Figure 9 - Hydraulic conductivity test results for soil-bentonite mixtures.

Table 5 - Average values of hydraulic conductivity results.

Test	k (m.s^{-1})			
	S00	*S03*	*S05*	*S07*
1	1.2×10^{-6}	4.4×10^{-8}	2.2×10^{-9}	6.8×10^{-10}
2	3.3×10^{-6}	5.3×10^{-8}	2.4×10^{-9}	7.5×10^{-10}
3	3.0×10^{-6}	7.2×10^{-8}	3.1×10^{-9}	8.8×10^{-10}
Average	2.5×10^{-6}	5.6×10^{-8}	2.6×10^{-9}	7.7×10^{-10}

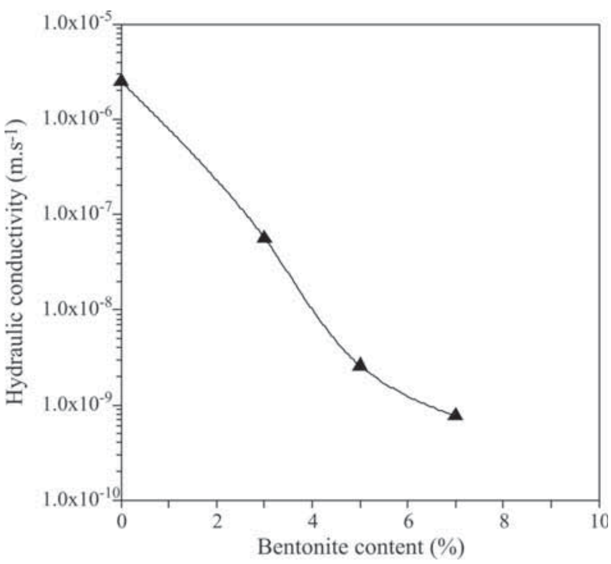

Figure 10 - Average hydraulic conductivity *vs.* bentonite content.

3.3. Shear strength test results

Figure 11 shows the maximum deviator stress for different confining pressures and different bentonite contents. It is observed that the shear strength of the soil decreases with bentonite addition. However, among the mixtures the shear strength tends to increase when bentonite content is increased. This behavior was also observed by Magistris *et al.* (1998). The shear strength parameters are shown in Table 6 and total and effective stress failure envelopes are shown in Figs. 12 and 13, respectively.

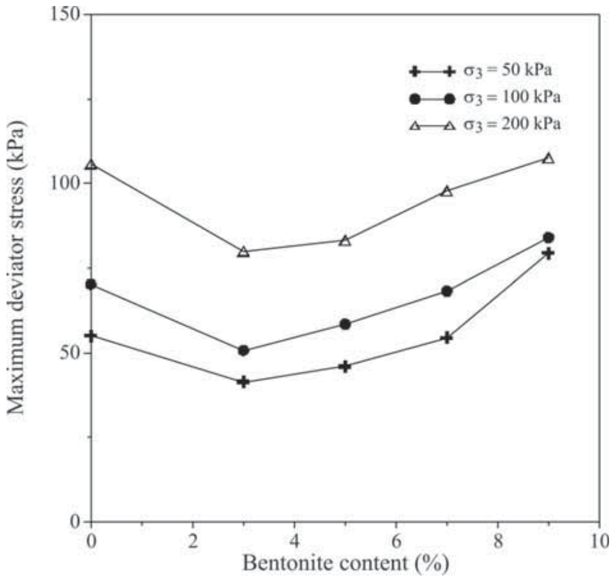

Figure 11 - Maximum deviator stress *vs.* bentonite content.

Table 6 - Shear strength parameters of compacted soil-bentonite mixtures.

Bentonite content (%)	Total parameters		Effective parameters	
	ϕ (°)	*c* (kPa)	ϕ' (°)	*c'* (kPa)
0	10.0	10.1	20.9	5.9
3	6.7	11.9	13.4	14.4
5	6.3	15.1	11.3	15.7
7	7.2	17.6	15.5	14.4
9	6.4	25.8	15.7	22.1

ϕ = total friction angle. c = total cohesion. ϕ' = effective friction angle. c' = effective cohesion.

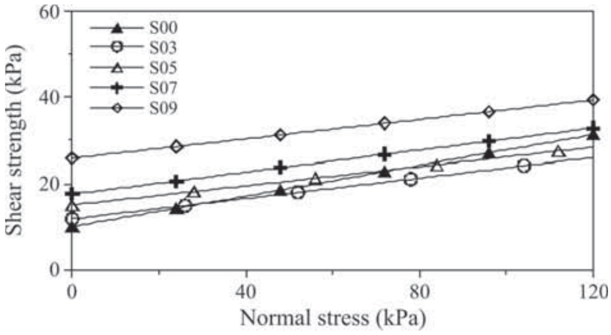

Figure 12 - Total stress failure envelopes.

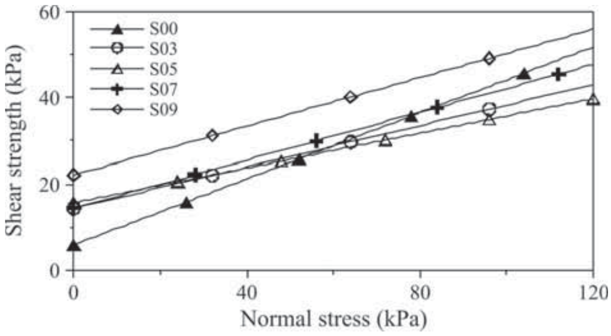

Figure 13 - Effective stress failure envelope.

As shown in Table 6, the total and effective friction angle of compacted soil-bentonite mixtures decreases from 10.0° to 6.3° and from 20.9° to 11.3°, respectively, when bentonite content is increased from 0 to 5%. The natural soil shows the highest friction angle, for both total and effective stresses. The addition of bentonite to natural soil causes the friction angle to decrease. However, it cannot be concluded from test results, that the higher the bentonite content, the lower the friction angle. One explanation for this behavior is that the bentonite swelling causes the mixtures to become loose. Nevertheless, for bentonite content of 7%, the total and effective friction angles increased to 7.2° and 15.5°, respectively. For bentonite content of 9%, the total and effective friction angles found are 6.4° and 15.7°, respectively, showing a modification of the mixture behavior.

In contrast, the cohesion increases when the bentonite content is increased, as shown in Table 6. The total and effective cohesion of the soil-bentonite mixtures increased from 10.1 kPa to 25.8 kPa and 5.9 kPa to 22.1 kPa, respectively, when the bentonite content was increased from 0 to 9%. From shear strength test results it can be observed that there is a tendency of the cohesion to increase when the bentonite content is increased. This behavior was also observed by Chalermyanont & Arrykul (2005).

Magistris *et al.* (1998) also reported that the shear strength parameters are affected by the addition of bentonite. According to these authors, this is in agreement with the microstructural changes reflected by the increase in plasticity.

3.4. Unconfined compression tests results

Figures 14 to 18 show the stress-strain curves, obtained from unconfined compression tests, for samples *S00*, *S03*, *S05*, *S07* and *S09*. The corresponding unconfined compression results are shown in Table 7. Figure 19 shows the variation of the unconfined compression strength with the bentonite content, for three different relative compaction values.

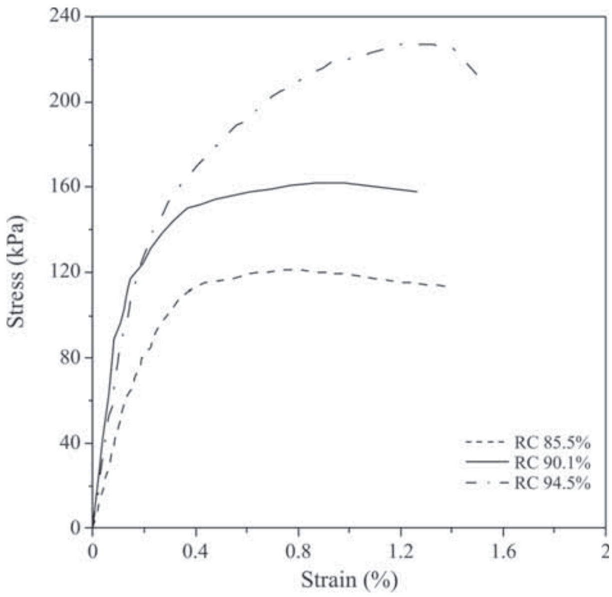

Figure 14 - Stress-strain curve (*S00*).

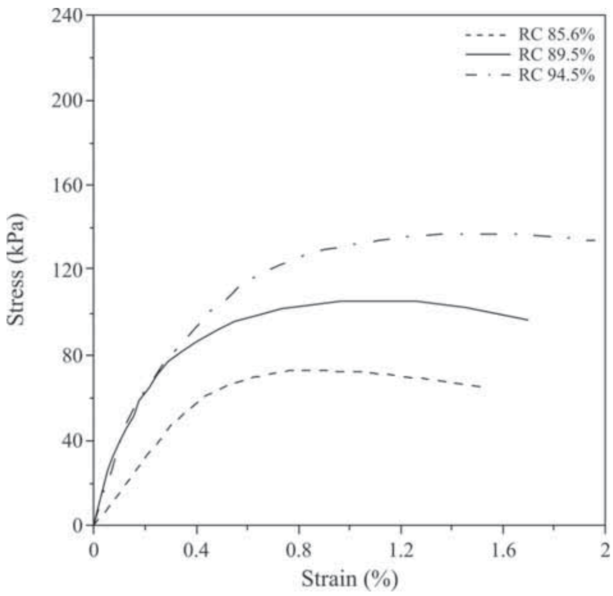

Figure 15 - Stress-strain curve (*S03*).

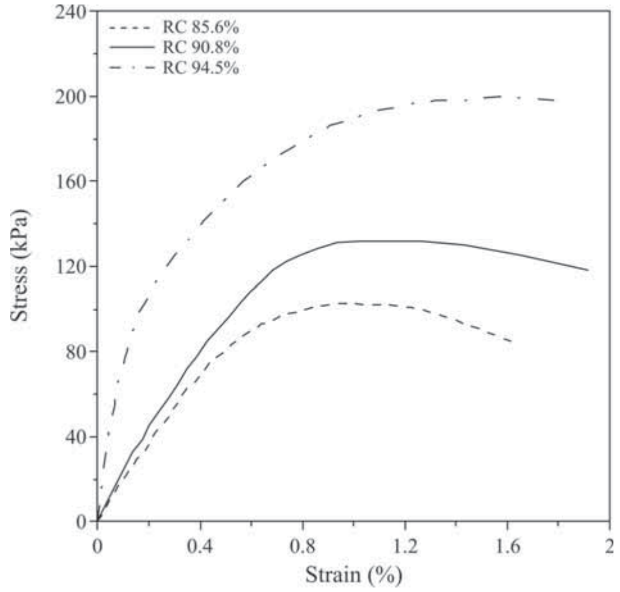

Figure 16 - Stress-strain curve (*S05*).

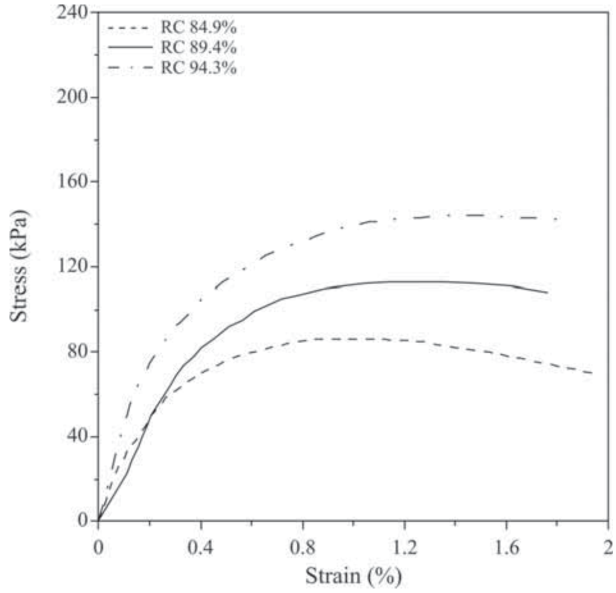

Figure 18 - Stress-strain curve (*S09*).

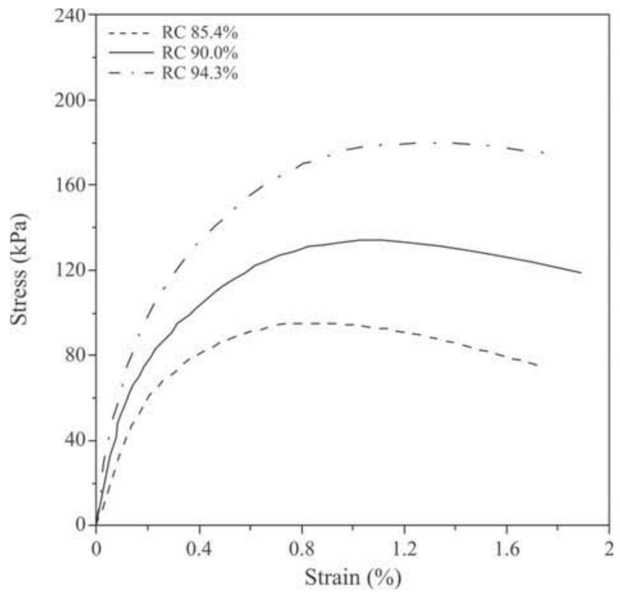

Figure 17 - Stress-strain curve (*S07*).

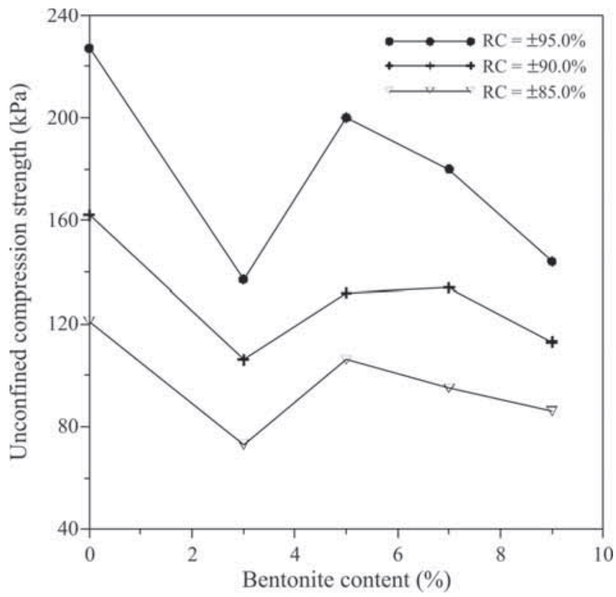

Figure 19 - Variation of the unconfined compression strength with the bentonite content.

It can be noticed that unconfined strength of the natural soil decreases with the addition of bentonite (Fig. 19). However, it can be observed that when the bentonite content is increased, the unconfined strength increases, reaching a maximum value, and then starts to decrease again. Figure 19 also shows that the higher the relative compaction, the higher the unconfined strength. According to Daniel e Wu (1993), the unconfined compression strength for the conduction of liners should be equal or higher than 200 kPa. Therefore, the 5% soil-bentonite mixture is suitable for liner constructions when relative compaction is equal or higher than 95%. The same authors reported that the higher molding water content, the lower the unconfined strength. This tendency can be observed in Fig. 19, although tests performed with mixture *S03* showed the lowest strengths.

4. Conclusions

The properties of compacted soil-bentonite mixtures were assessed by carrying out a series of hydraulic conductivity and shear strength tests. The following conclusions

Table 7 - Unconfined compression results.

	Specimen	RC (%)	UCS (kPa)
	01	85.5	121
S00	02	90.1	162
	03	94.5	227
	01	84.8	73
S03	02	89.5	106
	03	94.5	137
	01	85.6	106
S05	02	90.8	132
	03	94.9	200
	01	85.4	95
S07	02	90.0	134
	03	94.3	180
	01	84.9	86
S09	02	89.4	113
	03	94.3	144

RC = relative compaction. *UCS* = unconfined compression strength.

can be stated concerning the influence of bentonite content on the soil-bentonite mixture properties.

1. The grain size distribution do not show any significant changes by adding bentonite to the natural soil.

2. As it was expected, the liquid limit increases when the bentonite content is increased, while the plastic limit remains constant. Consequently, the bentonite addition significantly increases the plasticity of the natural soil.

3. The maximum dry unit weight decreases and the optimum water content increases when the bentonite content of the compacted soil-bentonite mixtures is increased. Compaction test results have shown that when the bentonite content varies from 0 to 7%, the maximum dry unit weight decreases from 18.90 to 17.86 $kN.m^{-3}$ and the corresponding optimum water content increases from 13 to 15.5%. It is also noticed that the higher the bentonite content, the lower the maximum dry unit weight. Moreover, there is a tendency showing that the higher the bentonite content, the higher the optimum water content, although for mixtures *S03* and *S05* the optimum water contents are alike.

4. As it was expected, the hydraulic conductivity of the soil-bentonite mixtures decreases when the bentonite content is increased. The hydraulic conductivity decreases two to four orders of magnitude when compared to the compacted natural soil. The results have shown that the relationship between the bentonite content and the reduction of the hydraulic conductivity is non-linear.

5. The usual municipal waste standards for compacted soil liners state that the hydraulic conductivity should be less than 10^{-9} $m.s^{-1}$. Therefore, for the studied soil, compacted soil-bentonite mixtures with bentonite content equal or higher than 6% are suitable for constructing liners.

6. Adding bentonite to the natural soil modifies its shear strength parameters. From shear strength test results it can be noticed that there is a tendency showing that the cohesion increases when bentonite content is increased. The addition of bentonite to natural soil causes the friction angle to decrease. However, it cannot be concluded from test results, that the higher the bentonite content, the lower the friction angle.

7. As it was already expected, the unconfined strength of natural soil is higher than the unconfined strength of soil-bentonite mixtures. The mixture with bentonite content of 5% shows higher unconfined strength than the other mixtures.

The laboratory test results of this research leads to the conclusion that the addition of 6% or more of bentonite to the studied lateritic soil makes it suitable for sanitary landfill liners with the purpose of retaining pollutants. However, it must be taken into account that the hydraulic conductivity in the field will be generally higher than that measured in laboratory tests. Likewise, it should be taken into account that the leachate viscosity affects the hydraulic conductivity and the potential interaction of soil-bentonite mixture and leachate.

Acknowledgments

The authors are very thankful to CNPq for the scholarship granted. Furthermore, the authors appreciate the helpful corrections and suggestions of this paper reviewers.

References

ABTN (1984) Solo-Análise Granulométrica. NBR 7181, Rio de Janeiro, 13 pp.

ABTN (1984) Solo-Determinação do Limite de Liquidez. NBR 6459, Rio de Janeiro, 6 pp.

ABTN (1984) Solo-Determinação do Limite de Plasticidade. NBR 7180, Rio de Janeiro, 3 pp.

ABTN (1986) Solo-Ensaio de Compactação. NBR 7182, Rio de Janeiro, 10 pp.

ABNT (2000) Solo- Determinação do Coeficiente de Permeabilidade de Solos Argilosos a Carga Variável. NBR 14545, Rio de Janeiro, 12 pp.

ASTM (1995) Standard Test Method for Consolidated Undrained Triaxial Compression Test for Cohesive Soils. D 4767, West Conshohocken, USA, 13 pp.

ASTM (2001) Standard Test Method for Measurement of Hydraulic Conductivity of Saturated Porous Materials Using a Flexible Wall Permeameter. D 5084, West Conshohocken, USA, 23 pp.

Anderson, S.A. & Hee, B.H. (1995) Hydraulic conductivity of compacted lateritic soil with bentonite admixture. Environmental & Engineering Geoscience, v. 1:3, p. 299-312.

Boscov, M.E.G. (2008) Geotecnia Ambiental. Oficina de Textos, São Paulo, 248 pp.

Chalermyanont, T. & Arrykul, S. (2005) Compacted sand-bentonite mixtures for hydraulic containment liners. Songklanakarin J. Sci. Technol, v. 27:2, p. 314-323.

Daniel, D.E. (1984) Predicting hydraulic conductivity of clay liners. Journal of Geotechnical Engineering, v. 110:2, p. 285-300.

Daniel, D.E. (1989) *In situ* hydraulic conductivity tests for compacted clay. Journal of Geotechnical Engineering, v. 115:9, p. 1205-1226.

Daniel, D.E. (1993) Clay liners. Daniel, D.E. (ed) Geotechnical Pratice for Waste Disposal. Chapter 1. Chapman & Hall, London, pp. 3-14.

Daniel, D.E. & Wu, Y.K. (1993) Compacted clay liners and covers for arid sites. Journal of Geotechnical Engineering, v. 119:2, p. 223-237.

Daniel, D.E. & Koerner, R.M. (1995) Waste Containment Facilities: Guidance for Construction, Quality Assurance and Quality Control of Liner and Cover System. ASCE, New York, 354 pp.

Dixon, D.A.; Graham, J. & Gray, M.N. (1999) Hydraulic conductivity of clays in confined tests under low hydraulic gradients. Canadian Geotechnical Journal, v. 36:5, p. 815-825.

Dourado, K.A. (2003) Condutividade Hidráulica de Materiais de Baixa Permeabilidade: Desenvolvimento, Construção e Teste de um Sistema de Medida. Masters Thesis, Escola de Engenharia de São Carlos, Universidade de São Paulo, São Carlos, 89 pp.

Farnezi, M.K. & Leite, A.L. (2007) Lateritic soil and bentonite mixtures assessment for liner usage purpose. Soils & Rocks International Journal of Geotechnical and Geoenvironmental Engineering, v. 30:2, p. 103-112.

Ferrari, A.A.P. (2005) Viabilidade da Utilização de Silte Compactado como Material de Impermeabilização em Aterros de Resíduos. Masters Thesis, Escola Politécnica, Universidade de São Paulo, São Paulo.

Gleason, N.H.; Daniel, D.E. & Eykholt, G.R. (1997) Calcium and sodium bentonite for hydraulic containment applications. Journal of Geotechnical and Geoenvironmental Engineering, v. 123:5, p. 438-445.

Gouveia Filho, P.P.F. (2006) Active layers for soil impermeability. Personal Communication.

Head, K. (1986) Manual of Soil Laboratory Testing. Pentech Press, London, v. 3, 712 pp.

Hoeks, J.; Glas, H.; Hofkamp, J. & Ryhiner, A.H. (1987) Bentonite liners for isolation of waste disposal sites. Waste Management & Research, v. 5:1, p. 93-105.

Khera, R.P. (1995) Calcium bentonite, cement slag and fly ash as slurry wall material. Proc. Geoenvironment 2000: Characterization, Containment, Remediation and Performance in Environmental Geotechnics, v. 1:46, p. 1237-1249.

Kumar, S. & Yong, W.L. (2002) Effect of bentonite on compacted clay landfill barriers. Soil and Sediment Contamination, v. 11:1, p. 71-89.

Lukiantchuki, J.A. (2007) Influência do Teor de Bentonita na Condutividade Hidráulica e na Resistência ao Cisalhamento de um Solo Arenoso Utilizado como Barreira Impermeabilizante. Masters Thesis, Escola de Engenharia de São Carlos, Universidade de São Paulo, São Carlos, 124 pp.

Magistris, F.S.; Silvestri, F. & Vinale, F. (1998) Physical and mechanical properties of a compacted silty sand with low bentonite fraction. Canadian Geotechnical Journal, v. 35:6, p. 909-925.

McBean, E.A.; Rovers, F.A. & Farquhar, G.J. (1995) Solid Waste Landfill Engineering and Design. Prentice Hall, New Jersey, 521 pp.

Mollins, L.H.; Stewart, D.I. & Cousens, T.W. (1996) Predicting the properties of bentonite-sand mixtures. Clay Minerals, v. 31:2, p. 243-252.

Rowe, R.K.; Quigley, R.M.; Brachman, R.W.I. & Booker, J.R. (2004) Barriers Systems for Waste Disposal Facilities. Spon Press, London, 587 pp.

Rowe, R.K. (2001) Barrier systems. Rowe, R.K. (ed) Geotechnical and Geoenvironmental Engineering Handbook. Chapter 25. Kluwer Academic Publishing, Norwell, pp. 739-788.

Sivapullaiah, P.V.; Sridharan, A. & Stalin, V.K. (2000) Hydraulic conductivity of bentonite-sand mixtures. Canadian Geotechnical Journal, v. 37:2, p. 406-413.

Tripathi, K.K. & Viswanadham, B.V.S. (2005) Ascertainment of bentonite content for sand-bentonite liners. Proc. 10th International Waste Management and Landfill Symposium, Sardinia.

Symbols

G_s: specific gravity
w_L: liquid limit
w_P: plastic limit
I_P: plasticity index
Δu: pore-pressure variation
$\Delta\sigma_3$: confining pressure variation
B: Pore-pressure parameter
a: capillary tube cross section area
A: mercury container cross section area
γ_{Hg}: mercury unit weight
γ_w: water unit weight
$D_{máx}$: maximum grain diameter
C_U: uniformity coefficient
C_C: coefficient of gradation
CEC: cation exchange capacity
SS: specific surface
CA: clay activity
L: specimen height
S: specimen cross section area
Y_i and Y_{i+1}: mercury column height at instants t_i and t_{i+1}

Δt: elapsed time between the readings of Y_i and Y_{i+1}.
k: hydraulic conductivity
$\gamma_{dmáx}$: maximum dry unit weight
w_{op}: optimum water content
S00: natural soil
S03: sample with 3% of bentonite (dry weight basis)
S05: sample with 5% of bentonite (dry weight basis)
S07: sample with 7% of bentonite (dry weight basis)
S09: sample with 9% of bentonite (dry weight basis)
ϕ: total friction angle
ϕ': effective friction angle
c: total cohesion
c': effective cohesion
RC: relative compaction
UCS: unconfined compression strength

Numerical Assessment of an Imperfect Pile Group with Defective Pile both at Initial and Reinforced Conditions

Renato P. Cunha, Ary F.B. Cordeiro, Maurício M.M. Sales

Abstract. The assessment of problems of imperfect, damaged, pile groups is scarce in the geotechnical literature. Besides, techniques of assessing the performance of the foundation system once a defect is found are seldom presented, as well as real examples of the behavior of large scale imperfect foundations after their remediation. Therefore, this paper has extended the design philosophy of "piled raft" foundations to predict the numerical behavior of imperfect pile group foundations at pre and post-remediated conditions. Focus will be given to the problem of groups with either defective shorter length or lower stiffness piles, caused by natural or man-made sources. The remediation of the group is considered via added reinforcement piles with either similar or dissimilar characteristics (length, diameter, stiffness) compared to the original undamaged piles. Although the results are limited, they allow preliminary generalizations of the overall group behavior at working conditions, once a pile flaw is noticed and after the remediation has taken place. Among other results the paper highlights the load sharing mechanism between foundation elements, which relates to the position and magnitude of damage of the defective pile, as well as to the overall characteristics of reinforcement one. It was concluded that a defect caused by an unwanted pile length variation can be more detrimental to the foundation system than an unexpected low structural stiffness for the constructed pile. The derived factor of safety (SF) of the system (overall value) and of its distinct components (individual values) are also influenced by aforementioned variables, leading to questions on how the reinforcement can be made in such manner to obtain well optimized SFs. As noticed throughout the analyses, defective piles share its load with system components, once a defect appears. Nevertheless, even when imperfect such piles continue to absorb some load, although to a lesser degree than the original value. The reinforcement piles tend to absorb (or retain) some of the load spread by the defective ones, in a proportion which depends to its general characteristics (size, position, stiffness). Again, questions about an optimization procedure have to be made in order to wisely and economically use this particular observed feature on the remediation design.
Keywords: defective pile, imperfect pile group, remediation, numerical analysis, piled raft.

1. Introduction

The design of deep foundations underneath high-rise buildings or bridges almost invariably assumes that most, if not all, of the piles are of the same characteristics (length, diameter, stiffness) and constructed without structural or geotechnical imperfections (defects).

Such hypotheses may be valid for many constructions, although quality control of the executed pile is rarely undertaken on conventional works, with exception of some special pile types, as continuous flight augers with their instrumented insertion procedures. Therefore, it may be possible to find, in many pile groups, piles of different lengths or even piles with defects arising from careless construction techniques.

Once the defect, or imperfection of the pile, is found, it is necessary to assess the possible performance of the overall foundation system, to see if it will continue (or not) to be favorable in regard to initial design considerations. Otherwise, some sort of remedial action may be required, such as the insertion of reinforcement piles combined with a geometrical change of the top raft (cap) of the imperfect pile group. Of course geometrical changes of the group would be feasible only if the imperfection could be found out at early stages of the construction, when the loading of the foundation is not at its upmost value.

Given the fact that, according to Janda *et al.* (2009), the term "piled raft" is generally expressed (and was defined in this publication) as a "foundation system in which both structural components (piles and top raft) interact with each other and with the surrounding soil to sustain vertical, horizontal or moment loads coming from supported superstructures", one should realize that any imperfect foundation group with defective(s) pile(s) will behave as a "piled raft". That means, the system will share load in between its elements (raft, piles, surrounding soil) due to an uneven performance of the good quality and the defective pile(s) in the same foundation system. In other words, interaction between dissimilar piles and the raft will unavoidably take place. Therefore, the analysis of pile groups with defective pile(s) is a special analysis of a piled raft system, in which one or more piles have special distinct characteristics, such as length, diameter or stiffness.

Similarly, the remediation of the imperfect group by the insertion of similar or dissimilar piles can also be a

Renato Pinto da Cunha, Ph.D, Professor Associado 2, Departamento de Engenharia Civil e Ambiental, Universidade de Brasília, Brasília, DF, Brazil. e-mail: rpcunha@unb.br.
Ary Franck Baia Cordeiro, M.Sc., Departamento de Engenharia Civil e Ambiental, Universidade de Brasília, Brasília, DF, Brazil. e-mail: aryfranck@gmail.com.
Maurício Martines Sales, Doutor, Professor Adjunto 3, Escola de Engenharia Civil, Universidade Federal de Goiás, Goiania, GO, Brazil. e-mail: sales.mauricio@gmail.com.
Submitted on April 13, 2009; Final Acceptance on October 29, 2009; Discussion open until December 31, 2010.

problem related to the behavior of a piled raft system, especially if it can be assumed that the reinforcement piles (and geometry change) are considered in the beginning of the loading process, thus compatible with the fact that the imperfection was detected at an early work stage.

The motivation of this particular (piled raft) analyses and discussion comes from the fact that the assessment of problems of imperfect pile groups is scarce in specialized publications and, not rarely, is hidden to practitioners/researchers under confidentiality or commercial non publication clauses. Few publications deal with this topic, particularly related to site behavior of pile groups with defective pile(s) of distinct categories (shorter length, lower stiffness, structural damages, and so on), and their performance once some sort of remediation is put in place. Also, techniques of assessing the performance of the foundation system, either analytically or numerically, are seldom presented in technical literature, as well as successful examples of large scale reinforced foundations.

In this regard, and from the publications available to the authors, one may refer to Lizzi (1982), Sales & Costa (1996), Poulos (1997, 1999, 2005 and 2009), Gotlieb & Gusmão Filho (1999), Ferreira *et al.* (2000), Lima & Costa Filho (2000), Knigmuller & Kirsch (2004), Milititsky *et al.* (2005), Ziccareli & Valori (2006) and Cordeiro *et al.* (2008a, b) to read more about imperfect pile groups and possible reinforcement systems. Note that, with exception of some of Poulos papers, none of them present in a clear manner the analytical approach used for the insertion of additional piles, *i.e.*, how calculations and decisions were made as well as field performance of the reinforced group(s).

This paper will therefore focus on the problem of defective pile groups with either (a) shorter length or (b) lower stiffness piles, caused by natural or man-made imperfections. It will detail the conventional numerical methodology to forecast the behavior of traditional piled raft groups, and how this methodology can be used to perform parametric analyses of hypothetical post-reinforced cases. That means, pile groups in which the remediation was carried out at early stages of construction work, hence where it was possible to implement a geometrical increment of the top raft combined with the insertion of a reinforcement pile to substitute the defective one. It needed to be considered as an "insertion" at initial stages of loading due to limitations of the adopted numerical tool.

The reinforcement pile was considered either with similar or dissimilar characteristics (length, diameter, stiffness) as the original undamaged piles of the group.

The paper will present all the parametric analyses for a particular case in study derived by a M.Sc. recently defended in this area (Cordeiro, 2007). Although a unique example is shown, due to paper size limitations, the discussion and conclusions apply for other hypothetical cases of similar characteristics.

2. Concepts On Imperfect Pile Groups

According to Poulos (2005) in his state of the art (40th Terzaghi Lecture) the imperfections that may have impact on pile foundation performance may arise from a number of sources, including natural and construction aspects, inadequate ground investigation, pile load testing, and loading during operation.

In terms of natural sources, the dissimilar piles arise from the existence of layers that are not horizontal or continuous, or from undetected boulders within a soil layer, from sloping bedrock, intrusions of rock over limited areas of the site, from cavities in limestone rock, or simply by the presence of softer layers below what might be regarded as suitable founding strata for the piles. These aspects are shown in Fig. 1.

On the other hand, construction related imperfections arise from processes inherently linked to execution aspects of the piles, *i.e.*, either from inadequate field quality control or from inevitable consequences of construction (man made) activities, as for instance: (a) soft base on bored piles due to inadequate base cleaning; (b) necking or other defects within the shaft of piles; (c) inadequate forecast of the real founding conditions; (d) lack of proper base inspection in manually excavated foundations; (d) ground movements developed due to drilling, or construction activities (dewatering, excavations, surficial loading) during pile execution; (e) careless use of some intrinsically related technologies to particular piles, as excessive driving, poor quality bentonite mud, etc.

So, according to Poulos (2005) the construction-related imperfections in piles can be broadly classified into

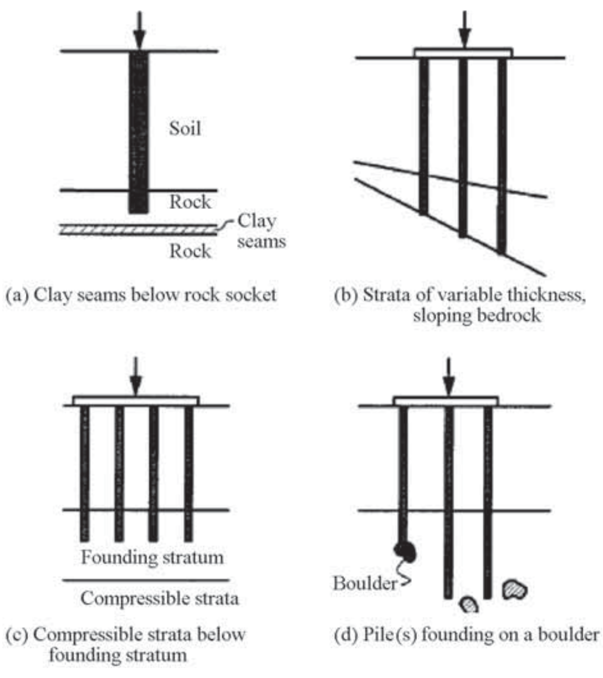

Figure 1 - Examples of imperfections by natural sources (after Poulos, 2005).

two main categories, which are related either to structural defects or to geotechnical ones. For instance, structural defects can result in dissimilar size, strength, and/or stiffness for some piles, being therefore of distinctive characteristics compared to others in the same group, or as initially assumed in design. Geotechnical defects usually arise from either a poor assessment of the in situ conditions during design and construction, or else from construction related problems, and may result in dissimilar piles with distinctive (reduced) shaft friction and end bearing resistance from others of the same group, or with different operational conditions as initially forecasted by designers. These aspects are visualized in Fig. 2.

Hence, according to Poulos (2005) the imperfections that have impact on pile foundation performance may arise from a number of sources, including natural sources, inadequate ground investigation, construction, pile load testing, and loading during operation.

Based on a history of problems noticed by the authors in foundation sites for conventional residential and commercial buildings within the respective areas of their (academic and technical) interactions, it can be said that most of the detected problems are indistinctively related to both natural and construction sources. In fact, many of the problems appear to be related to shorter than designed piles, due to natural sources (boulders, hard strata), man-made construction mistakes, or structural defects (as necking). In many cases where necking appears to exist (via post execution pile integrity tests), it may be possible to consider the tested pile of dissimilar characteristics in relation to others of the same group, with a shorter length valid up to the point where the potential necking is detected. Moreover, in a particular case of knowledge by some of the authors, geotechnical related problems made necessary the overall reinforcement of a building simply by the fact that the piles were not properly founded on competent strata (hence, with lower than forecasted end bearing).

Therefore, the paper will focus on piles with dissimilar characteristics which are related to either shorter length

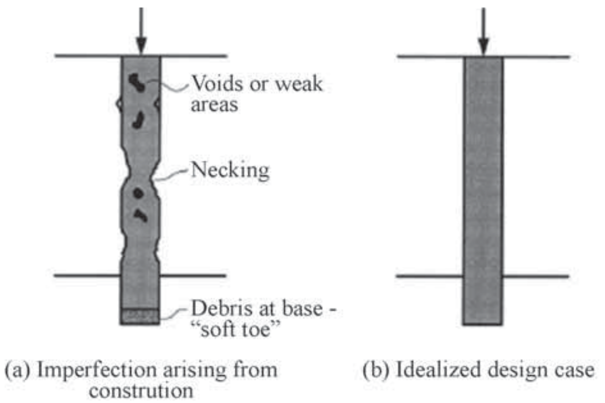

Figure 2 - Examples of imperfections by construction aspects (after Poulos, 2005).

or lower stiffness than others of the same group, as according to local experience this seems to be the major problem found on imperfect pile groups of the region. Besides, only hypothetical cases of reinforcement are presented, given the lack of good examples, or, better, unclassified examples where one could openly apply the numerical technology to be described herein.

3. Numerical Methodology

A specific numerical program was adopted in order to handle the simulations with all requirements for the analyses, in which one could take on account all (or most) of the aforementioned imperfections listed for typical defective piles. In particular, the analyses would need to handle some key aspects of the problem, as already mentioned by Poulos (2005):

• Heterogeneous or different soil profiles along the piles of the same group;

• Piles of different length or diameter within the same group, including consideration of interaction among dissimilar piles;

• Piles containing structural defects or changes in diameter or size along the length;

• Piles that would be activated part-way through the loading process to simulate the installation of reinforcement piles;

• Vertical loadings to be imposed from ground movements, as well as from normal structural loadings; and

• Piles with nonlinear shaft-soil response, and also nonlinear structural behavior.

From the available programs, the software GARP7 (*Geotechnical Analysis of Raft with Piles*; Poulos and Small 1998, modified by Sales, 2000) was adopted by Cordeiro (2007) in his Thesis to evaluate the behavior of the several imperfect pile groups with defective piles, some of them presented herein. This program is based on a simplified form of boundary element program in which the raft is represented as a linear elastic plate and the soil can be modeled either as an elastic layered continuum or as a Winkler spring medium. The piles are represented by elastic-plastic springs that can interact with each other and with the raft. Limiting values of contact pressure (beneath the raft) and pile capacity (shaft friction plus tip end bearing) can also be specified, and the raft is analyzed using the finite element technique, rather than via finite differences.

This particular software has already been used under another study (Cunha *et al.* 2001) for the analyses of standard piled raft groups, and has proved to be preferable to be used as the initial step for an academic study of this particular topic, given its high degree of approximation, simplicity and speed for usage, and facility to be adapted for carrying out parametric studies as well as solving real-world problems.

This opinion is also similar to that of Poulos (2005) in his state of art Report, who states that more complex (3D finite element – FEM) programs may take on account most, or eventually all, of the important aspects inherently related to defective pile studies, but "at the expense of a relative greater amount of time involved in setting up and modifying distinct meshes, plus the general difficulties of discerning broad patterns of behavior from the parametric studies".

On the other hand, GARP7 can effectively and quickly simulate defective pile groups with most of the aforementioned requirements, as nonlinear pile-soil response, dissimilar piles with distinctive length, diameter and stiffness in the same group, or heterogeneous soils profiles.

However, the activation of reinforcement piles at any stage of the loading process (or once the defect is more noticeable) is not possible, which has turned the analyses to be valid solely for post-reinforced systems in which the remediation was carried out at early stages of construction work and (vertical) loading. Nevertheless, an ongoing D.Sc. Thesis is presently underway to cover for reinforcement groups at distinct levels of the loading stage (using a more refined 3D FEM software – LCPC Cesar).

GARP7 considers "interaction factors" between the springs that represent the piles of similar or dissimilar characteristics. Such factors are computed via the use of another well-established software program called DEFPIG (*Deformation Analysis of Pile Groups*; Poulos, 1990). It was originally written for a group of identical elastic piles having axial and lateral stiffness that are constant with depth. However, it also allows for the eventual slippage between the piles and the surrounding soil, and it can take into account the effects of soil non-homogeneity along the length of the pile. The stress distributions are computed from the theory of elasticity, more specifically from Mindlin's solutions for an isotropic, homogeneous, linear elastic medium.

The first stage of the DEFPIG analyses is the evaluation of the interaction factors, by using a two pile (pile to pile) integration approach via Mindlins theoretical equations. GARP program then evaluates other factors (raft to raft, pile to raft) based on Boussinesqs equations and a fraction of aforementioned obtained (pile to pile) values. In sequence it constructs the matrices of interaction factors for the specified group (pile to pile, pile to raft and raft to raft) and moves towards the assessment of the computed stresses in each of the system components (pile, raft and soil elements).

GARP program uses two methodologies to determine the interaction factors, namely those from Randolph (1985) and from Poulos (1988). The main difference between them is the fact that the former adopts non homogeneity for the soil along the pile length whereas the latter employs a homogeneous soil condition throughout the length. Cordeiro (2007) has demonstrated that both methodologies yield slightly different answers in terms of non dimensional charts of the interaction factors *versus* pile spacing over diameter (S/D) of the piles when related to some of the system variables, as the relation of deformable strata over pile length (H/L). Given this particular aspect, it was suggested by Cordeiro (2007), and adopted herein, Randolph's methodology since it has proven to lead to a more uniform output of results. Nevertheless, as already pointed out elsewhere, this is an open point which still requires further validation – especially for Brazilian non classical (tropical) soil conditions.

In the present series of studies the following characteristics for the simulated groups were adopted:

• A linear elastic flexible 60 cm thick initial rectangular raft (2.3 x 3.8 m) , with 6 piles of 50 cm diameter (D) and 10 m of length (L_p) equally spaced 3D apart;

• Linear elastic piles with either similar (length, diameter and stiffness) or dissimilar characteristics;

• Linear elastic, isotropic, horizontally semi-infinite soil medium, free from adjacent loadings or interferences, with a thickness of 20 m up to the rigid base (2 times the similar pile length);

• Defects related to either distinct length or stiffness for the defective (dissimilar) pile. The variation of pile length simulates broken joints, necking or geotechnical aspects (boulders, etc.), whereas the variation of the structural stiffness denotes man-made construction problems (as pile molding, concrete quality, etc.) that could generate imperfect piles;

• Remediation related to reinforcement piles of either similar characteristics of the original pile group or dissimilar characteristics (50% of length, diameter, or stiffness of original piles). The remediation was simulated by four hypothetical scenarios, each one with a unique reinforcement pile located at an enlarged position of the original raft;

• Vertical constant load level equivalent to the work condition of the original similar pile group (4.6 MN applied at the geometrical center of the raft). This value leads to an overall geotechnical factor of safety for the group equal to 2 - level where the effect of a defective pile is simulated. The remediation is also simulated at this level, but considering that the reinforcement pile was incorporated at an early stage of pile group construction, and load was carried out up to the work level;

• Results in terms of load sharing and distribution, raft moment and displacement, pile reaction, and individual pile, and overall group, safety factor are presented for pre and post-reinforcement scenarios.

The stiffness (K = load/settlement) of each structural pile element of the foundation system was determined with the use of the program DEFPIG, assuming soil conditions and pile geometry in accordance to each analysis (to be presented next). For each particular condition that was analyzed, for instance for the cases with shorter length or variable Young modulus, this program has calculated and given distinct stiffness values K, used in following GARP analyses. Hence, by doing so, the defective pile was simulated with a different K value as those of the original intact piles, and the reinforcement pile had similar or distinct characteristics as those of the original piles, depending on the remediation conditions (similar or dissimilar piles). Constant K values were respectively adopted for undamaged and defective piles since the load-settlement curves were assumed as linear elastic.

Having said that, the adopted values are given as follows:

• K of intact pile equals to reinforcement pile ("similar" pile case) = 192678 kN/m;

• K of defective pile equals to reinforcement pile ("dissimilar" pile case) = distinct for each case of shorter length L or lower modulus E:

a. 80%L: $K_{80\%L}$ = 187969 kN/m;
b. 50%L: $K_{50\%L}$ = 153609 kN/m;
c. 30%L: $K_{30\%L}$ = 71942 kN/m;
d. 80%E: $K_{80\%E}$ = 175746 kN/m;
e. 50%E: $K_{50\%E}$ = 143266 kN/m;
f. 30%E: $K_{30\%E}$ = 113895 kN/m;

4. Parametric Analyses

Based on previous descriptions, Fig. 3 introduces a perspective, cross section and upper view of the original group of similar piles studied herein, whereas Table 1 presents some of the variables depicted in Fig. 3.

The following charts show the behavior of the raft in the AA cross section, *i.e.*, central section of the raft. The paper has adopted settlements in form of normalized displacements to a vertical constant load level, which is equivalent to the working conditions of the original similar pile group.

4.1. Initial conditions of the imperfect group

The behavior of the original (perfect) model group once an imperfection (defective pile) is imposed was studied at mid width of the raft, *i.e.*, at the (AA) cross section depicted in Fig. 3 which passes through its geometrical center. For that, a particular section of the finite element mesh was considered at this position.

Table 1 - Variables for group of similar piles.

Variable/symbol	Value
Raft length (L)	3.8 m
Raft width (B)	2.3 m
Load column side (a)	0.5 m
Pile distance (d)	1.5 m
Young modulus of raft (E_{raft})	20 GPa
Poisson of raft (ν_{raft})	0.2
Young modulus of pile (E_p)	20 GPa
Poisson of pile (ν_p)	0.2
Young modulus of soil (E_s)	50 MPa
Poisson of soil (ν_s)	0.3

Also in this same figure, it is possible to notice the denomination (numbering) of the similar piles. For the purpose of this paper, piles number 1 and 3 are those which will be simulated (non simultaneously) as defective in the following analyses.

Figure 4 (a) and (b) presents the normalized displacement behavior (ρ is the vertical settlement at each point) along the raft length for an imperfection respectively on pile 1 (P1) and pile 3 (P3). For each defective pile, a simulation was made on its length (80, 50 and 30% of the original length of the similar piles) and on its Young modulus (80, 50 and 30% of the original value of the similar piles).

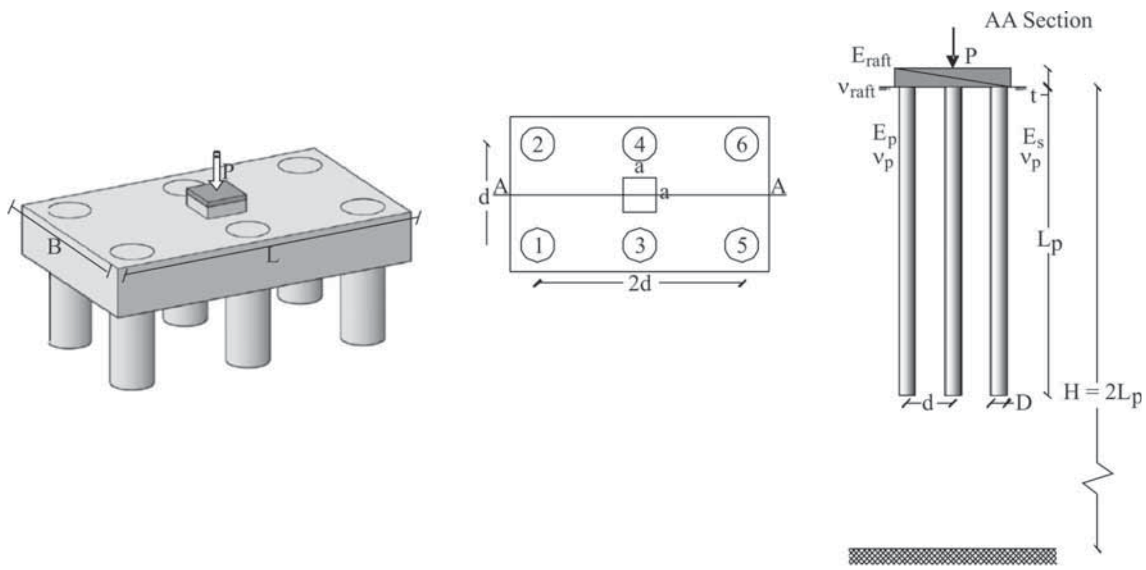

Figure 3 - General characteristics of the original group of similar piles.

Figure 5 (a) and (b) presents similar set of analyses for the raft moment generated along its length. In both cases, the "perfect group" condition refers to the original case, where the group of similar piles is loaded without any sort of imperfection.

From these initial set of results, one may notice that:

• A pile defect caused by a variation on its length is more influential on the raft settlement and moment than a proportional defect caused by a variation on the pile stiffness;

• A distinct position for the defective pile generates a slightly different pattern of observed results for both normalized settlement and moment of the imperfect pile group. It also changes the percentage difference of either normalized settlement or moment when it is generated by a length versus a stiffness defect. For instance, for a defect on pile 1, and for the highest level of defect (30%), the results in terms of normalized settlement can vary to up 25% depending on the defect type (length or stiffness). On the other hand, if the same defect is on pile 3, such maximum percentage difference drops to around 5%. The percentage difference is also variable along the raft's length;

• For any case of imperfect pile group, the normalized settlement is more influenced by the defect than the raft moment. For instance, for a defect on the length of pile 1, and for the highest level of defect (30%), the normalized settlement can be up to 45% higher than the equivalent value for the original (perfect) group. On the other hand, on similar conditions, the maximum difference of moments drops to 10%;

• Also for any case, the imperfect pile group attains higher values of normalized settlement and moment than equivalent ones of the original perfect group. For the particular cases of P1, the imperfection not only causes a higher settlement, but also starts to tilt the raft towards the position of the defective pile.

Figure 6 and Table 2 respectively present the reactions and the safety factor (SF) for the imperfect pile group once the defect is located on pile 1, whereas Fig. 7 and Table 3 present similar results valid for a defect on pile 3. The SF is expressed in terms of (a) individual values for each of the piles, *i.e.*, the amount of individual bearing capacity divided by the load they receive at working conditions; and (b) the overall value for the whole group, *i.e.*, the amount of bearing capacity of the raft plus all piles divided by the working load.

It should be noted that such definition of overall safety factor was adopted for simplicity reasons, given the fact that a cross comparison of results was the main objective here. It is known that a more refined definition for piled rafts could be adopted (Sanctis and Mandolini, 2006).

Tables 2 and 3 are also divided, line by line, on the level (severity) of group imperfection. The first line refers to original (perfect) group conditions, where all piles are operative and similar, while the last one refers to a fully defective condition for either piles 1 or 3, *i.e.*, assuming that they simply do not exist. Imperfections related to a distinct length or stiffness for the defective dissimilar pile are also presented.

From these results, one may notice that:

• At perfect conditions the overall safety factor is 2, whereas individual factors for each pile vary from ~1.5 to 2.5. Such variation is normal, given the fact that the raft is not perfectly flexible and readjusts itself to the applied load,

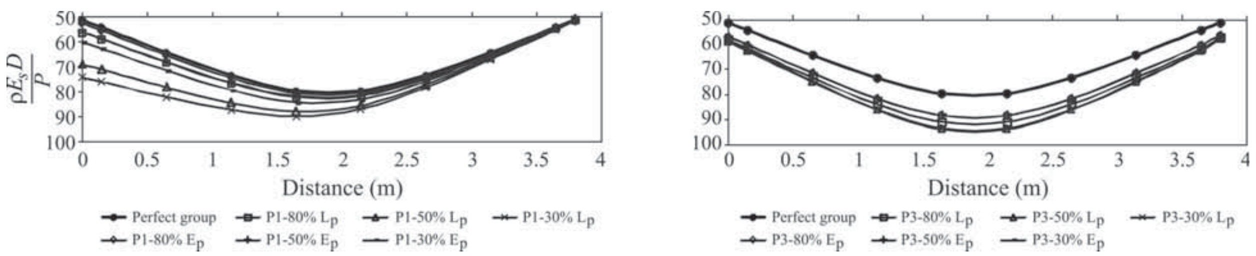

Figure 4 - Group behavior in terms of normalized vertical settlement for imperfection on (a) pile 1 and (b) pile 3.

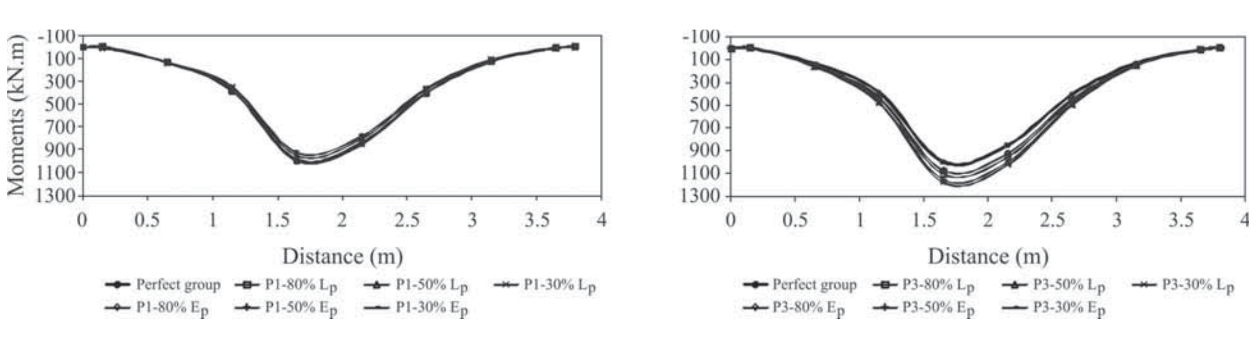

Figure 5 - Group behavior in terms of raft moment for imperfection on (a) pile 1 and (b) pile 3.

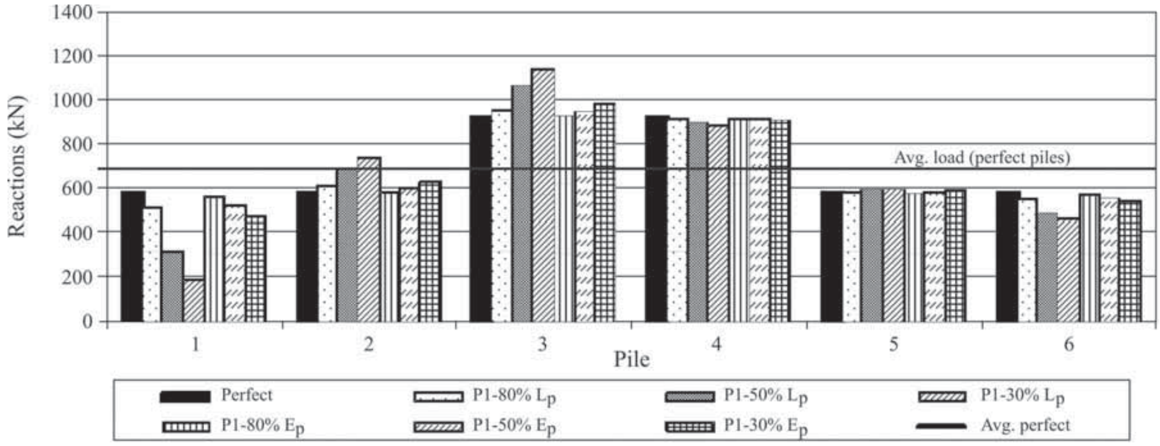

Figure 6 - Generated pile loads for imperfection on pile 1.

Table 2 - SF for imperfection on pile 1.

Damage level	Pile 1 (defective)	Pile 2	Pile 3	Pile 4	Pile 5	Pile 6	Overall SF
Perfect group	2.50	2.50	1.57	1.57	2.50	2.50	2.00
80% Lp	1.00	2.39	1.51	1.58	2.49	2.61	1.80
80% Ep	2.58	2.48	1.55	1.57	2.50	2.53	2.00
50% Lp	1.00	2.11	1.36	1.61	2.43	2.97	1.75
50% Ep	2.77	2.40	1.52	1.58	2.49	2.59	2.00
30% Lp	1.00	1.96	1.26	1.64	2.42	3.16	1.73
30% Ep	3.06	2.32	1.48	1.58	2.46	2.67	2.00
Fully damaged	-	1.78	1.16	1.64	2.37	3.47	1.69

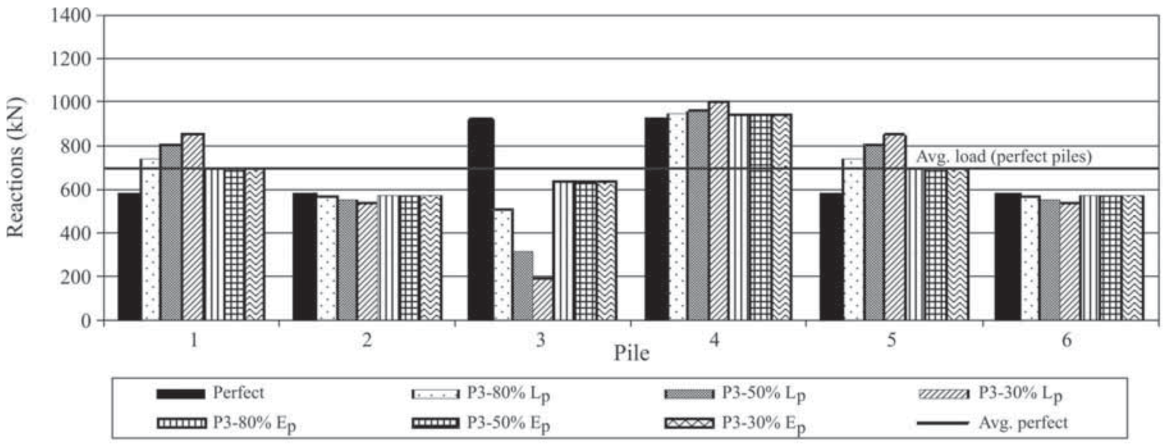

Figure 7 - Generated pile loads for imperfection on pile 3.

differently spreading it through the piles. Notice that piles 3 and 4 are those in the lower limit of SF, by their closer proximity to the column load. Such behavioral contrast between piles 3,4 and 1,2,5,6 will hold for all studied cases;

• For the case of imperfection caused by pile length variation it can be seen that the overall SF tends to decrease as the severity of the defect increases. At worst (fully damaged) conditions, the SF drops to values in the range of 1.7.

Table 3 - SF for imperfection on pile 3.

Damage level	Pile 1	Pile 2	Pile 3 (defective)	Pile 4	Pile 5	Pile 6	Overall SF
Perfect group	2.50	2.50	1.57	1.57	2.50	2.50	2.00
80% Lp	1.96	2.55	1.00	1.52	1.96	2.55	1.80
80% Ep	2.10	2.53	2.27	1.54	2.10	2.53	2.00
50% Lp	1.78	2.60	1.00	1.50	1.78	2.60	1.75
50% Ep	2.10	2.53	2.27	1.54	2.10	2.53	2.00
30% Lp	1.69	2.69	1.00	1.45	1.69	2.69	1.73
30% Ep	2.10	2.53	2.27	1.54	2.10	2.53	2.00
Fully damaged	1.57	2.68	-	1.39	1.57	2.68	1.69

Moreover, in terms of individual SF for each of the piles, independently on the defect position (pile 1 or 3), the individual SF caused by a variation on the pile length may, or may not, lead to lower individual SF than those caused by the stiffness variation. For instance, this can be noticed for pile 4 results in both tables;

• Although the overall SF is the same (at a particular imperfect condition) for both studied positions of the defective pile, individual factors for the piles vary considerably from one to another condition. Notice, for instance, that even defective, piles 1 and 3 continue to absorb load from the general distribution between raft and piles. But a defect (of any type) on pile 3 always leads this pile to lower individual SF than equivalent ones from pile 1. This is so given its aforementioned position in the raft, closer to the center of loading;

• Once a defect is imposed, for any of the imperfect group conditions, there is a transfer of load from the defective (dissimilar) pile to the similar ones of the group. The amount of load spread depends on the severity of the damage and leads to an increase of load (and reduction of SF) for some of the non-defective piles. For instance, for a defect on pile 1 the load is mainly spread to piles 2 and 3, while for a defect on pile 3 this same load is mainly spread to piles 1 and 5 and to a lesser degree to pile 4;

• It is also clear that the transference of load not only occurs from the defective pile to similar non-defective ones, but also from similar to similar piles. For instance, in any of the cases of defective pile 1, some load is spread from pile 6 to adjacent ones, leading to a decrease of load in this pile and correspondent increase of its individual SF. This happens due to aforementioned tilting of the raft towards the position of the defective pile.

Finally, Fig. 8 presents the load distribution for each of the studied cases of imperfect group, at both conditions of variable pile length and stiffness. The figure depicts the percentage value absorbed by the raft in all conditions, including the original perfect case.

From this one, it is clear that a pile defect caused by a variation on its length is more influential on the raft load than a proportional defect caused by a variation on the pile stiffness. As the severity of the defect increases, more load is gradually transferred from the piles to the raft.

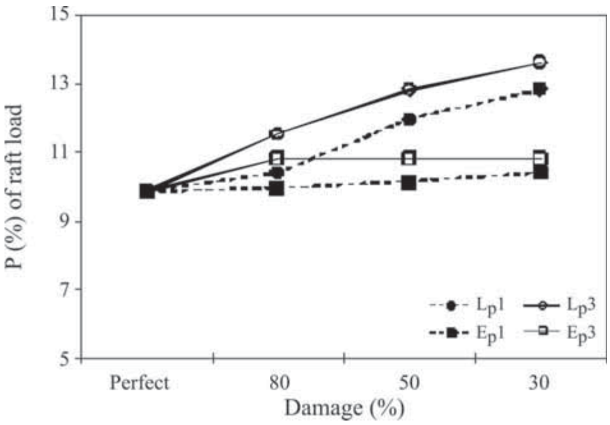

Figure 8 - Load distribution for imperfection on pile 1. (L_p1, E_p1) and pile 3 (L_p3, E_p3).

Although the transference was small (maximum of 4% of working load), it definitively indicates a tendency of load transfer towards the raft in imperfect pile groups, transfer which may be of considerable amount in other rather more severe cases.

4.2. Post-reinforced conditions of the imperfect group

This section introduces the parametric analysis of the remediation of the imperfect group, by the insertion of a similar or dissimilar pile at a particular distance from the defective one.

In order to simplify the analysis, a few basic considerations were adopted, as:

• Just one defective pile was considered, in a fully defective condition, *i.e.* assuming that it simply did not exist at the reinforced case. This is a common assumption adopted in the remediation design of similar imperfect groups. For the analysis, pile 1 was chosen as the defective one, due to the more severe conditions imposed on the group, as noted before;

• Just one reinforcement pile was considered, located close to the defective one, in the region of the raft potentially subjected to more damage. It was assumed that the reinforcement was carried out by a previous geometry change of the raft, in the beginning of the process. Although it changes the geometrical and loading center, this is exactly what is done in some practical cases;

• The reinforcement pile was considered either with similar or dissimilar characteristics (length, diameter, stiffness) compared to the original undamaged piles of the group. This is also normally considered on remediation jobs of this type.

Figure 9 presents the general view of the four remediation cases considered herein, namely cases 1 to 4, respectively related to reinforcement piles R1 to R4. The equivalent distance to the defective pile, and cross section AA, are also depicted. The results will be shown in relation to this particular raft section.

4.2.1. Remediation with similar pile

Figures 10 and 11 respectively present the results in terms of normalized vertical settlement and moment generated along the raft length, for all cases of reinforcement. The perfect original (undamaged) condition and the fully damaged one (unreinforced case) are also depicted.

In this particular series of analyses the remediation was considered to have taken place solely with a similar reinforcement pile, *i.e.*, with the same length, diameter and stiffness as the original piles of the group.

From this series of results one may notice that:

• Once fully damaged, the pile group behaves very distinctively from the original condition in terms of normalized settlements. Nevertheless, in terms of generated moments, there are few numerical differences between the results at both conditions;

• All remediation cases improve the behavior of the reinforced raft in terms of normalized settlement, *i.e.*, decreasing the values along the studied section. By considering the average pattern all along original and extended raft, it appears that remediation cases 2 and 4 are more effective than cases 1 and 3, although with small differences.

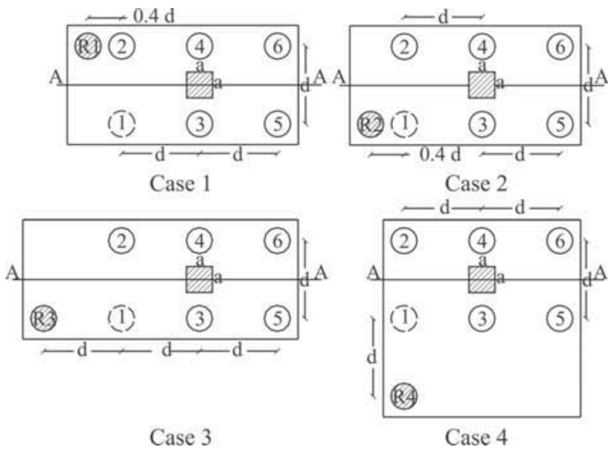

Figure 9 - General characteristics of the distinct cases of group remediation.

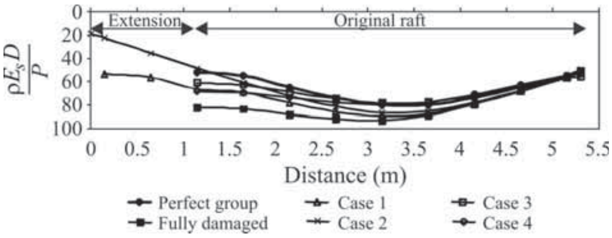

Figure 10 - Group behavior in terms of normalized vertical settlement for a similar reinforcement pile.

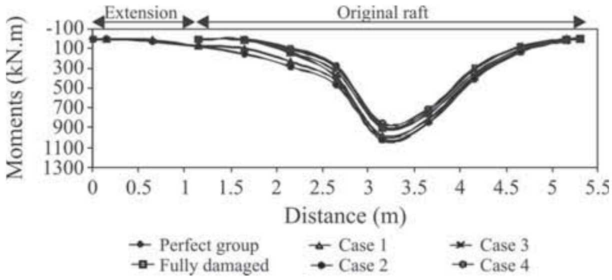

Figure 11 - Group behavior in terms of raft moments for a similar reinforcement pile.

• Contrary to what was initially expected, all remediation cases slightly aggravate the behavior in terms of moments, increasing them in relation to original (and fully damaged) conditions. The moment pattern is similar for all considered cases, and is largely influenced by the change on the raft's geometrical center and average flexibility once the reinforcement is imposed. From the studied conditions, and with minor differences, it appears that cases 3 and 4 are preferable to 1 and 2;

Figure 12 and Table 4 respectively present the reactions and the safety factors for all considered conditions, *i.e.*, perfect original, fully damaged and reinforced group.

Table 4, in particular, presents individual safety factors for each of the original and reinforcement piles, as well as the overall SF of the group for all considered cases. The overall SF considered the enlarged condition of the raft plus the contribution of the reinforcement pile, at each remediation case.

From these results, one may notice that:

• The overall SF has increased to acceptable values (> 2) in all reinforcement cases, reaching original pre-defect conditions. However, as for the imperfect group, there is a natural variation of individual factors for each pile. This variation holds for all cases, and, as before, piles 3 and 4 continue to be those in the lower limit of SF;

• Once reinforced, the group returns to a more uniform condition when compared to the fully damaged case. In the latter case, given the absence of one of the piles and

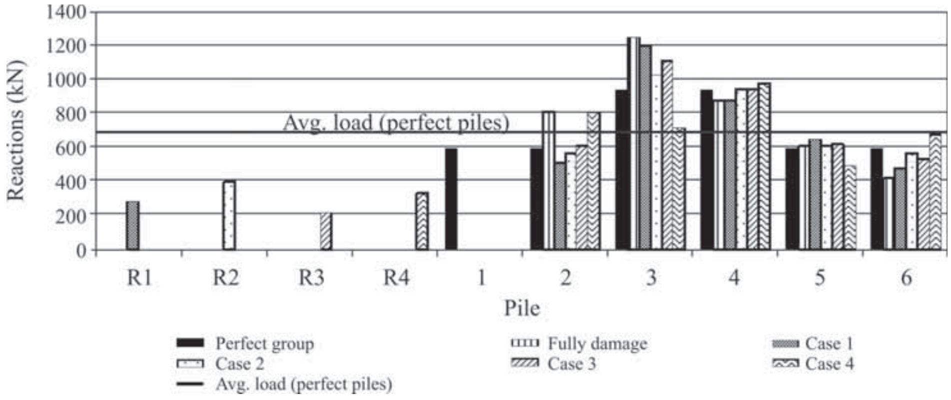

Figure 12 - Generated pile loads for all reinforced cases.

Table 4 - SF for reinforced cases of similar pile.

Pile	Perfect group	Fully damaged	Reinforcement type			
			Case 1	Case 2	Case 3	Case 4
R1	-	-	5.23	-		-
R2	-	-	-	3.67	-	-
R3	-	-		-	6.97	-
R4	-	-	-	-	-	4.48
1	2.5	-	-	-	-	-
2	2.5	1.78	2.84	2.55	2.38	1.79
3	1.57	1.16	1.21	1.41	1.29	2.03
4	1.57	1.64	1.64	1.53	1.53	1.47
5	2.5	2.37	2.24	2.40	2.33	2.94
6	2.5	3.47	3.07	2.55	2.71	2.14
Overall SF	2.00	1.69	2.00	2.00	2.02	2.03

the resultant spread of load, there is a large variation on the individual SF (1.78 to 3.47). For instance, taking on account the general pattern of load distribution and individual SF, it is clearly seen that, once the group is reinforced, piles 2 and 3 decrease their load, while piles 4 and 6 increase it. Also, depending on the reinforcement type, pile 5 may increase or decrease its internal load. This behavior is undoubtedly related to each pile position within the group, to their individual proximity to the defective one, plus aforementioned effects of the raft's geometrical center and average flexibility;

• Although all reinforcement cases proved to remediate the group to acceptable levels (of presented variables), the reinforcement piles failed to behave efficiently on working conditions. That means, they lacked to absorb most (or all) of the load spread caused by pile's 1 defect, hence they behaved conservatively in all cases. A better design, not implemented herein, would enhance the performance of piles 3 and 4 at post-reinforced conditions, leading them to a SF closer to original (undamaged) values. Note for instance the low individual SF of pile 3 at reinforcement cases 1 to 3, and of pile 4 at cases 2 to 4;

• It is also clear that for some piles, when comparing to original perfect conditions, there was an aggravation of the behavior by the imposed remediation, *i.e.*, they had a lower individual SF in relation to initial values. Perhaps, in other more severe situations some of the piles would be fully mobilized, even at the reinforced raft stage;

• Indeed, to lessen the conservative performance, the reinforcement piles could have been designed with distinct characteristics from the original ones, perhaps with shorter lengths or diameters. This aspect will be explored in the next topic.

Finally, Fig. 13 presents the load distribution for each of the studied reinforced cases, and their comparison to original and fully damaged values. From this one it is noticed that, by reinforcing the raft, it tends to transfer load back to the piles (original and reinforcement ones).

Depending on the reinforcement case, more load is gradually transferred from raft to piles, but, as previously

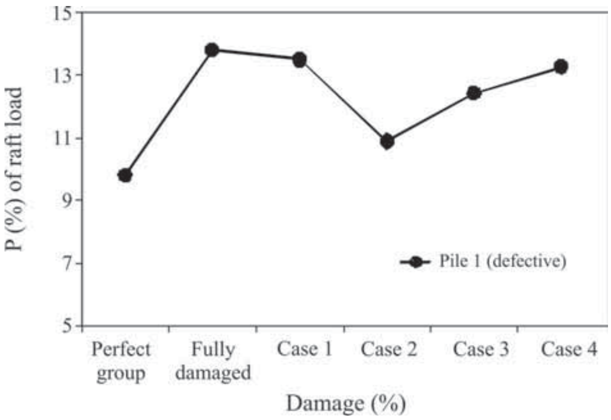

Figure 13 - Load distribution for reinforced cases.

commented, the effectiveness of the reinforcement systems was not ideal. That means, they failed to return the raft load to original perfect conditions, although some improvement is made in regard to the fully damaged case.

4.2.2. Remediation with dissimilar pile

The remediation with a dissimilar pile adopted solely the reinforcement case 4 as the parameter for comparison, due to its better performance on previous analyses. The dissimilar pile was simulated with respectively 50% of the original length, diameter, and stiffness, of the original piles.

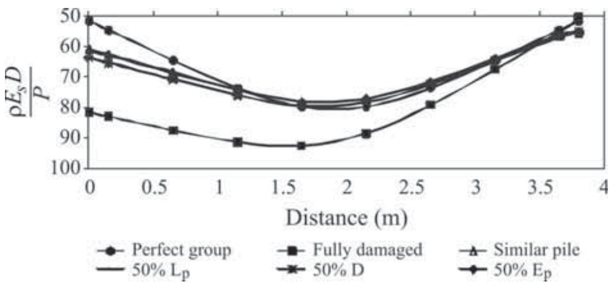

Figure 14 - Group behavior in terms of normalized vertical settlement for dissimilar reinforcement pile.

A comparison with former results (similar pile reinforcement) is also provided.

Hence, Fig. 14 and Table 5 respectively present the results in terms of normalized vertical settlement and safety factors for all considered cases.

From them, it can be noticed that:

• In terms of normalized settlements (and moments, not shown), there isn't much difference in reinforcing the raft with similar or dissimilar piles. All the results are good enough to be accepted in practical terms. Nevertheless, the reinforcement with dissimilar piles may prove to be more economical;

• In terms of individual SF it is clear that the dissimilar piles with 50% length or diameter behave less conservatively at working conditions than the similar pile. Nevertheless the overall SF values of the group for these cases tended to be lower than the minimum value advocated by normal standards;

• On the other hand, in terms of individual and overall SF for the reinforcement with a dissimilar pile with 50% of the original stiffness, it can be noticed results as good as those of the reinforcement with a similar pile. Hence, it appears from these (limited) tested cases that the usage of dissimilar piles with reduced stiffness seems to be preferable in a reinforcement event. However, this conclusion needs further validation, also taking into account the economical aspects of the problem.

5. Conclusions

This paper has explored and extended the design philosophy of "piled raft" to forecast the numerical behavior of imperfect pile group foundations at pre and post-remediated conditions.

Although the results are restricted to the conditions of the analyses, they allow preliminary generalizations of the overall behavior. Moreover, they do highlight the fact that the phenomena involved with such processes are rather complex, but feasible to be simulated in a simplified manner. More elaborate analyses could have been employed to

Table 5 - SF for reinforced cases of dissimilar pile.

Pile	Perfect group	Fully damaged	Reinforcement type			
			Similar pile	50% Lp	50% D	50% Ep
R4	-	-	4.48	1.66	2.10	5.05
1	2.5	-	-	-	-	-
2	2.5	1.78	1.79	1.77	1.76	1.78
3	1.57	1.16	2.03	1.95	1.89	1.96
4	1.57	1.64	1.47	1.49	1.49	1.48
5	2.5	2.38	2.94	2.95	2.94	2.93
6	2.5	3.47	2.14	2.21	2.24	2.19
Overall SF	2.00	1.69	2.03	1.79	1.82	2.07

cope with most (or all) of the aspects involved in the simulations, but at the expense of a much more complex numerical tool and longer time span.

The analyses have also allowed a reasonable insight into some of the most relevant variables that affect the behavior of the group foundation once it is damaged, *i.e.*, once it is loaded with the presence of a defective pile(s). They have as well provided a better understanding of the mechanisms which are involved by the remediation of this same foundation, via introduction of either similar or dissimilar (reinforcement) piles compared to those of the original group, at early loading stages.

From the general aspects observed with the analyses, some general conclusions can be drawn:

1. The behavior of the group foundation once an imperfection is imposed at working load will be undoubtedly degraded in relation to that which would occur at normal conditions. That means, settlements and moments on the raft will increase, and load transference between defective to normal, and normal to normal pile, will certainly take place. The level of load spread and raft tilting will depend on the severity of the defect, *i.e.*, the location and number of defective pile(s), the degree of defect and overall pile-raft characteristics (geometry and flexibility);

2. A pile defect caused by a variation on its length (reduced length in regard to normal similar piles) is more influential on the foundation variables than a proportional defect caused by a variation on the pile stiffness;

3. The foundation settlement is more influenced by the pile defect than the moment generated at raft, at working conditions;

4. Imperfect pile groups will also have degradation on the individual pile, and overall group, (geotechnical) safety factor. The overall SF will decrease as the severity of the defect increases, and individual pile SF may decrease (load gain) or even increase (load loss) due to load redistribution that normally occurs during this stage;

5. Once an imperfection is imposed there is a normal variation (or transference) of load from the piles to the raft. During this process, the defective pile transfers some of its original load to the raft as well as to adjacent normal piles, depending on the geometry of the raft, pile position and severity of the defect. Once remediated, the group tends to transfer less load from the piles to the raft, though the transfer continues to exist;

6. Even when imperfect, the defective pile continues to absorb some load, but to a lesser degree than the original value (of the perfect group condition). This particular feature can be wisely used in design;

7. The remediation of the foundation via insertion of a unique reinforcement pile close to the defective one improves the group behavior in terms of settlement and overall group SF, if such procedure is carried out at early stages of loading;

8. On the contrary, it can also degrade the foundation behavior in terms of raft moments, from the fact that it will inevitably change the raft's geometrical center and overall flexibility;

9. The reinforcement also provides a redistribution of load within group components, *i.e.*, the load spread from the defective pile will be partially absorbed by the reinforcement one, and some of the normal piles of the group may lose load (increasing their individual SF), while others, on the contrary, may gain load (decreasing their individual SF). This behavior is related to each pile position within group, type of reinforcement (*i.e.*, similar or dissimilar pile), plus aforementioned aspects of defect severity and raft geometry;

10. At extreme cases of imperfection, not carried out herein, it is feasible that some of the normal piles of the reinforced group can be fully mobilized, *i.e.*, with individual SF very close or equal to unity;

11. An optimization of the remediation is required to enhance the performance of the group at post-reinforced conditions, *i.e.*, to have most of the load of the defective pile transferred to the reinforcement one, with minimum levels of interference on adjacent normal piles;

12. Such optimization will undoubtedly take place by an initial study of the better location of the reinforcement pile on the original or extended raft, and by a suitable (in technical and economical terms) choice for the type of reinforcement, which most probably will be the use of dissimilar piles in relation to the normal ones of the group;

13. The effectiveness of the reinforcement, considered solely on technical terms (*i.e.*, safety factors) is better when adopting dissimilar piles with reduced stiffness, than when reinforcing the raft with a dissimilar pile of reduced length or diameter. This conclusion, however, is still subjected to further validation.

Acknowledgments

This study was made possible through a joint technical co-operation research program from the Universities of Sydney, Brasília and Federal of Goiás. In this regard, the authors are grateful to the kind support and comradeship provided by both Prof. H.G. Poulos and J.C. Small.

The authors also thank the Brazilian sponsorship organizations CNPq and CAPES for all related support in this and all other studies carried out by the group, in terms of personal research grants, or sabbatical & student scholarships.

English review kindly provided by Prof. Patrick Stewart from BCIT, Canada, is also acknowledged.

References

Cordeiro, A.F.B. (2007) Avaliação numérica de reforço de grupo de estacas pela introdução de estacas adicionais (Numerical assessment of the reinforcement of pile groups by the addition of extra piles). M.Sc. Thesis, Universidade de Brasília, 118 pp.

Cordeiro, A.F.B.; Cunha, R.P.; Sales, M.M.; Kuklík, P. & Broucek, M. (2008a) Influence of interaction factors and defective piles on piled raft behavior. 2nd BGA International Conf. on Foundatons, ICOF'08, Dundee, v. 1, pp. 475-483.

Cordeiro, A.F.B.; Cunha, R.P.; Broucek, M. & Sales, M.M. (2008b) Piled rafts with defective piles: Influence of reinforcement systems. 2nd BGA International Conf. on Foundations, ICOF'08, Dundee, v. 1, pp. 485-492.

Cunha, R.P.; Poulos, H.G. & Small, J.C. (2001) Investigation of design alternatives for a piled raft case history. J. Geot. & Geoenv. Eng., v. 127:8, p. 635-641.

Ferreira, C.D.; Machado, M.M.; Ferreira, R.S. & Kucera, C.F. (2000) Reforço de Fundações: um caso histórico (Reinforcement of foundations: A case history). Seminar on Special Foundation Eng. & Geotechnics, SEFE IV, São Paulo, v. 2, pp. 222-231.

Gotlieb, M. & Gusmão Filho, J.A. (1999) Reforço de fundações (Reinforcement of Foundations). In: Fundações, Teoria e Prática (Foundations, Theory and Practice), ABMS/ABEF and Pini Editors, São Paulo, pp. 471-493.

Janda, T.; Cunha, R.P.; Kuklík, P. & Anjos, G.M. (2009) Three dimensional finite element analysis and back-analysis of CFA standard pile groups and piled rafts founded on tropical soil. Soils and Rocks, v. 32:1, p. 3-18.

Knigmüller, O. & Kirsh, F. (2004) A Quality and safety issue for cast-in-place: 25 years of experience with low-strain integrity testing in Germany – From scientific peculiarity to day-to-day practice. ASCE Geot. Special Pub., Reston, n. 125, pp. 202-221.

Lima, S.P. & Costa Filho, L.M. (2000) Reforço de fundações de estrutura de prédio industrial (Reinforcement of the foundations from the structure of an industrial building). Seminar on Special Foundation Eng. & Geotechnics, SEFE IV, São Paulo, v. 2, pp. 391-401.

Lizzi, F. (1982) The Static Restoration of Monuments: Basic Criteria-Case Histories. Sagep Publisher, Genova, 146 pp.

Milititsky, J.; Consoli, N.C. & Schnaid, F. (2005) Patologia das Fundações (Pathology of Foundations). Oficina de Texto Editors, São Paulo, 208 pp.

Poulos, H.G. & Small, J. C. (1998). GARP6 User's Manual. Coffey Partners International Pty Ltd., Sydney, 23 pp.

Poulos, H.G. (1988) Modified calculation of pile group settlement interaction. Journal Geot. Eng., v. 114:6, p. 697-706.

Poulos, H.G. (1990) DEFPIG User's Guide. University of Sydney, Sydney, 55 pp.

Poulos, H.G. (1997) Behavior of pile groups with defective piles. Proc. 14th Int. Conf. Soil Mechanics Foundation Engineering, Hamburg, v. 2, pp. 871-876.

Poulos, H.G. (1999) Pile Defects – Influence on foundation performance. Proc. 4th Int. Conference on Deep Foundation Practice Incorporating Piletalk. Singapore, pp. 57-69.

Poulos, H.G. (2005) Pile behavior – Consequences of geological and construction imperfections. 40th Terzaghi Lecture, J. Geot. & Geoenv. Eng., v. 131;5, p. 538-563.

Poulos, H.G. (2009) Simulation of the performance and remediation of imperfect pile groups. Proc. 5th International Symposium on Deep Foundations on Bored and Auger Piles – BAP VI. Ghent, Belgium, pp. 143-154.

Randolph, M.F. (1985) Chapter 4. Design of single piles. K. Fleming, A. Weltman, M. Randolph and K. Elson (eds), Pile Engineering. Taylor & Francis, New York, 398 pp.

Sales, M.M. & Costa, W.L. (1996) Dois casos históricos de reforço de fundação (Two historical cases of foundation reinforcement). Seminar on Special Foundation Eng. & Geotechnics, SEFE III, São Paulo, v. 1, pp. 243-254.

Sales, M.M. (2000) Análise do comportamento de sapatas estaqueadas (Analysis of the behavior of piled rafts). D.Sc. Thesis, Universdade de Brasília, 229 pp.

Sanctis, L. & Mandolini, A. (2006) Bearing capacity of piled rafts on soft clay soils. J. Geot. & Geoenv. Eng., v. 132:12, p. 1600-1610.

Ziccarelli, M. & Valore, C. (2006) Effetti della presenza di detrito sotto la punta dei pali (Effect of the presense of debris beneath the tip of piles). V Convegno Nazionale dei Ricercatori di Ingegneria Geotecnica-CNRIG. Bari, CDRom, pp. 1-22.

Technical Note

Soils and Rocks
v. 33, n. 2

Evolution of the Mechanical Properties of a Tropical Soil Stabilized with Lime and Ash of Rice Rind

Marco Antônio de Morais Alcantara, Lucas Pereira dos Santos, Dario Cardoso de Lima

Abstract. The ash of rice rind is a pozzolanic material that reacts with the calcium hydroxide (Ca $(OH)_2$) forming bonding composites, when finely worn out and in water presence. Considering this behavior, the objective of the present work was to evaluate the potential use of this residue in the enrichment of the content of pozzolanic materials of a tropical soil stabilized with a commercial hydrated lime. The laboratory testing program incorporated unconfined compression strength tests performed on the soil and on its mixtures with contents of 8% of lime enriched with 5 and 10% of ash of rice rind in relation to the soil dry mass. The results of the testing program supported that the use of the residue was effective in increasing the degree of reactivity of the soil that was also directly related with the increase in the ash content and the period of cure of the mixtures.

Keywords: soil improvement, soil-lime-ash of rice rind mixture, enrichment of pozzolanic activity, mixture unconfined compressive strength.

1. Introduction

The Brazilian road engineering experience with soil-lime mixtures dates back to the decade of 1960, initially at the research level that was reported by: (i) Pinto (1964), referring to the stabilization of a A-7-5 soil using little amounts of hydrated lime and measuring mixtures mechanical strength via unconfined compression and CBR tests; (ii) Pinto (1965), analyzing the data from a Brazilian study including an universe of eight soils and seven hydrated commercial limes; (iii) Baptista (1969), informing the results of a study including data on the grain size distribution, Atterberg limits and mechanical resistance of soils from the state of Rio de Janeiro, Brazil.

Regarding soil-lime mixtures, the Brazilian National Department of Transportation Infrastructure-DNIT (DNIT, 2006) defines soil-lime stabilization as those composites using lime contents in the range of 5 to 6% that develop expressive tensile strength for application as bases and sub-bases of road pavements, as well as modified soil-lime mixtures in those applications using lime contents of 1 to 3% that do not show high tensile strengths and can be classified as flexible pavement layers.

The soil-lime stabilization is characterized as a procedure that modifies the clayey soil particles surface chemical conditions in order to promote changes in soil CTC and formation of new cementing composites as reported by TRB (1976) and Alcântara (1995) that are, respectively, responsible for short and medium/long term changes in soil mechanical engineering behavior. According to Lima (1981), Pinto (1985) and Alcântara (1995) short term modifications in soil lime mixtures are those that happen just after addition of lime, commonly referred to an increase in the plasticity limit, and decreases in the liquidity limit and in the plasticity index, as well as flattening of the compaction curves with increase in the optimum moisture content and decrease in the dry density. On the other hand, medium and long term modifications are due to pozzolanic reactions with formation of calcium and aluminate silicates that improve soil mechanical strength and durability.

The pozzolanic reactions are understood as those that happen between the inorganic components of a soil and the Calcium hydroxide $Ca(OH)_2$, forming insoluble composites, even under immersion conditions, similarly to the obtained in the Portland cement hydration (Cincotto & Kaupatez, 1984). Alcântara (1995) emphasizes that a soil has a pozzolanic activity degree that is directly related to its clay fraction type and content.

Considering that soil-lime mixtures are soil composition dependent, each mixture demands an specific laboratory design, generally, based on unconfined compressive strength (general procedure), CBR (modified soil-lime mixtures) and dry/wetting durability specimen testing. In this sense, Alcântara (1995) analyzed the soil-lime stabilization of three soils from the city of Ilha Solteira, São Paulo State, Brazil, classified as A-2-4, A-4 and A-7-6 using lime contents ranging from 2 to 10% and mixtures curing times of 3, 7, 28, 90, 120 and 180 days. Another parameter that affects soil-lime mixtures mechanical response is the mixture dry density. Segantini and Alcântara (2007) understand that the soil-lime unconfined compressive strength resistance fundamentally depends on specimen laboratory molding conditions, water content and compaction effort.

Marco Antônio de Morais Alcantara, PhD., Assistant Professor, Departamento de Engenharia Civil, Faculdade de Engenharia de Ilha Solteira, Universidade Estadual Paulista "Júlio de Mesquita Filho", 15385-000 Ilha Solteira, SP, Brazil. e-mail: alcantar@dec.feis.unesp.br.
Lucas Pereira dos Santos, Civil Engineer, Stahldach Construções/Grupo Marko, 02518000 São Paulo, SP, Brazil. e-mail: lsantos@marko.com.br.
Dario Cardoso de Lima, PhD., Professor, Departamento de Engenharia Civil, Universidade Federal de Viçosa, 36570-000 Viçosa, MG, Brazil. e-mail: declima@ufv.br.
Submitted on May 19, 2009; Final Acceptance on December 8, 2009; Discussion open until December 31, 2010.

The ash of rice rind is a natural residue from rice industry classified as a pozzolanic material, according to Cincotto and Kaupatez (1984). When finely grounded and in presence of water, this material reacts with lime calcium hydroxide ($Ca(OH)_2$) forming cementitious compounds. In Brazil, the agro-industrial improvement and commercialization of rice stands out for the high production of this residue, representing an environmental problem. When it is not used in a direct way, as in the case of the hen house bed or as soil conditioning, the rice rind is discarded and thrown in embankments and local highways, burned to open sky or used as fuel for grain drying, producing tons of ashes that are considered harmful to the human health as emphasized by Milani (2005). Data from the Brazilian Institute of Geography and Statistics (IBGE, 2007) show that Brazil produced around 2.3 million tons of ash rice rind in 2006.

According to Barbosa (2007), when ash of rice rind is roasted, 20% of it is turned into ashes reaching the available silica amount of 95%. Still according to this author, types of ash rice rind can be amorphous or crystalline, depending on the used burning process. Ashes produced at lower controlled temperature (450-500 °C) tend to be amorphous, while those produced at higher not controlled temperature tend to be crystalline; the first ones are considered to be the most reactive in soil stabilization processes.

This research was directed to the use of the ash of rice rind for the improvement of the clayey fraction of a tropical residual soil of gneiss stabilized with hydrated lime for road engineering applications taking advantage of its physical-chemical potentiality as a pozzolanic material and minimizing environmental drawbacks.

2. Materials and Methods

This research was developed at the Laboratory of Civil Engineering of the Faculty of Engineering of Ilha Solteira, UNESP, and at the Laboratory of Civil Engineering of the Energy Company of the State of São Paulo (CESP), Brazil.

2.1. Materials

A silt-clay-sand soil classified as A-4 (DNIT, 2006) and as red-yellow argissol (EMBRAPA, 2006) from the city of Ilha Solteira, State of São Paulo, Brazil, a commercial CH-III hydrated lime (ABNT, 2003), and a crystalline ash of rice rind from the city of Pelotas, State of Rio Grande do Sul, were used throughout the study.

The ash of rice rind was sampled after 30 min of grinding process in a mill of balls of the CESP's Laboratory of Civil Engineering located in Ilha Solteira, and specifically designed for the production of cement. Table 1 presents the physical and chemical characterizations of the sample of this residue.

2.2. Methods

After sampling, the soil sample was passed through the #4 sieve, and dried in air in order to determine its hygro-

Table 1 - Physical and chemical characterizations of the crystalline ash of rice rind.

Sample		Ash of rice rind	Requirements for pozzolanic materials (ABNT, 1992)	
			Minimum value	Maximum value
Apparent density (g/cm^3)		0.60	-	-
Absolute density (g/cm^3)		2.14	-	-
Grain size (micra)		20.13	-	-
Water content (%)		1.08	-	3.0
Chemical analysis data (%)	Fire loss	7.95	-	6.0
	SiO_2	85.37	-	-
	Fe_2O_3	0.86	-	-
	Al_2O_3	1.19	-	-
	CaO	1.34	-	-
	MgO	0.33	-	-
	SO_3	0.06	-	5.0
	$Al_2O_3 + Fe_2O_3$	2.05	-	-
	$SiO_2 + Al_2O_3 + Fe_2O_3$	87.42	70.0	-
	Na_2O equivalent alkaline (available)	0.42	-	-
	Na_2O	0.03	-	-
	K_2O	0.60		-

Table 2 - Soil, lime and ash rice rind mixture compositions used in the study.

Mixture	Soil, lime and ash of rice rind percentile composition
1	Soil + 8% lime + 0% ash of rice rind
2	Soil + 8% lime + 5% ash of rice rind
3	Soil + 8% lime + 10% ash of rice rind

scopic water content, and Table 2 presents the mixtures percentile combinations referred to soil dry mass used in the study.

Specimen preparation was carried through weighing the soil, lime and ash of rice rind, mixture of these materials in a plastic bag, addition of water in order to reach the optimum moisture content, mixture sieve through the #10 Brazilian Association of Technical Standards (ABNT) sieve mesh, and compaction at the Standard Proctor compaction energy using the mini-CBR molding apparatus (Nogami e Villibor, 1995) following the Brazilian NBR 12024 Standard (ABNT, 1990a). After molding triplicate 5 cm diameter to 5 cm height specimens, they were weighed and measured in order to determine their compaction degree, and kept curing for 7, 28, 60 and 90 days in a standard humidity chamber. After curing, the specimens were tested in laboratory under unconfined compression conditions using a 50 kN load frame apparatus according to the Brazilian NBR 12025 (ABNT, 1990b). The average value of the unconfined compressive strength of three tested specimens was adopted.

3. Results

3.1 Compaction testing data

Table 3 and Fig. 1 introduce, respectively, the soil and mixtures compaction curves and optimum compaction test parameters.

Table 4 shows the values of the degree of compaction of mixtures specimens compacted in the mini-CBR molding apparatus, where it can be noted that the values of degree of compaction ranges from 98 to 99.5%.

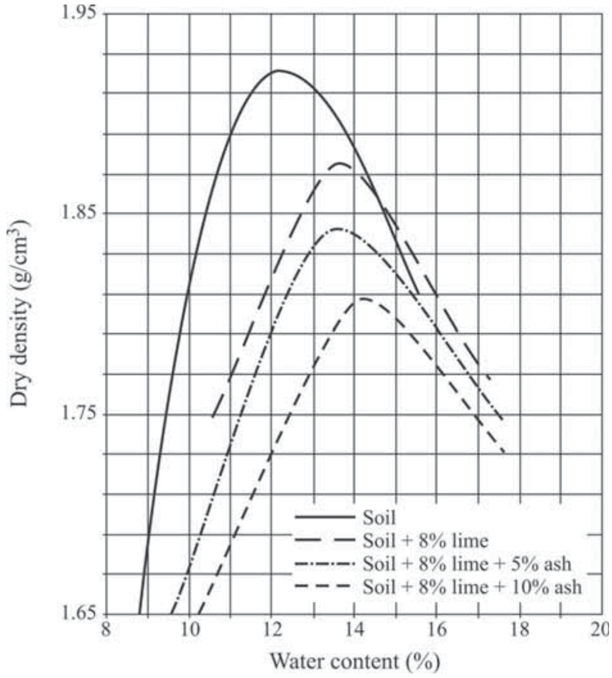

Figure 1 - Compaction curves of soil and its mixtures with lime and ash of rice rind.

Table 3 - Optimum compaction testing parameters of soil and mixtures: optimum moisture content (w_{ot}); maximum dry density (γ_{dmax}).

Soil and mixture compositions	w_{ot} (%)	γ_{dmax} (g/cm^3)
Soil	12.4	1.92
Soil + 8% lime	13.7	1.88
Soil + 8% lime + 5% ash of rice rind	13.7	1.84
Soil + 8% lime + 10% ash of rice rind	14.4	1.81

3.2 Unconfined compression testing data

Table 5 presents the mean values of the unconfined compressive strength, and Fig. 2 depicts the respective percentile variations of mixtures parameters.

Table 4 - Mean values (μ) and standard deviation (σ) of degree of compaction of mixtures specimens after periods of cure of 7, 28, 60 and 90 days.

Mixture content	Degree of compaction (%)							
	Period of cure (day)							
	7		28		60		90	
	μ	σ	μ	σ	μ	σ	μ	σ
Soil + 8% lime	99.0	2.31	98.5	0.40	98.5	0.5	98.5	0
Soil + 8% lime + 5% ash of rice rind	99.5	0	98.0	0.45	98.5	0.5	98.0	0

Table 5 - Mean values (μ) and standard deviation (σ) of the unconfined compressive strength of mixtures specimens after periods of cure of 7, 28, 60 and 90 days.

Mixture content	Unconfined compressive strength mean values (MPa)							
	Period of cure (day)							
	7		28		60		90	
	μ	σ	μ	σ	μ	σ	μ	σ
Soil + 8% lime	0.69	0.06	4.60	0.11	6.79	0.36	6.70	0.37
Soil + 8% lime + 5% ash of rice rind	0.64	0.015	4.13	0.55	6.54	0.29	7.81	0.73
Soil + 8% lime + 10% ash of rice rind	0.57	0.02	4.70	0.15	8.65	0.63	10.54	1.77

4. Discussions

Data from Fig. 1 and Table 3 support that addition of lime and ash of rice rind caused drops in the soil maximum dry density and increases in the soil optimum moisture content of the mixtures.

Table 5 presents the average values of unconfined compressive strength of soil-lime-ash of rice rind mixtures. For the first ages of cure, values of mechanical strength of the tested mixtures tend to be lesser than those of the reference mixture, mainly regarding the 7 days cure. On the other hand, for advanced periods of cure (60 and 90 days), the values of mechanical strength tend to surpass those presented by the reference mixture, especially for the period of cure of 90 days. Comparing the behaviors of the 10% ash and the reference mixtures, it is observed gains around 2, 27 and 57%, respectively, for the periods of cure of 28, 60 and 90 days.

Figure 2 shows that the addition of 10% of ash was highly efficient in promoting the increase of the unconfined compressive strength of the reference mixture, since after 28 days of cure the values of the percentile variation are positive. By contrast, the mixture with 5% of ash was less reactive, presenting negative percentile variation up to 60 days of cure; however, presenting a decreased trend in the difference, becoming positive for higher period of cure, that certifies the influence of the period of cure in the development of pozzolanic reactions in the ash mixture. Comparing the mechanical response of the 5 and the 10% ash content mixtures, it is observed that the later presented larger gains of mechanical strength at medium and long term periods of cure, indicating the significant influence of the addition of a higher content of ash in the development of pozzolanic reactions.

Figure 3 introduces the evolution of the mechanical strength of the tested mixtures with the period of cure. In this figure, the parameter unconfined compressive strength of the soil-lime mixture presents a stable behavior starting at 60 days of cure. On the other hand, at this period, the value of the mechanical strength of the mixture with 5% of ash already approaches the value presented by the reference composition, coming to overcome it at 90 days of cure as previously reported. Regarding the mixture with 10% of ash, it already reached the standard mixture mechanical strength at 28 days of cure being consistently higher than that of the 5% mixture of ash which emphasizes the influ-

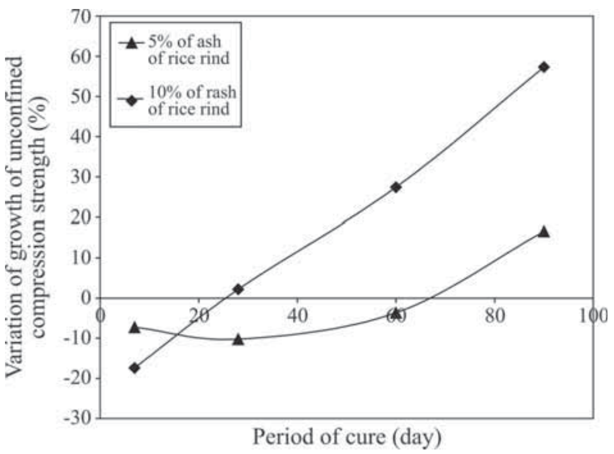

Figure 2 - Percentile variation of the increase of unconfined compressive strength versus periods of cure (7, 28, 60 and 90 days) adopting as reference the unconfined compressive strength of the soil-lime mixture.

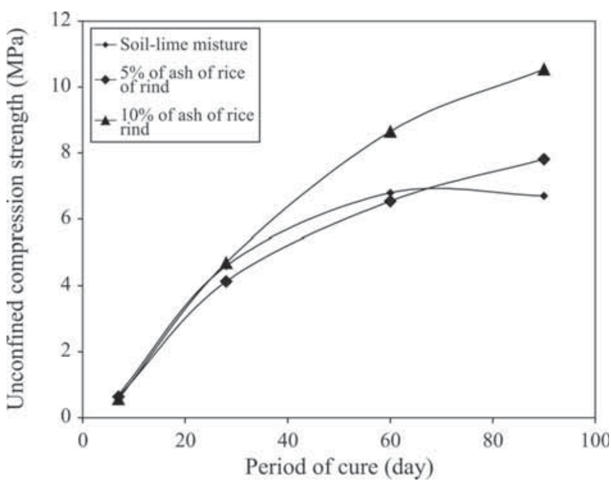

Figure 3 - Evolution of the mechanical strength of mixtures with the period of cure.

Table 6 - Dry density of mixture specimens tested after the periods of cure of 7, 28, 60 and 90 days.

Mixture	Dry density (g/cm^3)			
	Period of cure (day)			
	7	28	60	90
Soil + 8% lime	1.86	1.85	1.85	1.85
Soil + 8% lime + 5% ash	1.83	1.80	1.81	1.80
Soil + 8% lime + 10% ash	1.80	1.77	1.77	1.79

ence of the time and ash content on the evolution of the standard mixture mechanical response. This behavior can be also visualized through data presented in Fig. 4 which depicts the variation of the unconfined compressive strength with the ash contents of the standard mixture.

Table 6 illustrates the influence of addition of ash in the values of the dry density of the mixtures. Analyzing the data in this table and comparing with the standard mixture response, it is obvious that the drops in the values of dry density of the mixtures are related to the increase in the ash content, a lighter material than soil and lime. Certainly, the values of unconfined compressive strength presented in Table 5 reflect the possible influence of the variation of the dry density in the mechanical response of the mixtures, mainly reflecting the incipient development of pozzolanic reactions at 7 days period of cure (short term reactions). Larger periods of cure definitely increase the effect of the pozzolanic reactions in the gain of mechanical strength of the mixtures, also supplanting the deleterious effect of the observed dry density fall.

Finally, Fig. 5 shows an analysis of the relationship between dry density and unconfined compressive strength of all tested mixtures for different periods of cure. It is observed in this figure that there is no correlation between dry density and unconfined compressive strength of mixtures at the period of cure of 7 days. Increasing the period of cure, it is noticed the development of correlations between these two parameters that reaches a maximum at 90 days, emphasizing the effect of the period of cure on the development of the pozzolanic reactions in the tested mixtures.

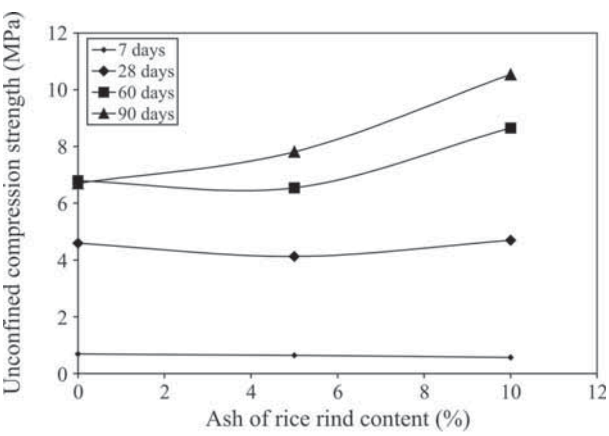

Figure 4 - Unconfined compressive strength versus ash of rice rind content and period of cure of mixtures.

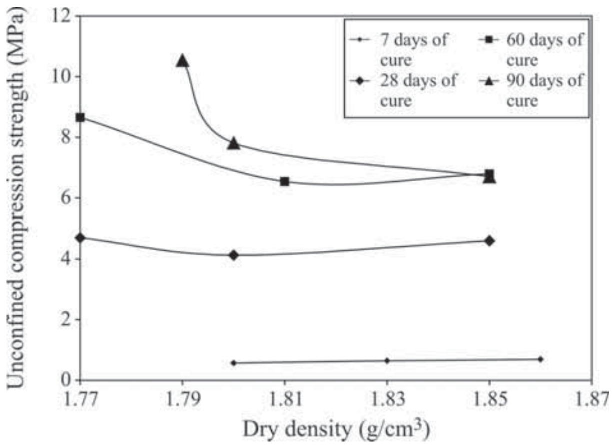

Figure 5 - Variations of dry density and unconfined compressive strength with periods of cure.

5. Conclusions

Based on the laboratory testing data, the conclusions are as follows:

• Addition of ash of rice rind increased the soil reactivity degree, and the increase in the pozzolanic effect was directly related to the ash content and the periods of cure of mixtures;

• The pozzolanic effect of the addition of the ash of rice rind to the soil-lime mixture compensated the effect of the decrease on the dry density of the mixtures for periods of cure of 60 and 90 days;

• The 10% ash content produced the largest increase on the mechanical strength of the soil-lime mixtures.

Acknowledgments

The research described in this technical note was supported by FAPESP. This support is gratefully acknowledged. The authors wish to thank the technicians of the Laboratory of Civil Engineering of the Energy Company of the State of São Paulo (CESP), and of the Laboratory of Materials of Construction of the UNESP-Ilha Solteira, for their support and collaboration in the execution of the tests.

References

Alcântara, M.A.M. (1995) Estabilização Química de Solos para fins Rodoviários: Técnicas Disponíveis e Estudo de Caso Dirigido à Estabilização Solo-Cal de Três Solos de Ilha Solteira-SP (Chemical Stabilization of Soils for Road Engineering Applications: Available Techniques and Case Study Directed to the Stabilization of Three Soils from Ilha Solteira). MSc. Dissertation, Universidde Federal de Viçosa, Viçosa, 91 pp.

ABNT (2003) NBR 7175: Cal Hidratada para Argamassas. Associação Brasileira de Normas Técnicas, Rio de Janeiro, RJ, Brazil, 4 pp.

ABNT (1992) NBR 12653: Materiais Pozolânicos - Especificação. Associação Brasileira de Normas Técnicas, Rio de Janeiro, RJ, Brazil, 3 pp.

ABNT (1990a) NBR 12024: Solo-Cimento – Moldagem e Cura de Corpos-de-Prova Cilíndricos. Associação Brasileira de Normas Técnicas, Rio de Janeiro, RJ, Brazil (in Portuguese), 5 pp.

ABNT (1990b) NBR 12025: Solo-Cimento – Ensaio de Compressão Simples de Corpos-de-Prova Cilíndricos. Associação Brasileira de Normas Técnicas (Brazilian Association of Technical Standards), Rio de Janeiro, RJ, Brazil (in Portuguese), 2 pp.

Barbosa, M.B. (2006) A Utilização de Resíduos de Cinza de Casca de Arroz e Borracha de Pneus em Concreto de Alto Desempenho (The Use of Ashes of Peel of Rice and Rubber Tire in High Performance Concrete). M.Sc. Dissertation, Faculty of Engineering of Ilha Solteira, Ilha Solteira (in Portuguese), 161 pp.

Baptista, C.F.N. (1969) Pesquisa solo-cal. Proc. X Reunião Anual de Pavimentação (10th Annual Pavement Meeting), Salvador, ABPv-Associação Brasileira de Pavimentação, pp. 114-142.

Cincotto, M.A. & Kaupatez, R.M.Z (1984) Seleção de materiais quanto a atividade pozolânica. A Construção São Paulo, n. 37, p. 15-18.

DNIT (2006) Manual de Pavimentação. 3rd ed. Instituto de Pesquisas Rodoviária, Rio de Janeiro, Publication IPR-719, 274 pp.

EMBRAPA (2006). Sistema Brasileiro de Classificação de Solos. 2nd ed. Embrapa, Rio de Janeiro, 306 pp.

IBGE (2007) Instituto Brasileiro de Geografia e Estatística, Available in: www.ibge.gov.br. Access in June 1, 2007.

Lima, D.C. (1981) Algumas Considerações Relativas a Aspectos da Estabilização de Solos, em Particular a Estabilização Solo-Cal (Considerations on Aspects of Soil Stabilization, in Particular to Soil-Lime Stabilization). M.Sc. Dissertation, Escola de Engenharia de São Carlos, São Carlos, 171 pp.

Milani, A.P.S. (2005) Avaliação Físico-Mecânica de Tijolos de Solo-Cimento e de Solo-Cal Adicionados de Casca de Arroz (Physical-Mechanical Evaluation of Soil-Cement-Ash of Rice Rind and Soil-Lime-Ash of Rice Rind Bricks). M.Sc. Dissertation, University of Campinas, Campinas, 131 pp.

Nogami, J.S. & Villibor, D.F. (1995) Pavimentação de Baixo Custo com Solos Lateríticos (Lateritic Low Cost Pavements). Ed. Villibor, São Paulo, 240 pp.

Pinto, C.S. (1985) Estabilização de pavimentos com cal (Soil-lime pavements). Bulletin n. 14. Associação Brasileira de Produtores de Cal, São Paulo, pp. 79-112.

Pinto, C.S. (1964) Estudo da Variação da Capacidade de Suporte de um Solo pela Adição de Pequenas Quantidades de Cal ou de Cimento (Study of the Variation of the Bearing Capacity of a Soil with the Addition of Small Amounts of Lime or Cement). Publication n. 49, Instituto de Pesquisas Rodoviárias, Rio de Janeiro, 41 pp.

Pinto, C.S. (1965) Estudo de Solo-Cal com Solos Brasileiros (Study of Brazilian Soil-Lime Mixtures). Publication n. 64, Instituto de Pesquisas Rodoviárias, Rio de Janeiro, 17 pp.

Segantini, A.A. & Alcântara, M.A.M. (2007) Solo-Cimento e Solo-Cal. (Soil-Cement and Soil-Lime). In: Materiais de Construção Civil e Princípios de Ciência e Engenharia de Materiais (Construction Materials and Science Principles Applied to Materials Engineering), v. 2. IBRACON, São Paulo, pp. 833-861.

TRB (1976) State of the art - lime stabilization: Reactions, properties, design, construction. Transportation Research Board, Report n. 180, Washington, DC: TRB, 31 pp.

Discussions

Soils and Rocks
v. 33, n. 2

The use of a High-Capacity Tensiometer for Determining the Soil Water Retention Curve

Discussion by

Claudio Fernando Mahler, Ronaldo Luiz dos Santos Izzo

The technical note presented by the authors is interesting. The use of high-capacity tensiometers has been reported for some time by other authors as well, such as Ridley & Burland (1993), cited in the note, and others, like Mahler *et al.* (2002), who presented a tensiometer made of acrylic and using another type of transducer (see Figs. 1, 2 and 3) that is much cheaper than the Entran transducers used by Ridley & Burland (1993) and the authors. If fact, Mahler *et al.* (2002) already proposed the use of high-capacity tensiometers together with TDR probes to determine soil moisture to obtain characteristic curves. One of these is presented in Fig. 4, obtained in soils used in a mini-lysimeter that was collected near Rio de Janeiro from gently rolling terrain. It can be characterised as sandy soil and the grain size curve is given in Fig. 5. This mini-lysimeter is depicted in Figs. 6 and 7. The description of the soil preparation and subsequent placement in the pot can be seen in Mahler *et al.* (2001). The initial saturation water content was approximately 20%, very near to field capacity. The results of the tensiometer presented here were compared to those of other devices also installed in a mini-lysimeter at the same depth as the equitensiometer (Fig. 8). More information on the equipment utilized in this study can be seen in Mahler *et al.* (2002). Figure 9 shows the results obtained with the then-new tensiometer and equitensiometer.

The main final remarks so far are as follows:

• The high bubbling pressure of the ceramic stone inhibits the presence of air bubbles, but the response is slower for suction values greater than 200 kPa;

• The saturation process used for the ceramic stone, which can be seen in Mahler *et al.* (2002) and Pacheco (2001), worked very well;

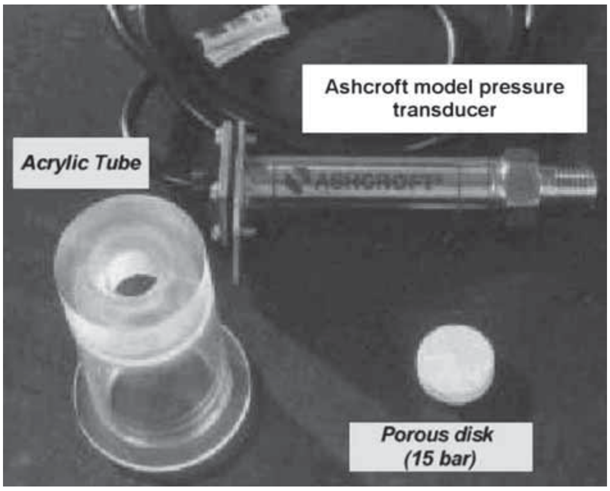

Figure 1 - Components of the new instrument (Pacheco, 2001 and Mahler *et al.*, 2002).

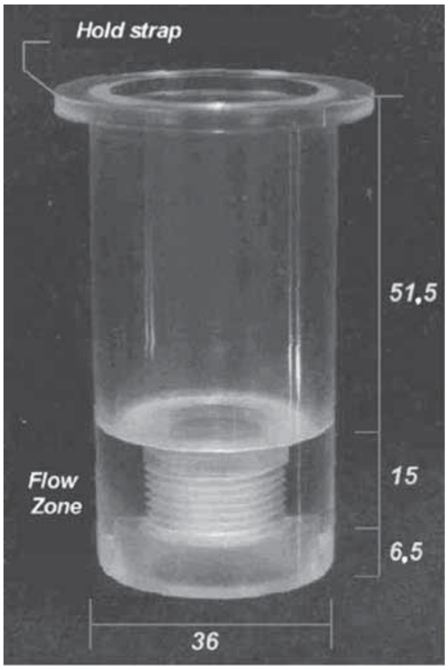

Figure 2 - Acrylic tube dimensions in milimiters (Pacheco, 2001 and Mahler *et al.*, 2002).

Claudio Fernando Mahler, LD, D.Sc., Professor, COPPE/UFRJ, Rio de Janeiro, R.J., Brazil. e-mail: mahler0503@yahoo.com.
Ronaldo Luiz dos Santos Izzo, D.Sc., Doutor, COPPE/UFRJ, Rio de Janeiro, R.J. Brazil. e-mail: ronaldoizzo@gmail.com.
The use of a High-Capacity Tensiometer for Determining the Soil Water Retention Curve by Marinho & Teixeira. Published in Soils and Rocks v. 32(2), p. 91.
Received and accepted on .

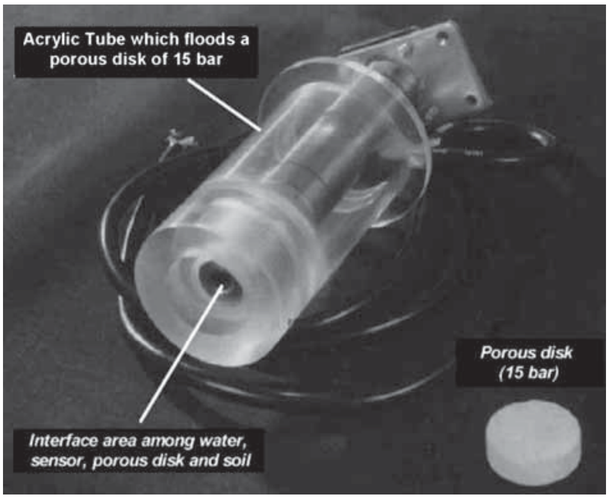

Figure 3 - View of the interface area among water, sensor, porous disk and soil (Pacheco, 2001).

• As expected, the position of the equitensiometer influences the values measured;

• The T5 tensiometer T5 measured values of over 100 kPa (about 150 kPa) quite accurately;

• The mini-lysimeter system proved to be a very good alternative for laboratory tests and for the development of instruments that measure suction;

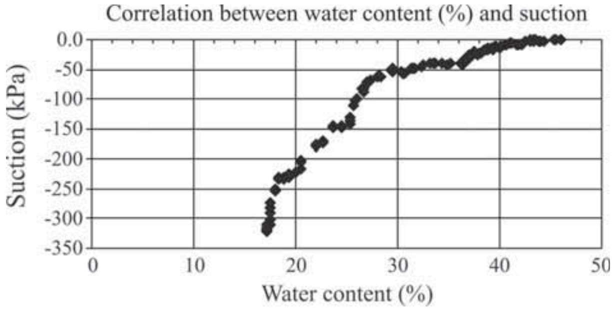

Figure 4 - Correlation between the measurement of the new tensiometer and the TDR probe (Pacheco, 2001).

• Tthe new instrument presented herein proved to be a good and an economical alternative for measuring matrix suction in the soil.

Later, Diene (2004), Mahler & Diene (2004) and Diene & Mahler (2006), among others, continued developing high-capacity tensiometers and managed to measure suction values of nearly 1500 kPa. The characteristic curves determined with high-capacity tensiometer and TDR proves are presented in Fig. 10, while Fig. 11 shows the suction results measured with two high-capacity tensiometers compared with those of a equitensiometer, the

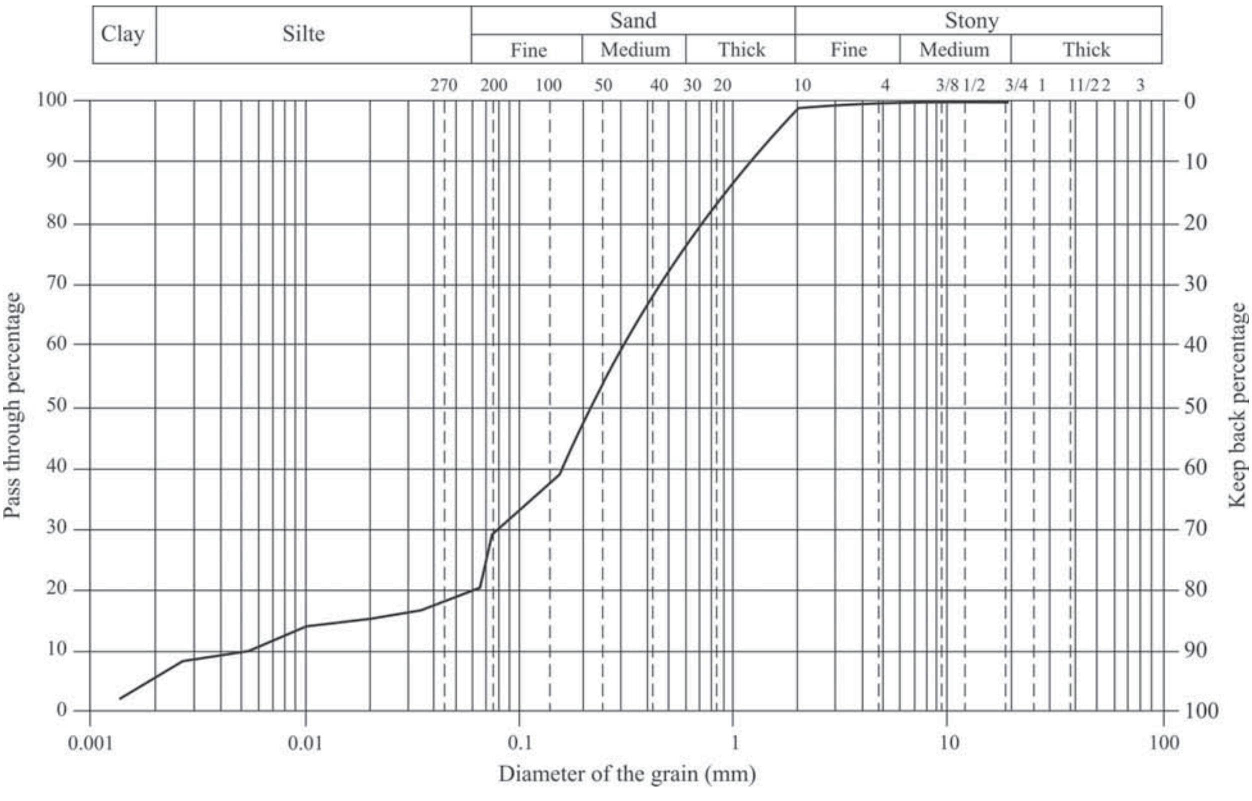

Figure 5 - Grain size curve the soil used (Pacheco, 2001).

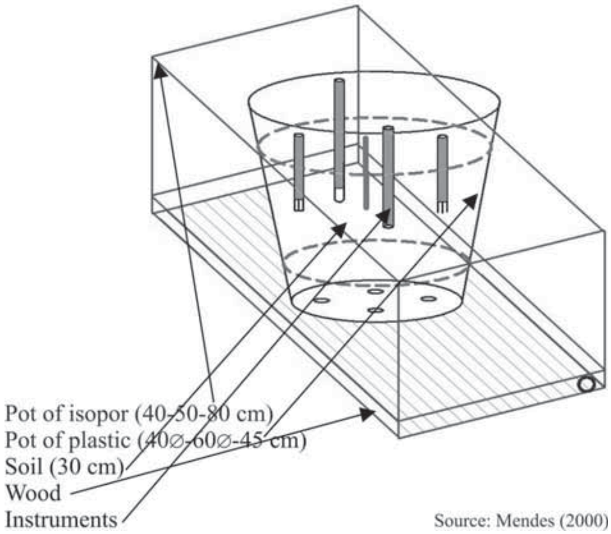

Figure 6 - Mini-lysimeter used in the lab (Pacheco, 2001 and Mahler *et al.*, 2002).

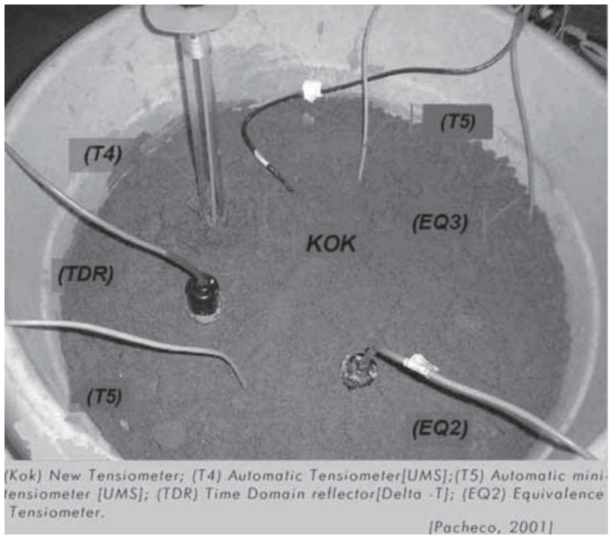

Figure 7 - Position of instruments installed in the mini-lysimeter.

Figure 8 - Equitensiometer (EQ2) [Delta - T Devices].

former having measured values of almost 1500 kPa, as mentioned.

More information on the equipment, procedures and soil used in this study can be seen in the articles cited above and in the master's dissertation of Diene (2004).

The results of the tensiometer presented at the time and those of the equitensiometers placed horizontally and vertically at the same level in laboratory lysimeters were very near.

The procedure used in the experiments carried out by Huse (2007) and Santos (2008) is very similar to that proposed by the authors of the technical note, Marinho & Teixeira. In these two earlier works, a device was developed to study soil drying using a tensiometer, as in the device described by Marinho & Teixeira, but providing more information, such as sample moisture (easily calculated from the sample weight variation) and volumetric variation (obtained directly by the wrapping on the flexible wall around the sample - Fig. 12). In this respect, the device used by Huse (2007) and Santos (2008) is more complete than that presented by Marinho & Teixeira.

One of the results obtained from using the set of equipment to study soil drying is the characteristic curve of

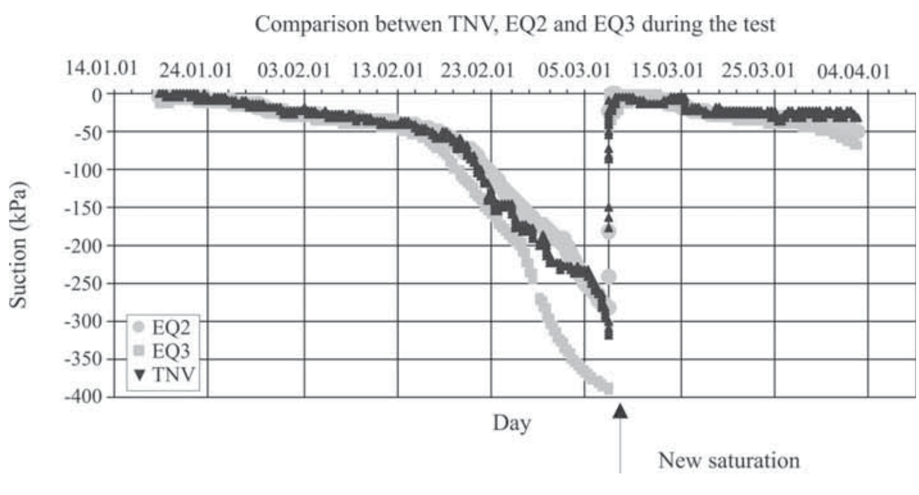

Figure 9 - Results of the new tensiometer and the equitensiometer in the mini-lysimeter (Pacheco, 2001 and Mahler *et al.*, 2002).

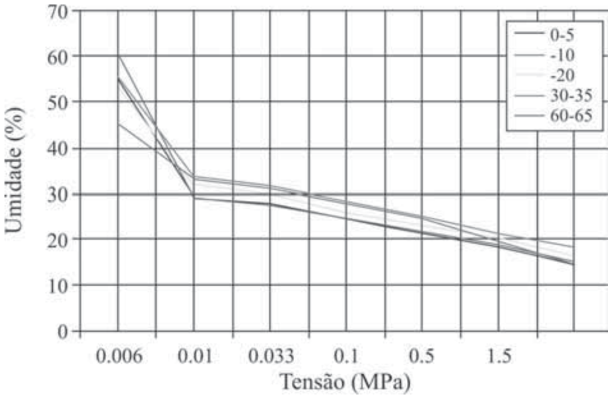

Figure 10 - Characteristic moisture retention curves of the soil from tank B (Laps-Embrapa/Cnps).

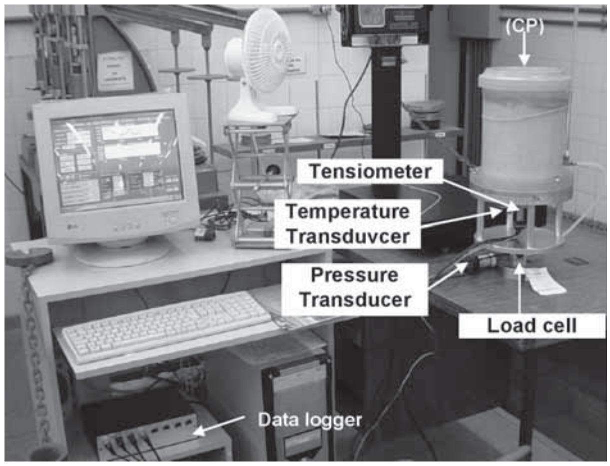

Figure 12 - View of the equipment set-up developed to drying in soil and soil mixed with bentonite (Santos, 2008).

the soil studied, which can be seen in Fig. 13 (Huse, 2006) and Fig. 14 (Santos, 2008).

The study by Huse (2007) was designed to analyze the formation of cracks in landfill cover soil caused by shrinkage from drying, and that by Santos (2008) was aimed at protection of embankments and hillsides. In both cases the authors studied use of mixtures of soil with bentonite.

In closing, it is important to use new types of tensiometers and other equipment to determine the characteristic curves in the laboratory, combined with procedures to determine the moisture content, that associate precision and low cost. The equipment set-up shown above is very flexible. It can be used in various ways and in association with other geotechnical tests.

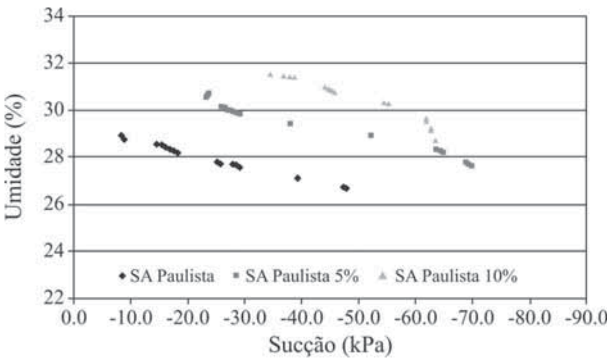

Figure 13 - Characteristic curves obtained by Huse (2006) using the equipment developed to study drying of soil and soil mixed with bentonite.

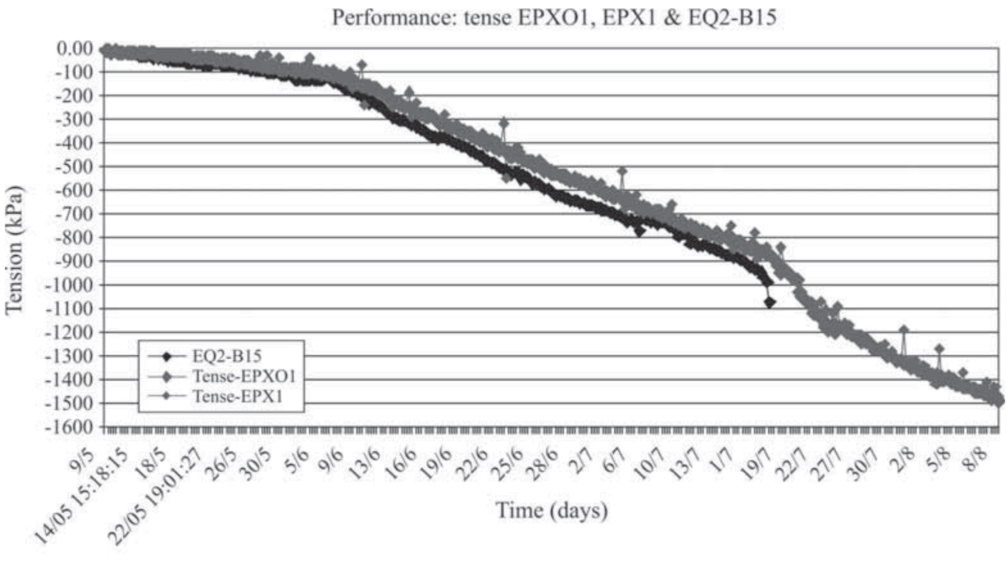

Figure 11 - Suction versus time measurements in two TENSE tensiometers anda n equitensiometer (Diene, 2004).

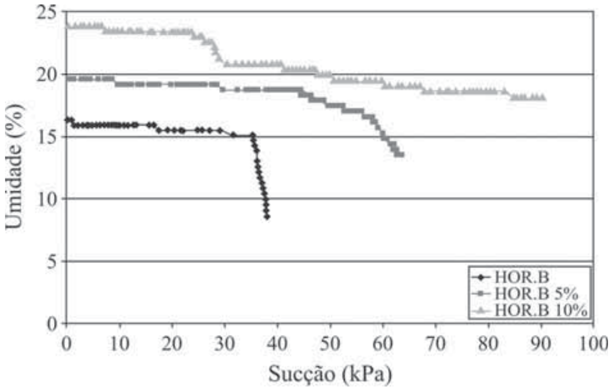

Figure 14 - Characteristic curves obtained by Santos (2008) using the equipment developed to study drying of soil and soil mixed with bentonite.

References

Diene, A.A. (2004) Desenvolvimento de Tensiometros para Sucção Elevada Ensaiados em Lisimetros para Laboratório (Development for High Suction Tensiometers Analysed in Laboratory Lysimeters in the Study of Drainage). Master Dissertation, Departamento de Engenharia Civil, COPPE/UFRJ, 173 pp.

Diene, A.A. & Mahler, C.F. (2007) Um instrumento para medida de potencial matricial nos solos sem ocorrencia de cavitação. Revista Brasileira de Ciência do Solo, v. 31:6, p. 1261-1270.

Huse, K. (2007) Estudo da Formação de Trincas na Camada de Cobertura de um Aterro (Influence of the Top Layer Shrinkage in Water Balance of a Solid Waste Landfill). Master Dissertation, COPPE/UFRJ, 126 pp.

Mahler, C.F.; Pacheco, A.C.C.S. & Goncalves, H.S. (2002) Development of an automatic tensiometer in the laboratory using a Mini-Lysimeter. Proc. 3th International Congress on Unsaturated Soils, UNSAT 2002, Recife, v. 3.

Mahler, C.F.; Diene, A.A. & Goncalves, H.S. (2005) Um novo instrumento para medida de sucção nos solos. Solos e Rochas, v. 28:3, p. 309-318.

Pacheco, A.C.C.S. (2001) Desenvolvimento de um Novo Tensiômetro para Medidas de Tensão Acima de 1 atm (Development of a new tensiometer for suction measurement over 1 atm). Master Dissertation, Departamento de Engenharia Civil, COPPE/ UFRJ, 95 pp.

Ridley, A.M. & Burland, J.B. (1993) A new instrument for measuring soil moisture suction. Geotechnique, 43:2, p. 321-324.

Santos, L.V. (2008) Influencia da Bentonita em um Solo Residual para uso como Camada Selante. (The Influence of Bentonite in a Residual Soil for Use as a Sealant Layer). Master Dissertation, COPPE/UFRJ, 140 pp.

Authors' reply to the discussion presented by Mahler, C.F. & Izzo, R.L.S.

The Authors thanks the Writers to the opportunity to clariffy some aspects associated or not with the papers presented but that were risen by the Writers. Our comments will try to focus on the use of tensiomneter to measure SWRC and will not deeply comment on others insue rised by the Writers, that are not related to technical note published.

The Writer sugested the use of TDR for obtaing the soil water retention curve (SWRC). TDR is inapropriated to be used for soil water retention curve unless the sample used is of a size that the boundary effects can be disconsidered. The eventual change in volume of the specimen during the increase in suction can also cause problems (see Vieira *et al.*, 2005). There is only one SWRC presented by the Writers that seems to go beyond 100 kPa of suction. Considering the way these result are presented (Fig. 10) it is not clear how the experimental data was obtained and how the TDR probes were used in this case.

The Writers did not presented any comparison between their attempt to obtain the SWRC and conventional methods. Since there is no comparison at least a calibration curve should be presented showing the acuracy of the equipment. The tensiometer mentioned by the Writers made of acrilic cannot work for high suction (higher than aproximatelly 200 kPa) if a conditioning process is not used. The conditioning process (see Marinho *et al.*, 2008), can only be applied if the tensiometer is robust enouth to suport the high level of pressure that is necessary for avoiding cavitation. Other possibility is the development of a chemical saturation which is not mentioned by the Writers.

The Writer did not read the paper with the proper care since they did not undestood the results presented. The work did measure the water content that was “easilly” back calculated by weighting the sample during the drying process. The volume of the sample was also obtained since the volumetric water content is given. Volumetric water content can only be used if the specimen does not change volume during drying or if the volume of the specimen is obtained.

The Authors also would like to call attention to the writers to do not make confusion between pressure and suction. In Figs. 4, 9 and 13 suction is presented as a negative number. This is pressure not suction. Care also should be taken when using the term “tension”. The water is only under tension when it is below atmospheric pressure and in this way cannot be used as it is used in Figs. 10 and 11. Fig. 11 presents results sugesting that the tensiometer used by the Writers can sustain suction higher than 500 kPa for months. The Authors cannot agree with that result unless sufficient scientific evidence is shown.

SOILS and ROCKS
An International Journal of Geotechnical and Geoenvironmental Engineering

Publication of

ABMS - Brazilian Association for Soil Mechanics and Geotechnical Engineering
ABGE - Brazilian Association for Engineering Geology and the Environment
SPG - Portuguese Geotechnical Society

Volume 33, N. 2, May-August 2010

Author index

Instructions to Authors

Category of the Papers

Soils and Rocks is the scientific journal edited by the Brazilian Society of Soil Mechanics and Geotechnical Engineering (ABMS) and by the Brazilian Society of Engineering and Environmental Geology (ABGE). The journal is intended to the divulgation of original research works from all geotechnical branches.

The accepted papers are classified either as an Article paper, a Technical Note, a Case Study, or a Discussion according to its content. An article paper is an extensive and conclusive dissertation about a geotechnical topic. A paper is considered as a technical note if it gives a short description of ongoing studies, comprising partial results and/or particular aspects of the investigation. A case study is a report of unusual problems found during the design, construction or the performance of geotechnical projects. A case study is also considered as the report of an unusual solution given to an ordinary problem. The discussions about published papers, case studies and technical notes are made in the Discussions Section.

When submitting a manuscript for review, the authors should indicate the category of the manuscript, and is also understood that they:

a) assume full responsibility for the contents and accuracy of the information in the paper;

b) assure that the paper has not been previously published, and is not being submitted to any other periodical for publication.

Manuscript Instructions

Manuscripts must be written in English. The text is to be typed in a word processor (MS Word or equivalent), using ISO A4 page size, left, right, top, and bottom margins of 25 mm, Times New Roman 12 font, and line spacing of 1.5. All lines and pages should be numbered. The text should be written in the third person.

The fist page of the manuscript is to include the title of the paper in English, followed by the names of the authors with the abbreviation of the most relevant academic title. The affiliation, address and e-mail is to be indicated below each author's name. An abstract of 200 words is to be written in English after the author's names. A list with up to six keywords at the end of the abstract is required.

Although alteration of the sequence and the title of each section may be required, it is suggested that the text contains the following sections: Introduction, Material and Methods, Results, Discussions, Conclusion, Acknowledgements, References and List of Symbols. A brief description of each section is given next.

Introduction: This section should indicate the state of the art of the problem under evaluation, a description of the problem and the methods undertaken. The objective of the work is to be clearly presented at the end of the section.

Materials and Methods: This section should include all information needed to the reproduction of the presented work by other researchers.

Results: In this section the data of the investigation should be presented in a clear and concise way. Figures and tables should not repeat the same information.

Discussion: The analyses of the results should be described in this section. **Conclusions**: The text of this section should be based on the presented data and in the discussions.

Acknowledgenments: If necessary, concise acknowledgements should be written in this section.

References: References to other published sources are to be made in the text by the last name(s) of the author(s), followed by the year of publication, similarly to one of the two possibilities below:

"*while Silva & Pereira (1987) observed that resistance depended on soil density*" or "*It was observed that resistance depended on soil density (Silva & Pereira, 1987).*"

In the case of three or more authors, the reduced format must be used, *e.g.*: Silva *et al.* (1982) or (Silva *et al.*, 1982). Two or more citations belonging to the same author(s) and published in the same year are to be distinguished with small letters, *e.g.*: (Silva, 1975a, b, c.). Standards must be cited in the text by the initials of the entity and the year of publication, *e.g.*: ABNT (1996), ASTM (2003).

Full references shall be listed alphabetically at the end of the text by the first author's last name. Several references belonging to the same author shall be cited chronologically. Some examples are listed next:

Papers: Bishop, A.W. & Blight, G.E. (1963) Some aspects of effective stress in saturated and unsaturated soils. Géotechnique, v. 13:2, p. 177-197.

Books: Lambe, T.W & Whitman, R.V. (1979) Soil Mechanics, SI Version, 2nd ed. John Wiley & Sons, New York, p. 553.

Book with editors: Sharma, H.D.; Dukes, M.T. & Olsen, D.M. (1990) Field measurements of dynamic moduli and Poisson's ratios of refuse and underlying soils at a landfill site. Landva A. & Knowles, G.D. (eds) Geotechnics of Waste Fills - Theory and Practice, American Society for Testing and Materials - STP 1070, Philadelphia, p. 57-70.

Proceedings (printed matter or CD-ROM): Jamiolkowski, M.; Ladd, C.C.; Germaine, J.T & Lancellotta, R. (1985) New developments in field and laboratory testing of soils. Proc. 11th Int. Conf. on Soil Mech. and Found. Engn., ISSMFE, San Francisco, v. 1, pp. 57-153.(specify if CD – ROM)

Thesis and dissertations: Lee, K.L. (1965) Triaxial Compressive Strength of Saturated Sands Under Seismic Loading Conditions. PhD Dissertation, Department of Civil Engineering, University of California, Berkeley, 521 p.

Standards: ASTM (2003) Standard Test Method for Particle Size Analysis of Soils - D 422-63. ASTM International, West Conshohocken, Pennsylvania, USA, 8 p.

Internet references: Soils and Rocks available at http://www.abms.com.br.

On line first publications must also bring the digital object identifier (DOI) at the end.

Figures shall be either computer generated or drawn with India ink on tracing paper. Computer generated figures must be accompanied by the corresponding digital file (.tif, .jpg, .pcx, etc.). All figures (graphs, line drawings, photographs, etc.) shall be numbered consecutively and have a caption consisting of the figure number and a brief title or description of the figure. This number should be used when referring to the figure in text. Photographs should be black and white, sharp, high contrasted and printed on glossy paper.

Tables shall be numbered consecutively in Arabic and have a caption consisting of the table number and a brief title. This number should be used when referring to the table in text. Units should be indicated in the first line of the table, below the title of each column. Abbreviations should be avoided. Column headings should not be abbreviated. When applicable, the units should come right below the corresponding column heading. Any necessary explanation can be placed as footnotes.

Equations shall appear isolated in a single line of the text. Numbers identifying equations must be flush with the right margin. International System (SI) units are to be used. The symbols used in the equations shall be listed in the List of Symbols. It is recommended that the used symbols be in accordance with Lexicon in 8 Languages, ISSMFE (1981) and the ISRM List of Symbols.

The text of the submitted manuscript (including figures, tables and references) intended to be published as an article paper or a case history should not contain more than 30 pages formatted according to the instructions mentioned above. Technical notes and discussions should have no more than 15 and 8 pages, respectively. Longer manuscripts may be exceptionally accepted if the authors provide proper explanation for the need of the required extra space in the cover letter.

Discussion

Discussions must be written in English. The first page of a discussion paper should contain:

• The title of the paper under discussion in the language chosen for publication;

• Name of the author(s) of the discussion, followed by the position, affiliation, address and e-mail. The discusser(s) should refer himself (herself, themselves) as "the discusser(s)" and to the author(s) of the paper as "the author(s)".

Figures, tables and equations should be numbered following the same sequence of the original paper. All instructions previously mentioned for the preparation of article papers, case studies and technical notes also apply to the preparation of discussions.

Editorial Review

Each paper will be evaluated by reviewers selected by the editors according to the subject of the paper. The authors will be informed about the results of the review process. If the paper is accepted, the authors will be required to submit a version of the revised manuscript with the suggested modifications. If the manuscript is refused for publication, the authors will be informed about the reasons for rejection. In any situation comprising modification of the original text, classification of the manuscript in a category different from that proposed by the authors, or refusal for publication, the authors can reply presenting their reasons for disagreeing with the reviewers' comments

Submission

The author(s) must submit for review:

1. A hard copy of the manuscript to Editors - Soils and Rocks, Av. Prof. Almeida Prado, 532 – IPT, Prédio 54 – DEC/ABMS, 05508-901 - São Paulo, SP, Brazil. The first page of the manuscript should contain the identification of the author(s), or

2. The digital file of the manuscript, omitting the authors' name and any information that eventually could identify them, should be sent to **abms@ipt.br**. The following must be written in the subject of the e-mail message: "*Paper submitted to Soils and Rocks*". The authors' names, academic degrees and affiliations should be mentioned in the e-mail message. The e-mail address from which the digital file of the paper was sent will be the only one used by the editors for communication with the corresponding author.

Follow Up

Authors of manuscripts can assess the status of the review process at the journal website (www.soilsandrocks.com.br) or by contacting the ABMS secretariat.

Volume 33, N. 2, May-August 2010

Table of Contents